ISTANBUL TECHNICAL UNIVERSITY ★ INSTITUTE OF SCIENCE AND TECHNOLOGY

IMPROVEMENT OF THE PROPERTIES OF ELECTROSPUN SILK FIBROIN NANOWEB

M.Sc. Thesis by
Nuray KIZILDAĞ

Department : Textile Engineering

Programme : Textile Engineering

FEBRUARY 2011

İSTANBUL TECHNICAL UNIVERSITY ★ INSTITUTE OF SCIENCE AND TECHNOLOGY

IMPROVEMENT OF THE PROPERTIES OF ELECTROSPUN SILK FIBROIN NANOWEB

M.Sc. Thesis by
Nuray KIZILDAĞ
(503081815)

Date of submission : 20 December 2010
Date of defence examination: 26 January 2011

Supervisor (Chairman) : Assist. Prof. Dr. Yesim BECEREN(ITU)
Members of the Examining Committee : Prof. Dr. Banu UYGUN NERGIS (ITU)
Assist. Prof. Dr. Murat TABANLI (ITU)

FEBRUARY 2011

İSTANBUL TEKNİK ÜNİVERSİTESİ ★ FEN BİLİMLERİ ENSTİTÜSÜ

İPEK PROTEİNİ FİBROİNDEN ELEKTROSPİNNİNG YÖNTEMİ İLE ÜRETİLEN NANOWEBİN ÖZELLİKLERİNİN İYİLEŞTİRİLMESİ

YÜKSEK LİSANS TEZİ
Nuray KIZILDAĞ
(503081815)

Tezin Enstitüye Verildiği Tarih : 20 Aralık 2010
Tezin Savunulduğu Tarih : 26 Ocak 2011

Tez Danışmanı : Yrd. Doç. Dr. Yeşim BECEREN (İTÜ)
Diğer Jüri Üyeleri : Prof. Dr. Banu UYGUN NERGİS (İTÜ)
Yrd. Doç. Dr. Murat TABANLI (İTÜ)

ŞUBAT 2011

FOREWORD

I would like to express my deep appreciation and thanks for my advisor Yesim IRIDAG for her invaluable guidance, encouragement and financial support throughout this study.

I also would like to express my thanks for Murat KAZANCI for his endless guidance, support and discussion.

A special thanks to Assist. Prof. Dr. Dilek CUKUL from Anadolu University for all of the SEM imaging, Prof. Dr. Oguz OKAY, Prof. Dr. Oya ATICI, Research Assistant Ilknur KARAKUTUK from Istanbul Technical University, Department of Chemistry for the freeze drier, Prof. Dr. Yusuf MENCELOGLU from Sabanci University, Department of Materials Science and Engineering, and Prof. Dr. Ali DEMIR from Istanbul Technical University, Department of Textile Engineering for the electrospinning setup, Research Assistants Elif OZDEN and Eren SIMSEK from Sabanci University, Department of Materials Science and Engineering and graduate students Aras MUTLU, Salih GULSEN and Nur BAYCULAR from Istanbul Technical University, Department of Textile Engineering for their help in electrospinning process, Prof. Dr. Gultekin GOLLER from Istanbul Technical University, Department of Metallurgical and Materials Engineering for the first SEM images depicting the fiber formation and, Prof. Dr. Ersin SERHATLI from Istanbul Technical University, Department of Chemistry for the FTIR spectroscopy.

I would like to extend my thanks to Dt. Elif Nurhak ERDAL for her help in supplying hypodermic needles.

I would like to thank my friends Serdar DEMIRCIOGLU from Dystar Kimya Sanayi ve Ticaret Ltd. Sti., and Mahmut ZAMAN from Ozen Mensucat A.Ş for their help in supplying the chemicals.

I would like to thank Research Assistants Ikilem GOCEK, Sena CIMILLI, and Melek GUL for their help in statistical analysis.

Finally, I would like to express my deepest appreciation to my family members. I am indebted to my dear husband Cagri KIZILDAG for his financial support, encouragement, patience and help in analysing SEM images.

December 2010

Nuray Kızıldağ

Textile Engineer

TABLE OF CONTENTS

Page

ABBREVIATIONS

Ala	**:** alanine
B. mori	**:** Bombyx mori
BCE	**:** before Common Era
BF	**:** Battlefield filter
BMP-2	**:** bone morphogenetic protein-2
CE	**:** common era
cm	**:** centimeter
Da	**:** dalton
DIN	**:** Deutsches Institut für Normung
DMF	**:** dimethylformamide
DNA	**:** deoxyribonucleic acid
D_r	**:** degumming ratio
DSC	**:** differential scanning calorimetry
ECM	**:** extra cellular matrix
EGF	**:** epidermal growth factor
FTIR	**:** Fourier Transform Infra Red
g	**:** gram
Gly	**:** glycine
h	**:** hour
HAEC	**:** human aortic endothelial cells
HCASMC	**:** human coronary artery smooth muscle cells
HFA	**:** hexafluoroacetone
HFIP	**:** 1,1,1,3,3,3-hexafluoro-2-propanol
hMSC	**:** human mesencymal stem cells
kDA	**:** kilodalton
kV	**:** kilovolt
mL	**:** mililiter
MPa	**:** mega pascal
MWCO	**:** molecular weight cut off
nm	**:** nanometer
PAA	**:** poly (acrylic acid)
PAN	**:** poly (acrylo nitrile)
PCL	**:** ε-poly (caprolactone)
PEG	**:** poly (ethylene glycol)
PEO	**:** poly (ethylene oxide)
PET	**:** poly (ethylene terephthalate)
PGA	**:** poly (glycolide)
PLA	**:** poly (lactide) acid
PLGA	**:** poly (lactic-co-glycolic acid)
PLLA	**:** poly (L-lactic acid)
PMMA	**:** poly (methyl methacrylate)
PS	**:** polystyrene
PVA	**:** poly (vinyl alcohol)

SEM : scanning electron microscope
Ser : serine
SF : silk fibroin
SLPF : silk like polymer fiber
TEM : transmission electron microscopy
TFA : trifluoroaceticacid
US : United States
w/v : weight per volume
w/w : weight per weight
WAXD : Wide-angle X-ray diffraction
wt : weight
µm : micrometer
µl : microliter

LIST OF TABLES

Page

LIST OF FIGURES

Page

IMPROVEMENT OF THE PROPERTIES OF ELECTROSPUN SILK FIBROIN NANOWEB

SUMMARY

Silks are fibrous proteins with remarkable mechanical properties produced in continuous form by spiders and silkworms. Cultivated silk from the *Bombyx mori* silkworm, which is and has always been the most common type of silk used, has a number of interesting and desirable properties that have been admired for over 5,000 years. It is popularly known in textile industry for its luster and mechanical properties. Besides its traditional use in textiles, the range of applications of silkworm silk is expanding mainly in the field of biomaterials.

Several different material morphologies such as gels, sponges, films, and nanowebs produced through regeneration of silk fibroin (SF) have been applied in a wide variety of biomedical applications such as cell or tissue scaffolds, drug delivery carriers, wound dressing, etc. Materials based on silk fibroin which is naturally biocompatible, biodegrable and mechanically superior, are promising candidates for biomedical applications. Especially the availability of silk nanofibers with high surface area to volume ratio and highly porous three dimensional structure through a simple process of electrospinning introduces a new set of potential uses that previously were unattainable.

In this study, an attempt was made to produce nanowebs from silk fibroin by electrospinning and to optimize the electrospinning parameters for the spinning of uniform, continuous and nanoscale silk fibroin fibers. The study involved the steps of, degumming; forming a silk fibroin solution comprising silk fibroin in an aqueous salt solution; removing the salt by dialysis and water by freeze-drying from the solution to form a regenerated silk fibroin material; forming an electrospinnable solution by redissolution of the resulting regenerated silk fibroin material in formic acid; and finally electrospinning to form nanowebs.

Nanowebs were electrospun from solutions of different concentrations, by varying the applied voltage, flow rate, tip-to-collector distance, and needle diameter. Solutions with concentrations of 6, 8, 10, 12, 15 and 18 wt% were prepeared by dissolving regenerated silk fibroin sponges in formic acid. Electrospinning was carried out by varying the applied voltage from 10 to 25 kV, tip-to-collector distance from 5 to 13 cm, flow rate from 0.006 to 2.0 mL/h and needle diameter from 0.7 to 1.25 mm. Fourier transform infrared (FTIR) spectrum was obtained in the spectral region of 400–4,000 cm^{-1} to observe the structural and conformational changes in silk fibroin caused by electrospinning. The effects of the varying parameters on bead formation and fiber diameter were investigated by scanning electron microscopy (SEM) and statistical analysis was carried out to test whether the diferences in the mean fiber diameters were of real significance.

As a result, electrospinning of regenerated silk fibroin was conducted successfully and fibers with diameters in the range of 37 to 437 nm which were much thinner than natural silk fiber were fabricated. Concentration appeared to be the most significant factor affecting the fiber spinnability, bead formation and fiber diameter. Also it is observed that the processing paramaters such as applied voltage, tip-to-collector distance, flow rate and needle diameter had considerable effect on bead formation and it is statistically approved that these parameters had significant effects on fiber diameter.

İPEK PROTEİNİ FİBROİNDEN ELEKTROSPİNNİNG YÖNTEMİ İLE ÜRETİLEN NANOWEBİN ÖZELLİKLERİNİN GELİŞTİRİLMESİ

ÖZET

İpek lifleri, ipekböcekleri ve örümcekler tarafından kontinü lif formunda üretilen üstün özelliklere sahip protein yapılı liflerdir. En yaygın şekilde kullanılmakta olan *Bombyx mori* ipekböceğinden elde edilen ipek, 5.000 yıldır beğeni toplayan, farklı ve çekici pekçok özelliğe sahiptir. Tekstil endüstrisinde parlaklığı ve mekanik özellikleri ile tanınan ipeğin kullanım alanları tekstil amaçlı kullanımlarının ötesinde biomateryaller alanında genişlemektedir.

İpek proteini fibroinin rejenerasyonu ile üretilen, jel, film, sünger ve nanoweb gibi farklı formlarda materyallerin, hücre ve/veya doku iskelesi, ilaç salınım sistemleri, yara örtücü yüzeyler olarak biomedikal alanda kullanımları ile ilgili olarak çalışmalar yapılmaktadır. Biyolojik olarak uyumlu, kendine kendine parçalanabilir, mekanik yönden üstün olan fibroin esaslı bu materyaller biomedikal uygulamalar için ümit verici adaylardır. Özellikle büyük yüzey alanına sahip, çok gözenekli, üç boyutlu yapıların, elektrospinning gibi basit bir yöntem ile üretilebilmesi, daha önce mümkün olmayan yeni kullanım alanları sunmaktadır.

Tez kapsamında, elektrospinning yöntemi ile ipek proteini fibroinden nanoweb üretilmesine ve düzgün, devamlı, nano boyutta rejenere ipek liflerinin elde edilmesi için parametrelerin belirlenmesine yönelik çalışılmıştır. Çalışma; serisinin uzaklaştırılmasını, fibroinin derişik tuz çözeltisinde çözülmesi ve bu çözeltiden tuzun diyaliz ile, suyun liyofilize işlemi ile uzaklaştırılarak toz halde rejenere fibroinin elde edilmesini, elde edilen rejenere fibroinin elektrospinning işlemine uygun bir çözeltide tekrar çözülmesini ve yeni çözeltiden elektrospinning yöntemi ile nanoweb üretilmesini kapsamaktadır.

Değişik konsantrasyonlarda çözeltilerden, voltaj değerinin, besleme hızının, iğne ile toplayıcı arasındaki mesafenin ve iğnenin değiştirilmesi ile nanoweb üretilmiştir. Rejenere fibroinin formik asit içerisinde çözülmesi ile %6, %8, %10, %12, %15 ve %18 konsantrasyonlarda çözeltiler hazırlanmıştır. Voltaj değerleri 10 kV ile 25 kV arasında, mesafe 5-13cm aralığında, besleme hızı 0,006 ile 2,0 mL/sa aralığında değiştirilerek ve 0,70, 0,90, 1,06, 1,25mm çaplara sahip farklı iğneler kullanılarak elektrospinning işlemi yapılmıştır. Fibroinin kimyasal ve konformasyonel yapısında oluşabilecek değişiklikler infrared spektroskopisi (FTIR) ile kontrol edilmiştir. Farklı parametrelerin boncuk oluşumu ve lif çapı üzerindeki etkileri taramalı elektron mikroskobu (SEM) ile araştırılmış ve ortalama lif çapında gözlenen değişikliklerin anlamlı farklar olup olmadıkları istatistiksel açıdan kontrol edilmiştir.

Çalışmanın sonucunda, ipek proteini fibroinden elektrospinning yöntemi ile nanoweb oluşturulmuş, doğal ipekten çok daha ince olan 37 nm ile 437 nm aralığında düzgün lifler elde edilmiştir. Konsantrasyonun lif eğrilebilirliği, boncuk oluşumu ve lif çapı üzerinde etkili olan en önemli parametre olduğu gözlenmiş ve konsantrasyon değişimine bağlı olarak ortalama lif çaplarında meydana gelen değişiklerin

istatistiksel açıdan önemli oldukları belirlenmiştir. Ayrıca uygulanan voltajın, iğne ile toplayıcı arasındaki mesafenin, besleme hızının ve iğne çapının da boncuk oluşumu ve lif çapı üzerinde belirli derecede etkiye sahip oldukları gözlenmiştir.

1. INTRODUCTION

1.1 Background

Silks are fibrous proteins with remarkable mechanical properties produced in continuous fiber form by spiders and silkworms.

Silk fibroin (SF) fiber, popularly known in the textile industry for its luster and mechanical properties, is produced by cultured silkworms [1]. It has been used as a surgical suture material for several centuries due to its good mechanical and biological properties including biocompatibility and low inflammatory reaction [2]. It has played an important role not only in political, cultural, and economic history (Silk Road, national costumes), but also in the history of technology (textile machines, Jacquard) and in science (protein chemistry, genetics, and genetic engineering). Despite the triumphal advance of synthetic fibers, silk maintains its place in the raw material market, in the textile and clothing industries, and in the retail trade because of its unique properties [3].

Besides its traditional use in textiles, the range of applications of silkworm silk is expanding mainly in the field of biomaterials [4]. Silks from silkworms (e.g., *Bombyx mori*) have been explored to understand the structure, the processing mechanisms and to exploit the properties of these proteins for use as biomaterials. They represent a unique family of structural proteins that are biocompatible, degradable, mechanically superior [1]. Silk-based biomaterials have demonstrated excellent biocompatibility in different material forms for various tissue regenerations. The degradation rate can be tailored from months to years after implanting *in vivo*, based on processing procedures employed during material formation. Moreover, the unique structural assembly of these proteins endows them with remarkable mechanical properties when compared with other commonly used biopolymer-based biomaterials. Also, they have characteristic properties including thermal stability, environmental stability, morphologic flexibility and the ability for amino acid side change modification to immobilize growth factors [1,5]. They have

been applied in a wide variety of biomedical applications such as a drug delivery carrier, a matrix for mammalian cell culture and enzyme immobilization and a scaffold for bone substitution in different material forms [2]. Regenerated from aqueous or solvent formulations of the natural fiber form of silk, several different material morphologies such as gels, sponges, films, and nanowebs produced by electrospinning can be utilized in biomaterials [1].

The electrospinning process became and remains attractive since it is a cost-effective method of producing nanofibers from a large variety of bulk starting materials in a moderately easy, repeatable, and simple fashion [6].

It is a process that creates nanofibers through an electrically charged jet of polymer solution or polymer melt [7]. Recently, researchers have begun to look into various applications of electrospun nanowebs as these provide several advantages such as high surface area to volume ratio, very high porosity and enhanced physico-mechanical properties as in this process, manipulation of the solution and process parameters can be easily done to get the desired fiber morphology and mechanical strength. The electrospinning process itself is a versatile process as fibers can be spun into any shape using a wide range of polymers. It has evinced more interest and attention in recent years due to its versatility and potential for applications in diverse fields [8].

Integrating the impressive properties of silk with unique advantages of electrospinning results in nanowebs with high surface area, high porosity and good biocompatibility and superior mechanical properties which have a potential for a variety of applications.

Silk was first electrospun and patented by Zarkoob *et al.* in 2000 [6]. Afterwards, there have been some simultaneous efforts to characterize the structure and morphology of nanofibers as a function of process parameters. However, limited study has been performed regarding the effect of flow rate on the morphology and diameter of SF nanowebs and no study has been performed regarding the effect of needle diameter.

In this study, a brief overview is provided for the regenerated fibers, structure of silk, electrospinning process, production of SF nanowebs and the effect of parameters

such as concentration, applied voltage, tip-to-collector distance, flow rate, and needle diameter on bead formation and fiber diameter are investigated.

1.2 Purpose of the Thesis

The purpose of the thesis is to fabricate uniform nanoscale SF fibers by electrospinning and to analyse the effects of the electrospinning parameters such as applied voltage, concentration, tip-to-collector distance, flow rate and needle diameter on bead formation and fiber diameter.

The study involves the steps of

a) extracting the silk fibroin by boiling the pieces of *Bombyx mori* cocoons in water containing 2 g/lt Na_2CO_3, rinsing several times to remove the sericine and drying in air;

b) forming a silk fibroin solution comprising silk fibroin in an aqueous salt solution;

c) removing the salt by dialysis and water by freeze-drying from the fibroin solution to form a silk fibroin material;

d) forming an electrospinnable solution by redissolution of the resulting regenerated silk fibroin material in formic acid;

e) electrospinning to form nanoscale silk fibroin fibers;

f) characterization to determine the structural changes in SF and the effects of different process and solution parameters on bead formation and fiber diameter.

2. LITERATURE SURVEY

2.1 Regenerated Fibers

The term 'regenerated' is applied to fibers which are formed from naturally occurring polymers by modifying and reforming the original material [9].

The raw materials like proteins or cellulose are reformed to produce fibers, filaments, and recently to produce nanowebs [10].

In the middle of the 20th century, the dominant textile fibers were two cellulosics, namely cotton, which was the cheap general-purpose fiber, and linen, which had superior quality, and two protein fibers, namely wool, which was warmer and more durable, and silk, which was a luxury fiber but also the toughest available fiber, used, for example, in parachutes. The advances in chemistry near the end of the 19th century led to attempts to emulate silk and wool [11]. Rayon appeared about a century ago as the first regenerated fiber mimicking silk. Rayon filament is made from wood pulp that is dissolved and wet-spun. Rayon is thus chemically composed of the same component (cellulose) as wood pulp [12]. After the acceptance of the idea of macromolecules, the production of rayon was followed by the synthetic fibers such as acrylics, polyamide, polyester and polypropylene. From 1935 onwards, the possibility of spinning regenerated fibers from proteins was investigated [11]. The sources of the proteins include soy, corn, peanuts, wool and silk wastes, spider silk, hagfish slime, and even milk [13]. The thought was that these fibers would be more like wool than the regenerated celluloses [11]. In the 1950s, casein from milk was used by Courtaulds Ltd. to make Fibrolane and by Snia to make Lanital; peanut protein was used by ICI to make Ardil; Vicara was made by the Virginia-Carolina Chemical Corporation from zein (corn protein); and soybean protein fiber was developed by the Ford Motor Company [14], and there were trials of many waste products, such as egg albumin, chicken feather protein, gelatin and silk waste [11]. The important positive aspects of textile fabrics made from protein fibers are comfort, high moisture regain of 11–12%, a soft warm comfortable hand [15] which

are typical of the main protein fibers, wool and silk [14], and competitively priced renewable sources as starting materials [15]. They could be processed on conventional textile machinery and colored with conventional dyes. Superior to wool in some regards, they did not prickle, pill or shrink. They could be produced as staple or filament, crimped or straight, with control over diameter, and dope-dyed if required. Their drawback was poor mechanical strength when wet. Dry fiber strength was acceptable due to interchain hydrogen bonding between protein macromolecules. In the wet state, however, the fiber became weak as hydrogen bonding occurred preferentially with water molecules and the density of interchain covalent crosslinks was insufficient to impart strength.

These technical issues, rising raw material and production costs and the ascent of the petrochemical synthetic fibers, with their constant and consistent supply of materials and superior performance, caused production of regenerated protein fibers to stop in the late 1950s.

Nevertheless research efforts were continued. Today, concern for the environment, rising oil prices, and the finite nature of oil reserves is driving the research into ways to replace petrochemical products with biobased materials. Targets include bioplastics, films, packaging, building materials, and a range of other products including fibers. Developing biobased alternatives offers a potential of significant environmental benefits. A further driver comes from consumer demand, with growth of the ‘eco-friendly’ and ‘organic’ markets in textiles as well as food and other areas, reflecting the increased interest and power of consumers in biobased materials. Surveys show environmental compatibility is increasing as a sales argument as demonstrated by organic cotton fetching a premium price over the nonorganic fiber, even though they are physically indistinguishable.

The desire for such products has led to a renaissance in fibers such as hemp and the adoption of nontraditional fibers, such as bamboo, for use in apparel. Attempts are being made to use lignocellulosic agricultural byproducts such as cornhusks, cornstalks, and pineapple leaves as alternative sources of cellulosic fibers.

Also there are efforts to produce regenerated protein fibers [14]. In nature, there exists an incredible variety of proteins tailored and tailorable to purpose [11]. To make a protein fiber for today’s market would require the wet-strength problem to be solved. The application of advances made since the 1950s in cross-linking

technology and use of nanoparticle reinforcing agents [14] and bicomponent fiber production techniques [15] to regenerated protein fibers offer the potential of improving tensile strength. Further, since the 1950s new protein sources have become available as agricultural byproducts (e.g. keratin from feathers, gluten from wheat) with concomitant infrastructure for large-scale production [14].

It is unexpected that the regenerated protein fibers, which can be produced at an economic rate, can achieve the performance needed for mainstream textile use but there are opportunities in specialist areas, such as medical textiles with wound-healing or other desirable attributes, where their natural origin may be beneficial [11].

Recently, the development of protein-based materials has received much attention for application in biomedical and biotechnological fields, in particular for tissue engineering, medical implant devices, bioactive surfaces, etc. [16]. In this context, materials based on the silk protein fibroin, which is naturally biocompatible, biodegrable and mechanically superior, are promising candidates. Especially the availability of silk nanofibers with high surface area to volume ratio and highly porous three dimensional structure through a simple process of electrospinning introduces a new set of potential uses that previously were unattainable.

2.2 Silk

According to DIN 60001, silk is a natural fiber, classified under the term animal fibers [3]. Silks are fibrous proteins with remarkable mechanical properties produced in fiber form by spiders and silkworms [1]. They are produced by more than 30,000 known species of spider, and by most of the 113,000 species in the insect order *Lepidoptera*, which includes mites, butterflies and moths. For every silk that has been characterized in any detail, over 1,000 uncharacterized silks are known to exist [17]. They are synthesized in specialized epithelial cells that line glands in these organisms. Silks provide structural roles in cocoon formation, nest building, traps, web formation, safety lines and egg protection [1].

The best-known type of silk which is also the subject of this study is obtained from the cocoons of the larvae of the mulberry silkworm *Bombyx mori*. A silkworm

spinning to build its cocoon, finished cocoons and silk in degummed, reeled fiber form are seen in Figures 2.1 a, b, and c, respectively.

a.  b.  c. 

Figure 2.1 : a.Silkworm spinning to build its cocoon [18]; b.Cocoons [18]; c.Silk [19]

The silkworm eats mulberry leaves, which are converted by enzymes into two proteins as fibroin and sericin in its body and then drags out silk thread to make a cocoon in order to protect themselves during their metamorphosis into moths [12,20,21]. The fibrous protein termed fibroin forms the thread core, and glue-like proteins termed sericins surround the fibroin fibers to cement them together [20]. After the cocoon is finished, the pupa is killed prior to its emergence as a moth and then cocoons are carefully sorted to eliminate the stained, deformed, double or otherwise inadequate ones which are unfit for reeling before cooking [22]. In conventional processing of silk, the first operation is cooking, which consists of passing the dry cocoons through a series of wet processes designed to soften the sericin binding the thread together. Sericin is not removed completely as it is needed throughout the industrial processes of throwing and weaving. The cooked cocoons are brushed with a stiff rotating brush to find the end of the continuous filament which forms the cocoon. Filaments of several cocoons are combined into one yarn in the operation called reeling. Raw silk yarn is generally too fine to be woven with no twist, except for some special fabrics. Before weaving or knitting they are twisted (thrown) together to achieve the thickness of the yarn required. They can be woven or knitted on a wide variety of looms and knitting machines. Once the fabric has been woven or knitted, the sericin is removed by degumming which is a critical operation in the preparation of the fabric for further finishing [23].

Recently, there are new methods developed for processing of silk and silks are explored for an extended variety of biomedical applications including cell support matrixes, drug delivery carriers, wound dressings, bone tissue, cartilage tissue, ligament tissue, tendon tissue, hepatic tissue, connective tissue, endothelial and blood

vessel engineering, antithrombogenesis in many different morphological forms as films, sponges, hydrogels and nanowebs [1,2,20].

2.2.1 History of silk

The earliest evidence of silk was found at the sites of Yangshao culture in Xia County, Shanxi in China where a silk cocoon was found cut in half by a sharp knife, dating back to between 4,000 and 3,000 BCE. The species was identified as *Bombyx mori*, the domesticated silkworm. Scraps of silk were found in a Liangzhu culture site at Qianshanyang in Huzhou, Zhejiang, dating back to 2,700 BCE [24], by carbon-14 dating [3]. Legend has it that a Chinese princess, Xi Lin Shi, was drinking tea in a mulberry garden when a cocoon dropped into her cup. The hot tea dissolved the hard outer layer of the cocoon. In trying to extract it with her long fingernail, she discovered that the cocoon contained a continuous filament. As she kept pulling on the thread, it continued to unwind. The princess had just invented the first technique of reeling silk. At that time in China's history, weaving was already well-established, so it was possible to convert this new-found fiber into fabric. Although it is difficult to prove with certainty, it is highly likely that the discovery of silk went hand-in-hand with some important improvements in the technology of weaving. Archaeological discoveries in China, notably in Hubei province in 1982, have brought to light fragments of some highly elaborate fabrics, over 2,000 years old, which could only have been produced on sophisticated looms. These fabrics included chiffons, brocades, and gauzes and the majority of them were embroidered. If the discovery of silk really did lead to vast improvements in weaving it is because of a special characteristic of silk, namely that it is the only natural fiber in the form of a continuous filament.

The Chinese were quick to realise the potential of the extraordinary fiber and they took every precaution to make sure that the secret of its origin was carefully guarded and made the revelation of its derivation on offence punishable by death [23]. The use of silk was confined to China until the Silk Road opened at the latter half of the first millennium BCE [24]. Large amounts of silk were carried over the Silk Road from Shanxi to the Phoenician parts of the eastern Mediterranean, from where they were shipped to all major cities of the west [3]. Though silk was exported to foreign countries in great amounts, sericulture remained a secret that the Chinese guarded carefully for a long time.

Silk cultivation spread to Japan in around 300 CE, and by 522 the Byzantines managed to obtain silkworm eggs and were able to begin silkworm cultivation. The Arabs also began to manufacture silk during this same time. As a result of the spread of sericulture, Chinese silk exports became less important, although they still maintained dominance over the luxury silk market. The Crusades brought silk production to Western Europe, in particular to many Italian states, which saw an economic boom exporting silk to the rest of Europe. Changes in manufacturing techniques also began to take place during the Middle Ages, with devices such as the spinning wheel first appearing. During the 16th century France joined Italy in developing a successful silk trade, though the efforts of most other nations to develop a silk industry of their own were unsuccessful. The Industrial Revolution changed much of Europe's silk industry. Due to innovations in spinning cotton, it became much cheaper to manufacture and therefore caused more expensive silk production to become less mainstream. New weaving technologies, however, increased the efficiency of production. Among these was the jacquard loom, developed for silk embroidery. An epidemic of several silkworm diseases caused production to fall, especially in France, where the industry never recovered. In the 20th century Japan and China regained their earlier role in silk production, and China is now once again the world's largest producer of silk. The rise of new fabrics such as polyamide reduced the prevalence of silk throughout the world, and silk is now once again a somewhat rare luxury good [24].

2.2.2 Structure of Bombyx Mori silk

2.2.2.1 Chemical structure

All animal fibers have the same basic chemical structure units, polyamides, in spite of the fact that the fibers come from a variety of different animals. Wool is produced by sheep and silk by the silkworm or spider but their basic structure is the same, as represented in Figure 2.2 where the R1 and R2 groups are the amino acid residues [25].

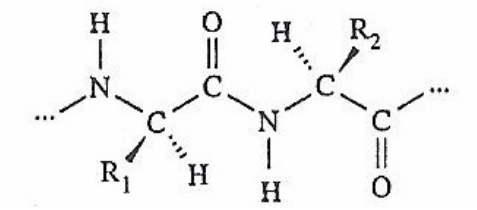

Figure 2.2 : Structure of natural proteins [25]

Silk fibers produced by cultivated silkworm *Bombyx mori* are composed of two protein groups, forming respectively the fibroin and the sericin [23]. They also contain minor amounts of residues of other amino acids and various impurities such as fats, waxes, dyes, and mineral salts [26]. Fibroin is the protein that forms the filaments of silkworm silk and gives silk its unique physical and chemical properties. Sericins are the group of gummy proteins which bind the fibroin filaments [17]. Depending on the cocoon strain, the fibroin content is 66.5-73.5%, and the sericin content is 26.5-33.5% by weight [26].

Fibroin is composed of polypeptide chains containing mostly non-polar amino acid residues, e.g about 44% glycine, 26% alanine and 12% serine with very low amounts of cysteine, acidic and basic amino acids [27]. In sericin, alanine and glycine together account for 15% of the total composition. The chief component of sericin is serine which makes up the 30% of the total [23]. Table 2.1 shows the chemical characteristics of silk fibroin compared to that of sericin, spider silk and wool keratin.

Table 2.1: Chemical structure of fibroin, sericin, spider silk and wool keratin

Type	Amino Acid	Side Group	Fibroin	Sericin	Spider Silk	Wool Keratin
Inert	Glycine	-H	43.70	13.90	37.10	8.40
	Alanine	-CH3	28.80	5.90	21.10	5.50
	Valine	$-CH(CH_3)_2$	2.20	2.70	1.80	5.60
	Leucine	$-CH_2CH(CH_3)_2$	0.50	1.10	3.80	7.80
	Isoleucine	$-CH(CH_3)CH_2CH_3$	0.70	0.70	0.90	3.30
	Phenylanine	$-CH_2C_6H_5$	0.60	0.50	0.70	2.80
Acidic	Aspartic Acid	$-CH_2COOH$	1.30	16.70	2.50	5.90
	Glutamic Acid	$-CH_2C_3COOH$	1.00	4.40	9.20	11.30
Basic	Lysine	$-(CH_2)_4NH_2$	0.30	3.30	0.50	2.60
	Arginine	$-(CH_2)_3NHC(NH)NH_2$	0.50	3.10	7.60	6.40
	Histidine	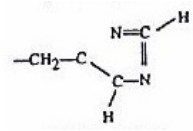	0.20	1.30	0.50	0.90
Hydroxyl	Serine	$–CH_2OH$	11.90	33.40	4.50	11.60
	Theronine	$-CH(OH)CH_3$	0.90	9.70	1.70	6.90
	Tyrosine	$-CH_2C_6H_4OH$	5.10	2.60	-	3.50
Ring	Proline	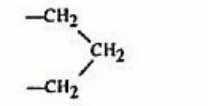	0.50	0.60	4.30	6.80
Double	Cystine	$-CH_2-S-S-CH_2-$	0.20	0.10	0.30	9.80
Other	Methionine	$-CH_2CH_2-S-CH_3$	0.10	0.04	0.40	0.40
	Tryptophan	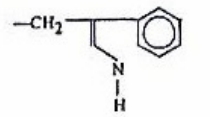	0.30	0.20	2.90	0.50

The primary structure of silk fibroin which mostly contains the amino acids of glycine, alanine, serine, in a specific repeating pattern [28] is represented in the Figure 2.3.

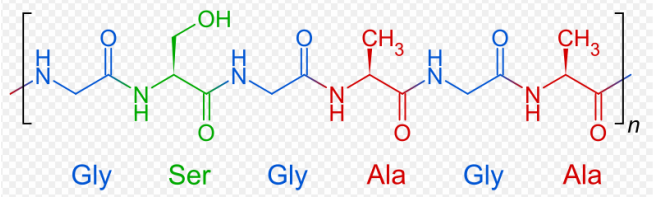

Figure 2.3 : Primary structure of silk fibroin [29]

This highly repetitive primary sequence leads to significant homogeneity in secondary structure [30].

Three main kinds of secondary structures such as random globules, α-helix (silk I) and β-sheet (silk II) are distinguished today. The α-helical structure is formed by intramolecular hydrogen bonds, with the hydrophobic fragments displaced to the periphery. In the β-sheet structure, the macromolecules are arranged in the paralel or antiparallel mode, forming a folded sheet.

Figures 2.4 and 2.5 show the projections of macromolecule segments forming the α-helical and β-sheet structures [26].

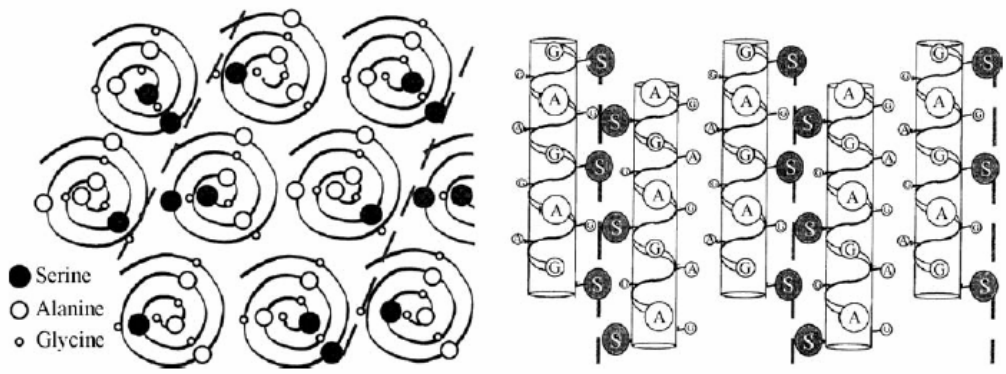

Figure 2.4 : α-helical structure of fibroin macromolecules [26]

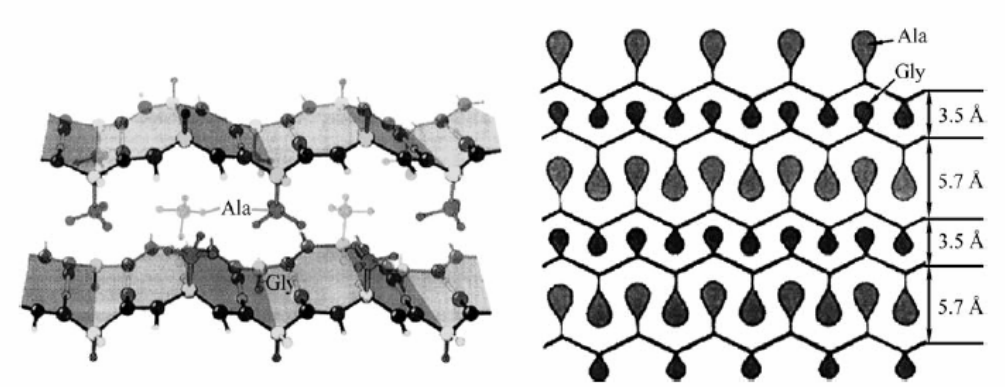

Figure 2.5 : β-sheet structure of fibroin macromolecules [26]

The fibroin macromolecules, generally take on a β-sheet secondary structure [31] due to the dominance of hydrophobic domains consisting of short side chain amino acids in the primary sequence. These structures permit tight packing of stacked sheets of hydrogen bonded anti-parallel chains of the protein. Large hydrophobic domains interspaced with smaller hydrophilic domains foster the assembly of silk and the strength and resiliency of silk fibers [1].

Antiparallel β-sheets of silk fibroin are packed in the face-to-face, back-to-back mode as represented in Figure 2.5. Double layer of glycine residues with an interplanar spacing 3.5A° and double layer of alanine/serine residues with an interplanar spacing 5.7A° forms the structure which is most favorable energetically for the hydrophobic fragments of macromolecules [26].

β-sheet structure together with α-helix form the crystalline areas whereas random globules form the amorphous areas in the silk fibroin. Fibroin of natural *Bombyx mori* fibers contains 56±5% macromolecules in the β-sheet form and 13±5% macromolecules in the α-helical form. Thus, the fraction of the crystalline areas of the polymer reaches to 60-70%. Liquid silk synthesized by the silkworm gland is a 26.0 vol% aqueous solution of fibroin in which the macromolecules have the conformation of globule or α-helix [26]. The organization of crystalline and amorphous regions is similar to that in cellulose-based natural fibers which can be depicted by a micellar model [25].

From the nineteenth century, attempts have been made to reproduce the qualities of natural silk. Although the chemical composition of silk is extremely well-known and the 'recipe' can be reproduced, no one has so far succeeded in spinning a continuous filament of natural silk. This is because the molecular organisation of the sericine-plus-fibroin combination is not the same when it is in the body of the silkworm and when it is extruded. For the time being, only *Bombyx mori* knows how to arrange the molecules into a continuous fiber [23]. The silkworm performs molecular orientation control very accurately by methods involving numerous sophisticated spinning technologies such as gel spinning, liquid crystal spinning, high speed spinning, self-exerted spinning, zone elongation and porous spinning, ion spinning, dry spinning, crimp spinning, and low energy spinning which cannot yet be duplicated by advanced arificial spinning technologies [17].

2.2.2.2 Physical structure

Silkworm fibers are naturally extruded from two silkworm glands as a pair of primary filaments (brin), which are stuck together with the sericin protein [32]. Thus, raw silk has a 'sheath-around-two-cores' composite structure**.** Anti-parallel β-sheet structure forming microfibrils is responsible for the crystalline nature of the silk fiber. The microfibrils are organized into fibril bundles, with several bundles leading to a single silk thread. The hierarchy of a fibroin filament, consisting of fibrils, microfibrils, and polymer molecules, is shown in Figure 2.6 [3].

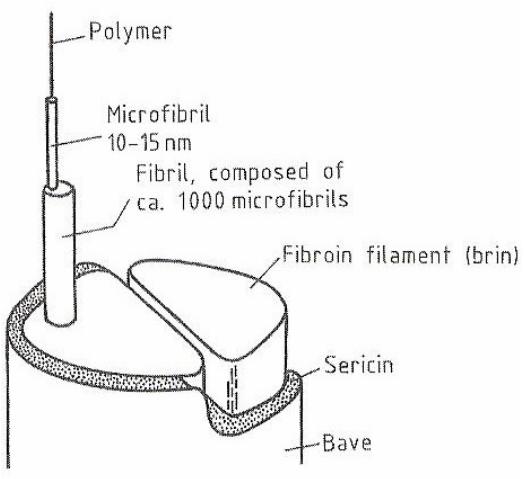

Figure 2.6 : Structure of silk [3]

The single filaments of degummed silk have round to trilobal cross-section [3] which is depicted in the SEM image in Figure 2.7.

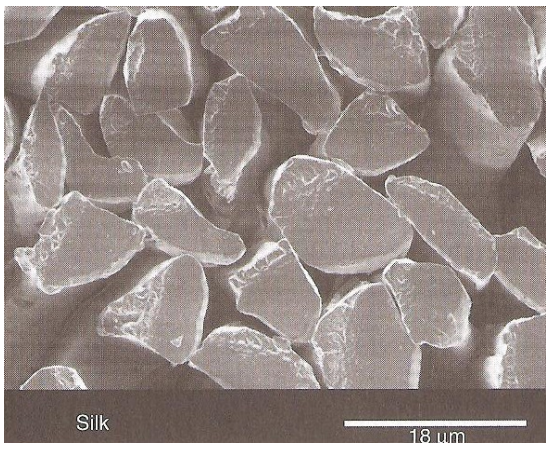

Figure 2.7 : SEM image showing cross-sectional shapes of mulberry silk fibers [22]

The fineness of the single filaments varies between 1 to 3.5 denier depending on their origin [3].The fineness of silk fiber can be seen in Table 2.2 in comparison with other fibers.

Table 2.2: Typical fiber deniers [25]

Fiber Type	**Denier**	**Within Sample CV**
Wool		
Minimum (Merino)	4	0.3
Maximum (carpet)	20	0.14
Vicuna	1.7	0.15
Chinese cashmere	1.8	0.19
Silk	1	
Cotton		
Minimum (St. Vincent Sea Island)	1	
Maximum (native Indian)	3	
Vicara	2.5	0.12
Synthetic		
Minimum (melt blown)	0.01	>1
Maximum (monofilament)	10000	
Typical apparel	0.9-3	0.12
Typical industrial	3	0.06
Typical carpet	6-20	0.12

The length of the filaments has reached to 1,600 metres today as a result of centuries of selection and development of the silkworm. In ancient times the yield is estimated to be between 100 and 150 metres per cocoon [23]. The length of silk can be seen in Table 2.3 in comparison with some other common fibers.

Table 2.3: Typical fiber lengths [25]

Fiber Type		Length (cm)
Cotton	Bengals	1.2-1.5
	American Uplands	1.9-3.0
	Egyptian Uplands	2.7-3.2
	Sea Islands	3.2-3.8
Other Vegetable	Flax	15-60
	Hemp	120-300
	Jute	150-360
Wood	Softwood	0.2-0.7
	Hardwood	0.1-0.3
Wool	Australian Merino (20μm diameter)	6.0-7.5
	Corriedale (30μm diameter)	7.5-9.0
	English Leicester (40μm diameter)	25-35
Mohair	Angora Goat	9-12
Silk	Cultured Silkworm	150,000

Under the microscope, silk has the apperance of a glass-like filament of uniform diameter which may bear striations along its length.

Silk fiber is smooth, unlike those of wool, cotton and other natural fibers. This is one of the reasons why silk fabrics are so lustrous and soft [23]. It has a high natural lustre and seen white in colour.

The density of silk is 1.32 g/cm³ [22].

2.2.3 Properties of Bombyx Mori silk

Cultivated silk from the *Bombyx mori* silkworm, which is and has always been the most common type of silk used, has a number of interesting and desirable properties that have been admired for over 5,000 years [33].

Silk is a natural fiber, in common with others such as cotton, wool, linen, cashmere, and mohair. Compared with other natural fibers, silk has certain specific characteristics which set it apart. First of all, it is the only natural fiber in the form of a continuous filament. All other natural fibers, wool, linen, cotton, cashmere, etc. have to be spun into a yarn from short fibers (This is also the way in which spun-silk is manufactured). Chemical fibers have made and continue to make enormous progress. They often possess characteristics which are far superior to those of silk, particularly in the field of washing and ironing. They even, in some cases, have the

appearance and the feel of silk. However, not one of the new fibers, for all their undoubted qualities, has so far succeeded in bringing together all the characteristics associated with silk [23].

Silks are remarkable materials in many respects [17].

Silk fiber from the *Bombyx mori* silkworm have a triangular cross section with rounded corners, 10-14 μm wide [3]. The triangular cross section gives it excellent light reflection capability [23] to reflect light at many angles, giving silk a natural shine. Silk has a smooth, soft texture that is not slippery, unlike many synthetic fibers [32].

Silks are a unique group of fibrous proteins with unusually high mechanical strength in fiber form [1]. Silk fiber from the *Bombyx mori* silkworm has a tenacity of approximately 4.8 grammes per denier which is slightly less than that of polyamide [17]. Part of the macromolecule is made up of amino acids with a low molecular weight, offering a series of crystalline regions which confer a high degree of tenacity on the fiber. The rest of the macromolecule is characterised by the presence of amorphous areas enclosing amino acids of a relatively higher molecular weight. The presence of both crystalline and amorphous zones makes for a combination of strength, flexibility and elasticity [23]. The elongation under the standard conditions is 17-25% [3]. Silk is relatively stiff and show good to excellent resiliency and recovery from deformation depending on the temperature and humidity conditions [22].

Silk is hygroscopic. Silk can absorb up to 30% of its weight in moisture without creating a damp feeling. Under normal atmospheric conditions silk absorbs 10% water based on the weight of water-free fiber. When moisture is absorbed it generates wetting heat which helps to explain why silk is comfortable to wear next to the skin [3,23].

Sunlight degrades silk rapidly [3].

Natural silk fibers dissolve only in a limited number of solvents, compared to globular proteins, because of the presence in fibroin of a large amount of intramolecular and intermolecular hydrogen bonds and its high crystallinity and specific physicochemical properties as wetting angle of 69°±3°.

Fibroin does not dissolve in water and in the majority of organic solvents, but only swells to 30-40%; 2/3 of the absorbed solvent is retained by the amorphous fraction of the polymer. The isoelectric point of fibroin varies in the range pH 3.6-5.2, depending on the conditions of solution preparation [26].

Silk, due to the virtual absence of cysteine, is not as resistant to acids as wool. However, the absence of alkali sensitive cysteine bridges gives silk a higher resistance to alkalis [3]. Silk is very resistant to organic solvents but soluble in hydrogen bond breaking solvents such as cupammonium hydroxide [22]. It dissolves in concentrated aqueous solutions of acids (phosphoric, formic, sulfuric, hydrochloric) and in concentrated aqueous, organic, and aqueous-organic solutions of salts [LiCNS, LiBr, $CaCl_2$, $Ca(CNS)_2$, $ZnCl_2$, NH_4CNS, $CuSO_4$+NH_4OH, $Ca(NO_3)_2$]. In concentrated solutions of acids, the fibroin macromolecules are solvated owing to strong ion-ion interaction, which becomes possible upon protonation of the amino and amide groups of the polymer. Dissolution in salt systems is due to interaction of solvent ions with functional groups of the fibroin macromolecules. The solvent ions interact with polar and charged groups of pendant chains of fibroin, breaking the hydrogen bonds between the macromolecules.

In some one-component organic solvents (e.g. hexafluoroisopropanol (HFIP), hexafluoroacetone (HFA)), fibroin can be dissolved only after its preliminary activation. The fibroin activation consists of the preliminary dissolution of the protein in an aqueous salt solution followed by dialysis of the solution and recovery of the polymer as a film or powder from aqueous solution by dry forming [26].

Strong oxidising agents such as hypochlorite will cause silk to rapidly discolour and dissolve, whereas reducing agents have negligible effect except under extreme conditions.

Silk exhibits favourable heat-insulating properties but owing to its moderate electrical resistivity, tends to build up static charge.

Unlike other natural fibers silk is more resistant to biological attack [22].

Silk is virtually unaffected by temperatures up to 140 ºC; above 150 ºC, thermal decomposition occurs [3].

Silk fiber also has some distinctive properties which make it suitable for biomedical applications such as wound healing, tissue engineering of bone, cartilage, tendon and

ligament tissues. The unique structure of silk, biocompatibility, versatility in processing, availability of different biomaterial morphologies, options for genetic engineering of variations of silks, the ease of sterilization, thermal stability, surface chemistry for facile chemical modifications to immobilize growth factors, and controllable degradation features make silk promising biomaterial for many clinical functions. Since the exploration of biomaterial applications for silks, aside from sutures, is only a relatively recent advance, the future for this family of structural proteins to impact clinical needs appears promising.

Silk biomaterials are biocompatible when studied *in vitro* and *in vivo*. Silk films implanted in vivo induced a lower inflammatory response than collagen films and poly (lactide) acid (PLA) films. Silk fibroin nonwoven mats implanted subcutaneously in rats induced a weak foreign body response and no occurrence of fibrosis. There was little upregulation of inflammatory pathways at the implantation site and no invasion by lymphocytes after six months *in vivo* [1].

Several primary cells have been successfully grown on different silk biomaterials to demonstrate a range of biological outcomes. Surface modification of silk fibroin biomaterials can be used to alter cell responses. Cell culture on silk-based biomaterials has resulted in the formation of a variety of tissues including bone, cartilage and ligament, both *in vitro* and *in vivo*. Silks can be chemically modified through amino acid side chains to alter surface properties or to immobilize cellular growth factors. Molecular engineering of silk sequences has been used to modify silks with specific features, such as cell recognition or mineralization.

The degradation of biomaterials is important in terms of restoring full tissue structure and function *in vivo*. Control over the rate of degradation is an important feature of functional tissue design, such that the rate of scaffold degradation matches the rate of tissue growth. According to the US Pharmacopeia an absorbable (suture) biomaterial is defined as one that 'loses most of its tensile strength within 60 days' post-implantation *in vivo*. Within this definition, silk is correctly classified as non-degradable since it retain more than 50% of its mechanical properties after two months of implantation *in vivo*. However, according to the literature, silk is degradable but over longer time periods due to proteolytic degradation usually mediated by a foreign body response. Several studies detail variable rates of silk absorption *in vivo* dependent on the animal model and tissue implantation site. In

general, silk fibers lose the majority of their tensile strength within 1 year *in vivo*, and fail to be recognized at the site within 2 years [1,30]. The degradability of silk biomaterials can be related to the mode of processing and the corresponding content of β-sheet crystallinity and can be altered by processing conditions. The rate of degradation depends upon the structure, morphology and mechanical and biological conditions at the location of implantation.

An important feature of silk as a biomaterial, compared with other fibrous proteins such as collagen, is the versatility of options for sterilization. Sterilization of silk fibroin scaffolds by autoclaving does not change morphology or β-sheet structure when heated to 120 °C. Comparatively, collagen denatures at these temperatures. Silk fibroin scaffolds can also be sterilized using ethylene oxide, g-radiation, or 70% ethanol [1].

2.2.4 Applications of silk

Silk has been primarily used in the textile industry due to its superior properties [17].

In its early days in China, even though some saw the development of a luxury product as useless, rules were used to regulate and limit its use to the members of the imperial family. For approximately a millennium, the right to wear silk was reserved for the emperor and the highest dignitaries. Later, it gradually extended to other classes of Chinese society. Silk began to be used for decorative means and also in less luxurious ways: musical instruments, fishing, and bow-making. Beginning in the 3rd century BCE paper, which is one of the greatest discoveries of ancient China, was made in all sizes with various materials including silk and paper made with silk became the first type of luxury paper [32].

Sutures braided from silk fibers which are obtained by reeling from cocoons have been used for centuries in gummed and degummed forms as sutures for surgical options [1].

Today the uses of silk cover a wide range of applications from ready-to-wear articles and home textiles to technical fabrics. Ready-to-wear articles include mainly mens' and womens' wear such as shirts, blouses, scarves, shawls, ties, formal dresses and high-quality evening clothes as well as lining materials, underwear, pyjamas, robes, night clothes, national dresses as kimonos and sarongs. Its' absorbency makes it comfortable to wear in warm weather and while active. Its low conductivity keeps

warm air close to the skin during cold weather. In home textiles, silk is most often used for furnishing fabrics, upholstery, wallpaper, velvet, plush, carpets, rugs, bedding, wall hangings and covers. Its' attractive luster and drape makes it suitable for many furnishing applications. In technical fabrics, silk is employed for typewriter ribbon, insulating material for cable covering, and surgical articles. Silk is also a very suitable material for sewing and embroidery thread because it can be dyed to give any shade [3].

Recently, silks from silkworms (e.g., *Bombyx mori*) and orb-weaving spiders (e.g., *Nephila clavipes*) have been explored to understand the processing mechanisms and to exploit the properties of these proteins for use as biomaterials. Biomaterial design is an important element of tissue engineering, incorporating physical, chemical and biological cues to guide cells into functional tissues via cell migration, adhesion and differentiation. Many biomaterials need to degrade at a rate commensurate with new tissue formation to allow cells to deposit new extracellular matrix (ECM) and regenerate functional tissue. In addition, biomaterials may need to include provisions for mechanical support appropriate to the level of functional tissue development. In general, biomaterials must be biocompatible and elicit little to no host immune response. Thus, silks have been investigated as biomaterials due to the successful use of silk fibers from *B. Mori* as suture material for centuries. Silks represent a unique family of structural proteins that are biocompatible, degradable, mechanically superior**.**

Silk fibroin is purified from sericins via boiling in an alkaline solution. As represented in Figure 2.8 the degummed or purified silk fibers can be processed into silk cords by twisting, non-woven silk mats by partial solubilization, or dissolved in concentrated salt solutions, dialysed and formed into aqueous silk fibroin solution for preparation of other materials as represented in Figure 2.9.

Silk proteins can be processed into a diverse set of morphologies such as films, hydrogels, sponges, and nanoscale electrospun webs from aqueous or solvent formulations of silk fibroin for utilization in biomedical and biotechnological applications such as tissue scaffolds, biocompatible coatings, drug delivery, biomineralization, solid supports for catalysts, etc. [1,21].

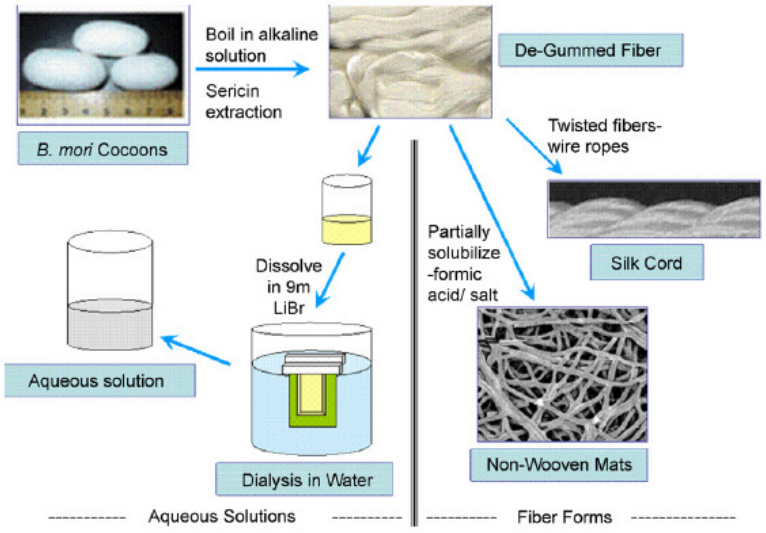

Figure 2.8 : Processing of silk fibroin [1]

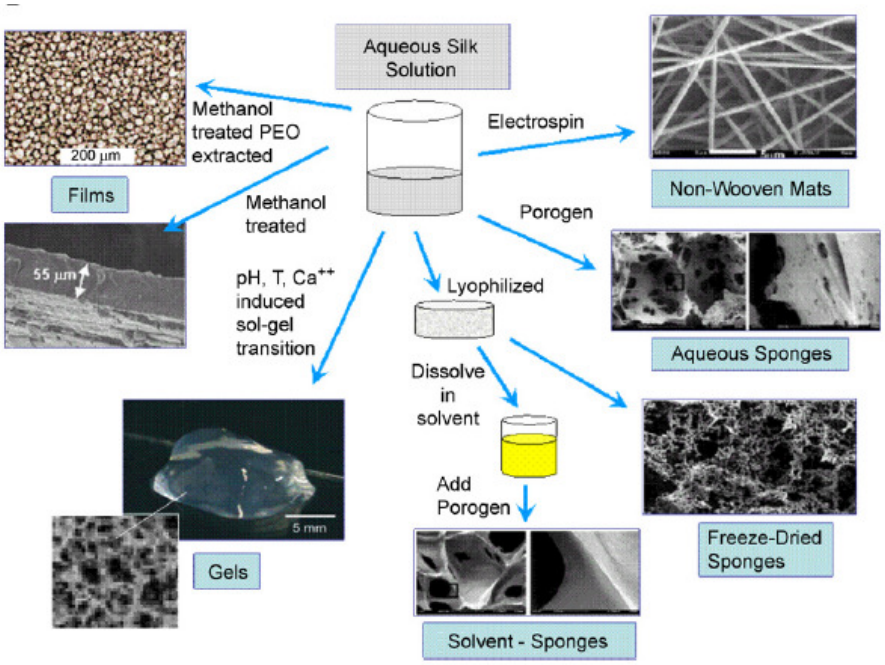

Figure 2.9 : Processing of silk morphologies from aqueous silk fibroin solution [1]

The complex secondary molecular structure of silks can be used to control specific interactions in different chemical and mechanical environments. The presence and amounts of particular secondary structure (silk I, silk II, α-helical or random coil) of silk fibroin can be modified and controlled through stretching, compression, or with chemical and annealing treatments. These conformational changes can be utilized in the formation of membranes of stable, thin films for a variety of barrier applications [17]. Films are generally prepared by casting solutions of silk proteins onto a

substrate and allowing the evaporation of the solvent. Once the solvent has evaporated, the films can be peeled off for further use, modified chemically (e.g. cross-linked), or modified structurally via treatment with another solvent [21]. Silk fibroin films have been cast from aqueous or organic solvent systems, as well as after blending with other polymers**.** Silk films prepared from aqueous silk fibroin solution had oxygen and water vapor permeability dependent on the content of silk I and silk II structures. Alteration of silk structure was induced by treatment with 50% methanol for varying times. Changes in silk structure resulted in differing mechanical and degradability properties of the films. Nanoscale silk fibroin films can also be formed from aqueous solution using a layer-by-layer technique. These ultrathin films were stable due to hydrophobic interactions and predictable film thickness could be obtained based on control of solution conditions. Fibroblast attachment to silk films has been shown to be as high as for collagen films. Other mammalian and insect cells also showed good attachment on silk fibroin films when compared with collagen films [1].

It has proven possible to prepare artificial blood vessels by coating steel wires with porous films of *B. mori* fibroin, and subsequently removing the wire template. Porous films were prepared by casting aqueous solutions of *B. mori* fibroin and polyethylene oxide (PEO) which is a fibroin immiscible porogen. Treatment of the films with aqueous methanol induces β-sheet formation and the PEO could subsequently be washed away with water yielding porous films. The level of porosity was controlled by varying the ratio of fibroin to PEO, and the diameter of the fibroin-based vessels was determined by that of the wire template. Low porosity microtubes demonstrated superior mechanical properties in terms of higher burst pressures, but displayed poor protein and cell permeability; whereas higher porosity tubes had lower burst strengths but increased permeability and enhanced protein and cell permeability [21].

Hydrogels are three-dimensional polymer networks which are physically durable to swelling in aqueous solutions but do not dissolve in these solutions. Hydrogel biomaterials provide important options for the delivery of cells and cytokines. Silk fibroin hydrogels have been prepared from aqueous silk fibroin solution. The pH of the silk fibroin solution impacted the rate of solution gelation. Other factors important in gelation included silk polymer concentration and Ca^{++}. An increase in

silk fibroin concentration, increase in temperature, decrease in pH and an increase in Ca^{++} concentration decreased the time of silk fibroin gelation. Hydrogel pore size was controllable based on silk fibroin concentration and temperature [1].

B. mori fibroin hydrogels have been used as a scaffold for human mesenchymal stem cells hMSC growth *in vitro*. The cells were able to grow, proliferate and survive for weeks in static culture conditions. Similarly, *B. mori* fibroin hydrogels have been used as scaffolds for bone tissue growth both *in vitro* and *in vivo* in rabbits without inflammatory effects [21].

Hydrogels formed from *B. mori* fibroin were demonstrated to control the release of model drugs with molecular weights ranging from ca. 350 Da to 4.5 kDa, and of buprenorphine (a morphine-like drug used in the treatment of acute pain) *in vitro*. Tuning of the gels' mechanical properties and rate of drug release was achieved simply by varying the concentration of fibroin. Hydrogels formed from engineered proteins based upon *B. mori* fibroin were demonstrated to similarly control the release of model drugs with molecular weights ranging from ca. 400 Da to 500 kDa, and of Pantarin (a mitotoxic protein) *in vivo* in guinea pigs, with no clinical signs of tissue reaction due to allergy, irritancy or toxicity after 28 days [21].

Porous sponge scaffolds are important for tissue engineering applications for cell attachment, proliferation, and migration, as well as for nutrient and waste transport. Regenerated silk fibroin solutions, both aqueous and solvent, have been utilized in the preparation of porous sponges. Sponges have been formed using porogens, gas foaming and lyophilization [1].

Sponges prepared from *B.mori* fibroin have been used as scaffolds for the attachment and proliferation of fibroblasts *in vitro*. It was observed that cell colonies were located preferentially at the surface of the foam, potentially due to the cell-seeding process, and/or lack of nutrients inside the sponge. Sponges seeded with hMSCs in chondrogenic medium formed cartilage-like tissue, whereas those in osteogenic medium formed bone-like tissue. Importantly, sponges seeded with adipose derived stem cells formed adipose-like tissue *in vivo* in rats.

Sponges prepared via freeze-drying the aqueous solutions of *B. Mori* fibroin and aspirin were demonstrated to be capable of controlled release of the aspirin trapped in the scaffold. Preliminary *in vitro* kinetic studies showed a burst release profile for

the aspirin, with a significant quantity of aspirin released in the first 2 h, followed by an almost constant rate of release thereafter [21].

Non-woven mats are of interest as biomaterials due to the increased surface area and rougher topography for cell attachment. Silk fibroin has been used to generate nanowebs from reprocessed native silk fibers or by electrospinning for use in biomedical applications as tissue scaffolding, drug delivery, medical prostheses, wound healing.

Fibers electrospun from aqueous solutions of *B. mori* fibroin and PEO were used as a scaffold for human aortic endothelial cells (HAECs) and human coronary artery smooth muscle cells (HCASMCs); in both cases *in vitro* culture in endothelial growth medium led to the formation of vascular tissues within a week.

Fibers electrospun from aqueous solutions of *B. mori* fibroin, PEO and bone morphogenetic protein-2 (BMP-2) were used as a scaffold for human mesenchymal stem cells hMSCs; *in vitro* culture in osteogenic media led to the formation of bone-like tissue. Addition of hydroxyapatite nanoparticles to the fibroin solution prior to electrospinning produced fibers with the nanoparticles embedded inside and was found to improve bone formation. *In vivo* implantation of electrospun *B. mori* fibroin fibers in calvarial defects in mice facilitated the complete healing of the defect with new bone within 12 weeks [21].

Schneider *e. al*. (2008) developed biofunctionalized electrospun silk mats as a topical bioactive dressing for accelerated wound healing. They produced nanowebs, made of electrospun nanoscale silk fibers containing epidermal growth factor (EGF), for the promotion of wound healing processes through acceleration of reepithelialization. They demonstrated that EGF is incorporated into the nanoweb and slowly released in a time-dependent manner (25% EGF release in 170 h) and when placed on the wounds as a dressing, aided the healing by increasing the time of wound closure by the epidermal tongue by 90%. The preservation of the structure of the nanowebs during the healing period as demonstrated by electronic microscopy, the biological action of the dressing, as well as the biocompatibility of the silk demonstrate that this biomaterial is a new and very promising material for medical applications, especially for patients suffering from chronic wounds [34].

2.3 Electrospinning Process

The process of spinning fibers with the help of electrostatic forces is known as electrospinning [35].

Electrospinning is an old polymer processing technique that has recently been rediscovered. It allows for the easy creation of nano-to-micro fibers that can be collected to form a non-woven structure, which is interchangeably called nanofiber membrane, nanofiber mesh or nanoweb [36].

Besides electrospinning, there are some other techniques like drawing, template synthesis, phase separation and self-assembly which can be used to produce polymeric nanofibers but electrospinning has gained much more attention in the last decade not only due to its versatility in spinning a wide variety of polymeric fibers but also due to its consistency in producing fibers in the submicron range. It seems to be the only method which can be further developed for mass production of one-by-one continuous nanofibers from various polymers [7,35,37].

In fiber science related literature, fibers with diameters below 100 nm are generally classified as nanofibers. In recent times, nanofibers have attracted the attention of researchers due to their pronounced micro and nano structural characteristics that enable the development of advanced materials that have sophisticated applications. More importantly, high surface area, small pore size, and the possibility of producing three dimensional structures have increased the interest in nanofibers. These fibers, with smaller pores and higher surface area than regular fibers, have enormous applications in nanocatalysis, tissue scaffolds, protective clothing, filtration, and optical electronics [35].

2.3.1 History of electrospinning

The first documented accounts of electrostatic spinning of a polymer solution into nanofibers were described in 1902 by J. F. Cooley and W. J. Morton [38]. In his patent entitled ‘Apparatus for electrically dispersing fibres’(US 692631) Cooley describes a method of using high voltage power supplies to generate yarn. Even at this early stage it was recognised that to form fibers rather than droplets the (i) fluid must be sufficiently viscous, (ii) solvent volatile enough to evaporate to allow

regeneration of the solid polymer, and (iii) electric field strength within a certain range [39].

In 1914, John Zeleny, published work on the behaviour of fluid droplets at the end of metal capillaries. His effort began the attempt to mathematically model the behaviour of fluids under electrostatic forces [40].

Further developments toward commercialisation were made by Anton Formhals, and described in a sequence of patents from 1934 to 1944 for the fabrication of continuous fine fibers using an electrostatic force [8,39].

Formhals's first invention consisted of a movable thread collecting device to collect the threads in a stretched condition, like that of a spinning drum in the conventional spinning. Formhals's process was capable of producing threads aligned parallel on to the receiving device in such a way that it can be unwound continuously. In his first patent, Formhals reported the spinning of cellulose acetate fibers using acetone as the solvent [35]. Cellulose acetate, was introduced into the electric field. The polymer filaments were formed, from the solution, between two electrodes bearing electrical charges of opposite polarity. One of the electrodes was placed into the solution and the other onto a collector. Once ejected out of a metal spinnerette with a small hole, the charged solution jets evaporated to become fibers which were collected on the collector [37]. This first spinning method adopted by Formhals had some technical disadvantages. It was difficult to completely dry the fibers after spinning due to the short distance between the spinning and collection zones, which resulted in a less aggregated web structure. In a subsequent patent, Formhals refined his earlier approach to overcome the aforementioned drawbacks. In the refined process, the distance between the feeding nozzle and the fiber collecting device was altered to give more drying time for the electrospun fibers. Subsequently in 1940, Formhals patented another method for producing composite fiber webs from multiple polymer and fiber substrates by electrostatically spinning polymer fibers on a moving base substrate [35].

Gladding also proposed the use of the process to produce staple fibers [39].

Electrospinning from a melt rather than a solution was patented by C.L. Norton in 1936 using an air-blast to assist fiber formation [40].

In 1938 N. D. Rozenblum and I. V. Petryanov-Sokolov, generated electrospun fibers, which they developed into filter materials known as "Petryanov filters". By 1939, this work had led to the establishment of a factory in Tver' for the manufacture of electrospun smoke filter elements for gas masks. The material, dubbed BF (Battlefield Filter) was spun from cellulose acetate in a solvent mixture of dichloroethane and ethanol [40]. The communistic government installed several factories starting from the year 1940 in the USSR. By 1960, the output of spun filtration material in these factories was claimed as 20 million m² per year. Some of these factories still exist and still produce Petryanov filters [41].

In 1966**,** Simons patented an apparatus for the production of non-woven fabrics of ultra thin and very light in weight with different patterns using electrical spinning. The positive electrode was immersed into the polymer solution and the negative one was connected to a belt where the non-woven fabric was collected. He found that the fibers from low viscosity solutions tended to be shorter and finer whereas those from more viscous solutions were relatively continuous [37].

Between 1964 and 1969 Sir Geoffrey Ingram Taylor produced the theoretical underpinning of electrospinning [39]. He studied the shape of the polymer droplet produced at the tip of the needle when an electric field is applied and showed that it is a cone and the jets are ejected from the vertices of the cone. This conical shape of the jet was later referred to by other researchers as the 'Taylor Cone' in subsequent literature. By a detailed examination of different viscous fluids, Taylor determined that an angle of 49.3 degrees is required to balance the surface tension of the polymer with the electrostatic forces. The conical shape of the jet is important because it defines the onset of the extensional velocity gradients in the fiber forming process [35]. Taylor also observed the emission of a fiber jet from the apex of the cone, which explained the generation of fibers with significantly smaller diameters compared to the spinneret [5].

In subsequent years, focus shifted to studying the structural morphology of nanofibers. Researchers were occupied with the structural characterization of fibers and the understanding of the relationships between the structural features and process parameters. Wide-angle X-ray diffraction (WAXD), scanning electron microscopy (SEM), transmission electron microscopy (TEM), and differential scanning calorimetry (DSC) have been used by researchers to characterize electrospun

nanofibers [35]. In 1971, Baumgarten investigated the effect of varying certain solution and processing parameters (solution viscosity, applied voltage, etc.) on the structural properties of electrospun fibers [42]. Baumgarten reported the electrospinning of acrylic microfibers whose diameters ranged from 500 to 1,100 nm. Baumgarten determined the spinability limits of a polyacrylonitrile/ dimethylformamide (PAN/DMF) solution and observed a specific dependence of fiber diameter on the viscosity of the solution. He showed that the diameter of the jet reached a minimum value after an initial increase in the applied field and then became larger with increasing electric fields. Larrondo and Mandley produced polyethylene and polypropylene fibers from the melt, which were found to be relatively larger in diameter than solvent spun fibers. They studied the relationship between the fiber diameter and melt temperature and showed that the diameter decreased with the increasing melt temperature [35].

Around this same time period others were beginning to examine the potential applications of electrospun fibrous mats in fields such as tissue engineering. In 1978, Annis and Bornat published work examining electrospun polyurethane mats for use as vascular prosthesis. As early as 1985, Fisher and Annis were examining the long-term *in vivo* performance of an electrospun arterial prosthesis [42].

In 1987, Hayati et al. studied the effects of electric field, experimental conditions, and the factors affecting the fiber stability and atomization. They concluded that liquid conductivity plays a major role in the electrostatic disruption of liquid surfaces. Results showed that highly conducting fluids with increasing applied voltage produced highly unstable streams that whipped around in different directions. Relatively stable jets were produced with semi conducting and insulating liquids, such as paraffinic oil. Results also showed that unstable jets produce fibers with broader diameter distribution [35].

In the early 1990s several research groups demonstrated that many organic polymers could be electrospun into nanofibers. Since then, the number of publications about electrospinning has been increasing exponentially every year [40].

First paper ‘Electrospinning process and applications of electrospun fibers’ was published by Darrel H. Reneker in 1993 and the word ‘electrospinning’ deriving from ‘electrostatic spinning’ was first used in this paper [39].

In 1996, a very important paper 'Nanometer diameter fibres of polymer, produced by electrospinning' was published by Reneker, which created a new era in electrospinning research. Before 1997, only Reneker had published several papers about electrospinning. After 1997, more and more researchers began to research electrospinning. However, only few papers had been published until 2000 [43].

Huang and co-workers noted that between 1995 and 2000 fewer than 10 journal papers were published annually, but from 2000 onwards the number of papers per year grew, reaching over 800 by 2008 and reflecting the growing interest in electrospinning by, at least, the academic community [39].

Using the keyword 'electrospinning' for a search in a scientific database (Compendex) returns about 1,400 papers (search performed 20/10/2010).

Figure 2.10 demonstrates the recent strong growth in this area by plotting the number of scientific papers on the subject published per year.

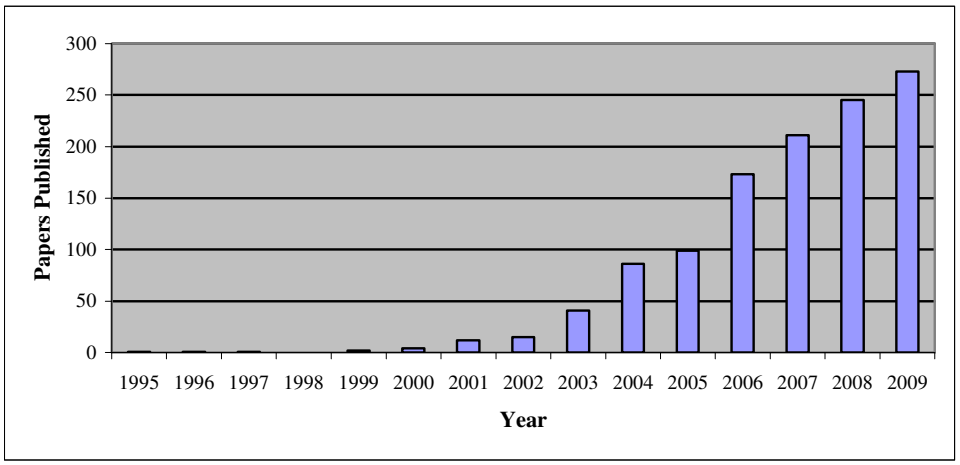

Figure 2.10 : Number of papers with the keyword 'Electrospinning' in a given year

Figure 2.11 shows which countries are most active in electrospinning research applications with the numbers obtained in 25/11/2008 [39]. The position of Turkey can also be seen in the figure.

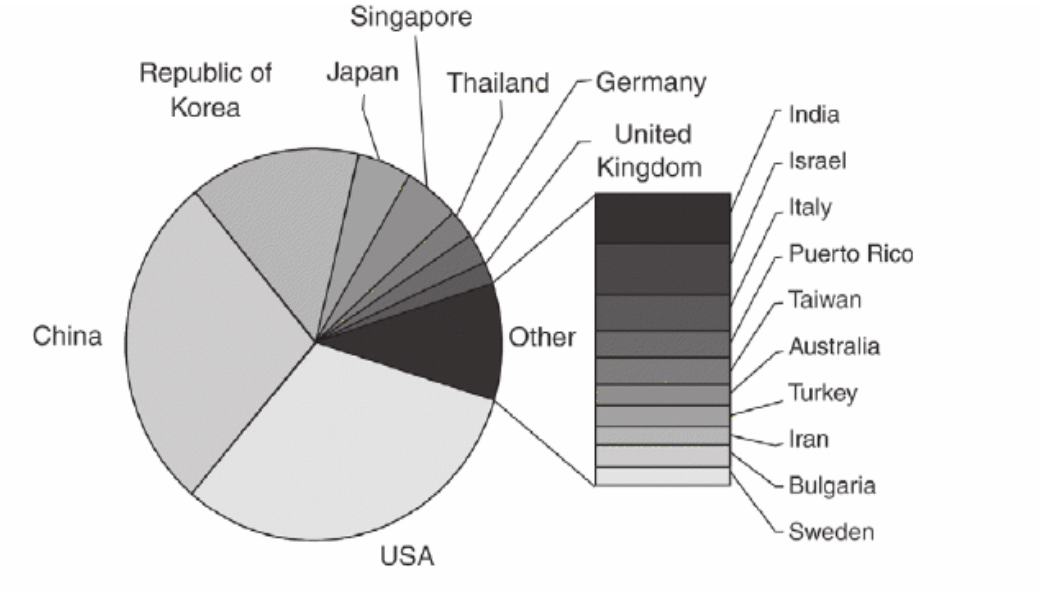

Figure 2.11 : Country of origin for papers containing keyword 'electrospinning' [39].

The popularity of the electrospinning process can also be realized by the fact that over 200 universities and research institutes worldwide are studying various aspects of the electrospinning process and the fiber it produces and also the number of patents for applications based on electrospinning has grown in recent years [7].

2.3.2 Principles of electrospinning

Electrospinning is a process that creates nanofibers through an electrically charged jet of polymer solution or polymer melt [7].

The apparatus used for electrospinning is simple in construction, which consists of a high voltage electric source with positive or negative polarity, a syringe pump with capillaries or tubes to carry the solution from the syringe or pipette to the spinnerette, and a conducting collector. Many researchers use an apparatus similar to the one given in Figure 2.12 with modifications depending on process conditions to spin a wide variety of fine fibers [35].

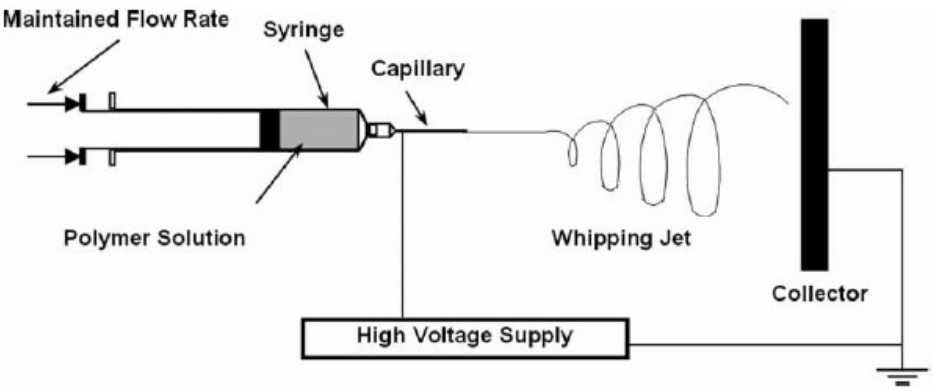

Figure 2.12 : Schematic diagram for parallel electrospinning setup [44].

Polymer solution or the melt that has to be spun is forced through a syringe pump to form a pendant drop of the polymer at the tip of the capillary. High voltage potential is applied to the polymer solution inside the syringe through an immersed electrode, thereby inducing free charges into the polymer solution. These charged ions move in response to the applied electric field towards the electrode of opposite polarity, thereby transferring tensile forces to the polymer liquid. At the tip of the capillary, the pendant hemispherical polymer drop takes a cone like projection in the presence of an electric field. And, when the applied potential reaches a critical value required to overcome the surface tension of the liquid, a jet of liquid is ejected from the cone tip. After the initiation from the cone, the discharged polymer solution jet undergoes an instability and elongation process, which allows the jet to become very long and thin and is field directed towards the oppositively charged collector [7,37]. As the jet travels through the atmosphere, the solvent evaporates, leaving behind a dry fiber on the collecting device, which collects the charged fibers as nanoweb [35,45]. For low viscosity solutions, the jet breaks up into droplets, while for high viscosity solutions it travels to the collector as fiber jets.

In electrospinning, the spinning of fibers is achieved primarily by the tensile forces created in the axial direction of the flow of the polymer by the induced charges in the presence of an electric field [35].

Important features of electrospinning are:

• Suitable solvent should be available for dissolving the polymer.

• The vapor pressure of the solvent should be suitable so that it evaporates quickly enough for the fiber to maintain its integrity when it reaches the target but not too quickly to allow the fiber to harden before it reaches the nanometer range.

• The viscosity and surface tension of the solvent must neither be too large to prevent the jet from forming nor be too small to allow the polymer solution to drain freely from the pipette.

• The power supply should be adequate to overcome the viscosity and surface tension of the polymer solution to form and sustain the jet from the pipette

• The gap between the pipette and grounded surface should not be too small to create sparks between the electrodes but should be large enough for the solvent to evaporate in time for the fibers to form.

Although electrospinning is a very simple process, requiring just simple laboratory equipment to yield fibers down to the nanoscale, the science behind it is not simple at all. Electrospinning process involves the understanding of electrostatics, fluid rheology and polymer solution properties such as rate of solvent evaporation, surface tension and solution conductivity. These fundamental properties are constantly interacting and influencing each other during the electrospinning process [7].

2.3.3 Polymers used in electrospinning

There are a wide range of polymers that are used in electrospinning and are able to form fine nanofibers within the submicron range used for varied applications [8].

Electrospun nanofibers have been reported as being from various synthetic nonbiodegradable materials such as polyesters, polyamides, polyurethanes, polycarbonates, polysulfones, etc., synthetic biodegradable materials such as polyglycolic acid, polycaprolactone, polylactic acid, polylactide-co-glycolide, etc., and natural materials such as collagen, gelatin, elastin, chitin, chitosan, alginate and hyaluronic acid, dextran, silk, protein, etc. Also, it is possible to incorporate electronic, magnetic, optical, and biological materials into the polymer to obtain multifunctional nanowebs. Over the years, more than 200 polymers have been electrospun successfully from several polymers and characterized with respect to their applications [8]. Polymers with attractive chemical, mechanical, and electrical properties like high conductivity, high chemical resistance, and high tensile strength

have been spun into ultrafine fibers by the electrospinning process, and their application potential in different areas like filtration, optical fibers, drug delivery systems, tissue scaffolds, and protective textiles have been examined [35].

Some of the polymers attempted to-date for electrospinning are tabulated in Table 2.4 with the solvents used, fiber diameters achieved and application perspectives.

Table 2.4: Some of the polymers used in electrospinning [8]

Polymers	Solvents	Fiber Diameter	Applications
Silk firoin / PEO	Water	590 ± 60	Bone tissue engineering
Gelatin	Acetic / Formic acid	109-761	Biomaterial scaffold
Collagen Type I	HFIP	100-600	Materials science and engineering
Collagen Type II	HFIP	496	Cartilage engineering
Gelatin / PVA	Formic acid	133-447	Controlled release of drugs
Chitosan	Acetic acid	130	Biomedical applications
PVA	Water	250-300	Drug delivery
Chitosan / PVA	Formic acid, TFA, HCl	330	Tissue engineering
Cellulose acetate	Acetone, DMF, Trifluoroethylene (3:1:1)	200-1000	Filtration
HA / Gelatin	DMF/ Water	190-500	Tissue engineering
Fibrinogen	HFIP	80 ± 30	Wound repair
Polyamide-6	m-Cresol Formic acid	98.3 ± 8.2	Biomedical applications
Polyurethane	Water	100-500	Tissue engineering
Polycaprolactone	DMF Methylene chloride	200	Wound healing
Collagen / chitosan	HFIP / TFA	300-500	Biomaterial scaffolds
Chitin	HFIP	163	Wound healing
PCL / Gelatin	TFE	470 ± 120	Wound healing
Polyaniline / Gelatin	HFIP	61 ± 13	Tissue engineering

2.3.4 Solvents used in electrospinning

Although molten polymers can be electrospun, it is more common to electrospin using polymer solution [7]. The solvent used in preparing polymer solutions has a significant influence on its spinnability. Basically, a solvent performs two crucial roles in electrospinning. Firstly to dissolve the polymer molecules for forming the electrified jet and secondly to carry the dissolved polymer molecules towards the collector. In Table 2.5, some solvents used in electrospinning and their properties

such as surface tension, dielectric constant and boiling point that should be kept in mind during the selection for electrospinning process are shown.

Table 2.5: The list of typical solvents used in the electrospinning process [8]

Solvents	Surface Tension (mN/m)	Dielectric Constant	Boiling Point °C	Density (g/mL)
Chloroform	26.5	4.8	61.6	1.498
Dimethyl formamide	37.1	38.3	153.0	0.994
Hexafluoro isopropanol	16.1	16.7	16.7	1.596
Tetrahydrofuran	26.4	7.5	7.5	0.886
Trifluoro ethanol	21.1	27.0	27.0	1.393
Acetone	25.2	21.0	21.0	0.786
Water	72.8	80.0	80.0	1.000
Methanol	22.3	33.0	33.0	0.791
Acetic acid	26.9	6.2	6.2	1.049
Formic acid	37.0	58.0	58.0	1.210
Dichloro methane	27.2	9.1	9.1	1.326
Ethanol	21.9	24.0	24.0	0.789
Tri fluoro acetic acid	13.5	8.4	8.4	1.525

The properties of solvents besides determining the spinability have a profound effect on fiber diameter. Various research groups have investigated the effect of solvents namely, chloroform, ethanol, dimethylformamide (DMF), mixture of tri-fluoroacetic acid and dichloromethane and water for electrospinning of poly (ethylene oxide) (PEO), polystyrene (PS) and poly (ethylene terephthalate) (PET) and showed the effect of solvent properties and polymer concentration on the morphology, structure, and mechanical and thermal properties while electrospinning. Thus the selection of an appropriate solvent system is indispensable for successful electrospinning [8].

2.3.5 Parameters that affect the electrospinning process

The electrospinning process is governed by many parameters, classified broadly into solution parameters, process parameters, and ambient parameters. Solution parameters include concentration, molecular weight, viscosity, surface tension, conductivity, polymer solubility and process parameters include applied voltage, tip to collector distance, type of collector, diameter of needle and feeding or flow rate.

In addition to these variables, ambient parameters encompass the humidity and temperature of the surroundings which play a significant role in determining the morphology and diameter of electrospun nanofibers.

Each of these parameters significantly affect the fibers' morphology obtained. With the understanding of these parameters, it is possible to come out with setups to yield fibrous structures of various forms and arrangements. It is also possible to create nanofibers of desired morphology and diameters by the proper manipulation of these parameters [7,8]. An optimal combination of these electrospinning parameters establish conditions to generate fibers with narrow variations in diameter and absence of beads [5].

2.3.5.1 Solution parameters

In order to carry out electrospinning, the polymer must first be in a liquid form, either as molten polymer or as polymer solution. The property of the solution plays a significant part in the electrospinning process and the resultant fiber morphology. The concentration, electrical property, surface tension and viscosity of the solution will determine the amount of stretching of the solution which will in turn have an effect on the diameter of the resultant electrospun fibers. The rate of evaporation will also have an influence on the viscosity of the solution as it is being stretched. The solubility of the polymer in the solvent not only determines the viscosity of the solution but also the types of polymer that can be mixed together [7].

Concentration

In the electrospinning process, for fiber formation to occur, a minimum solution concentration is required [8]. In other words solution concentration determine the 'spinnability' of the solution. If the solution is too dilute, the fiber breaks into microsize droplets before reaching the collector as a result of varicose jet instability and the phenomenon of electrospraying is observed instead of electrospinning. Electrospray is also observed when a polymer solution with low molecular weight is used [5]. If a solution with low concentration is used, a mixture of beads and fibers is obtained and as the solution concentration increases, the shape of the beads changes from spherical to spindle-like and finally uniform fibers with increased diameters are formed because of the higher viscosity resistance [8]. However, if the solution is too concentrated, it will be difficult for the polymer solution to flow through the

capillary due to high viscosity, therefore no fiber will form [5]. There should be an optimum solution concentration for the electrospinning process. Solution surface tension and viscosity play important roles in determining the range of concentrations from which continuous fibers can be obtained in electrospinning [8].

In many experiments it has been shown that within the optimal range of polymer concentrations fiber diameter increases with increasing polymer concentration. Megelski *et al*. found that by increasing the concentration of polystyrene in tetrahydrofuran (THF) the fiber diameter increased and the distribution of pore sizes became narrower. Deitzel *et al*. found that fiber diameter of fibers electrospun from PEO/water solution were related to PEO concentration by a power law relationship [42].

Another effect of higher concentration is seen by a smaller deposition area. Increased concentration means that the viscosity of the solution is strong enough to discourage the bending instability to set in for a longer distance as it emerges from the tip of the needle. As a result, the jet path is reduced and the bending instability spreads over a smaller area. This reduced jet path also means that there is less stretching of the solution resulting in a larger fiber diameter [7].

As is evident from the discussions, the concentration of the polymer solution influences the spinning of fibers and controls the fiber structure and morphology. [35].

Molecular weight

Molecular weight of the polymer has a significant effect on rheological and electrical properties of the solution such as viscosity, surface tension, conductivity and dielectric strength [8].

One of the conditions necessary for electrospinning to occur is that the solution consists of polymer of sufficient molecular weight and has sufficient viscosity. As the jet leaves the needle tip during electrospinning, the polymer solution is stretched as it travels towards the collection plate. During the stretching of the polymer solution, it is the entanglement of the molecule chains that prevents the electrically driven jet from breaking up thus maintaining a continuous solution jet. As a result, monomeric polymer solution does not form fibers when electrospun. The molecular weight of the polymer represents the length of the polymer chain, which in turn have

an effect on the viscosity of the solution since the polymer length will determine the amount of entanglement of the polymer chains in the solvent. Another way to increase the viscosity of the solution is to increase the polymer concentration. Similar to increasing the molecular weight, an increase in the concentration will result in greater polymer chain entanglements within the solution which is necessary to maintain the continuity of the jet during electrospinning [7].

Generally high molecular weight polymer solutions have been used in electrospinning as they provide the desired viscosity for the fiber generation. It has been observed that too low molecular weight solution tends to form beads rather than fibers and a high molecular weight solution gives fibers with larger average diameters.

Gupta *et al.* have synthesized poly (methyl methacrylate) (PMMA) varying in molecular weight from 12.47 to 365.7 kDa to investigate the effect of molecular weight of the polymer, and they found that as the molecular weight increased, the number of beads and droplets decreased [8].

Viscosity

Viscosity is a measure of the resistance of a material to flow and is affected by the factors such as polymer configuration, solvent type, temperature. The viscosity of the solution has a profound effect on electrospinning and the resultant fiber morphology. Viscosity and the factors that affect the viscosity of the solution affect the electrospinning process and the resultant fibers. Generally, the viscosity of the solution is related to the extent of polymer molecule chains entanglement within the solution. When the viscosity of the solution is too low, electrospraying may occur and polymer particles are formed instead of fibers. At lower viscosity where generally the polymer chain entanglements are lower, there is a higher likelihood that beaded fibers are obtained instead of smooth fibers and with very high viscosity there is difficulty in the ejection of jets from polymer solution and probability of the drying of the solution at the needle tip fibers. Thus there is a requirement of optimal viscosity for electrospinning. The optimal viscosity range at which spinning is done is different for various polymer solutions. Sukigara *et al.* have shown the significant effects of viscosity on silk nanofibers. Earlier, Larrondo and Manley also showed that viscosity was important when they electrospun fibers from the melt [7,8].

Viscosity, polymer concentration and molecular weight of polymer are correlated to each other. The solution viscosity has been strongly related to the concentration of the solution and the relationship between the polymer viscosity and /or concentration and fibers obtained from electrospinning has been studied in a number of systems, including poly(lactic-co-glycolic acid) (PLGA), poly(ethylene oxide) (PEO), poly (vinyl alcohol) (PVA), poly (methyl methacrylate) (PMMA), polystyrene, poly (L-lactic acid) (PLLA), gelatin and dextran**.** An increase in solution viscosity or concentration gives rise to a larger and more uniform fiber diameter [8]. This is probably due to the greater resistance of the solution to be stretched by the charges on the jet [7].

In electrospinning, viscosity of solution plays an important role in determining the range of concentrations from which continuous fibers can be obtained. For solution of low viscosities, surface tension is the dominant factor and just beads or beaded-fibers are formed while above a critical concentration, a continuous fibrous structure is obtained and its morphology is affected by the concentration of the solution**.**

Taken together, these studies indicate that there exist polymer specific, optimal viscosity values for electrospinning and this property has a remarkable influence on the morphology of fibers.

Surface tension

Surface tension, more likely to be a function of solvent compositions of the solution plays a critical role in the electrospinning process. Different solvents may contribute different surface tensions.

In electrospinning, the charges on the polymer solution must be high enough to overcome the surface tension of the solution [7].

The formation of droplets, bead and fibers depends on the surface tension of solution. Generally, the high surface tension of a solution inhibits the electrospinning process because of instability of the jets and results in the generation of sprayed droplets [8]. Surface tension has also been attributed to the formation of beads on the electrospun fibers [7]. By reducing the surface tension of a nanofiber solution; fibers can be obtained without beads [8].

Solvent such as ethanol has a low surface tension thus it can be added to encourage the formation of smooth fibers. Another way to reduce the surface tension is to add

surfactant to the solution. The addition of surfactant was found to yield more uniform fibers. Even when insoluble surfactant is dispersed in a solution as fine powders, the fiber morphology is also improved.

Conductivity / Solution charge density

For electrospinning process to be initiated, the solution must gain sufficient charges such that the repulsive forces within the solution are able to overcome the surface tension of the solution. Subsequent stretching or drawing of the electrospinning jet is also dependent on the ability of the solution to carry charges [7].

Solution conductivity is mainly determined by the polymer type, solvent used, and the availability of ionisable salts. It has been found that with the increase of electrical conductivity of the solution, there is a significant decrease in the diameter of the electrospun nanofibers whereas with low conductivity of the solution, there results insufficient elongation of a jet by electrical force to produce uniform fiber, and beads may also be observed [8].

Polymers are mostly conductive, with a few exceptions of dielectric materials, and the charged ions in the polymer solution are highly influential in jet formation. The ions increase the charge carrying capacity of the jet, thereby subjecting it to higher tension with the applied electric field [35].

Solvents used in electrospinning should have a certain level of conductivity. Although organic solvents are known to be non-conductive, many of them do have a certain level of conductivity. Solutions prepared using solvents of higher conductivity generally yield fibers without beads while no fibers are formed if the solution has zero conductivity [7].

The conductivity of the solution can be increased by the addition of ions when a small amount of salt or polyelectrolyte is added to the solution, the increased charges carried by the solution will increase the stretching of the solution. As a result, smooth fibers are formed which may otherwise yield beaded fibers. The increased in the stretching of the solution also will tend to yield fibers of smaller diameter. Since the presence of ions increases the conductivity of the solution, the critical voltage for electrospinning to occur is also reduced. Another effect of the increased charges is that it results in a greater bending instability. As a result, the deposition area of the

fibers is increased. This will also favor the formation of finer fibers since the jet path is now increased [7].

Baumgarten showed that the jet radius varied inversely as the cube root of the electrical conductivity of the solution. Zong *et al*. demonstrated the effect of ions by adding ionic salt on the morphology and diameter of electrospun fibers. They found that poly (D-lactide) acid (PDLA) fibers with the addition of ionic salts like KH_2PO_4, NaH_2PO_4, and NaCl produced beadless fibers with relatively smaller diameters ranging from 200 to 1,000 nm. [35,42]. This approach of increasing the solution conductivity by the use of salt addition has also been used for other polymers such as, PEO, collagen type I-PEO, PVA, polyacrylic acid (PAA), polyamide-6 and others [8].

Volatility

Solvent volatility plays a major role in the formation of nanostructures by influencing the phase separation process [35].

During the electrospinning process, the solvent evaporates as the electrospinning jet accelerates towards the collector. When most of the solvent has evaporated, individual fibers are formed as the jet reaches the collector. However, if the rate of evaporation of the solvent is too low such that the solution has not evaporated sufficiently when the electrospinning jet reaches the collector, fibers may not be formed at all and a thin film of polymer solution are deposited on the collector [7].

Polymer solubility

The solubility of the polymer in a particular solvent may affect the resultant fiber morphology. Polymer solubility is more complex than those of low-molecular weight compound due to size difference between polymer and solvent molecules, viscosity of the system, effects of the structure and molecular weight of the polymer. There are two stages when a polymer dissolves in the solvent. Firstly, solvent molecules diffuse slowly into the polymer bulk to produce a swollen gel. If the polymer-polymer intermolecular forces are high as a result of cross-linking, crystallinity or strong hydrogen bonding, the polymer-solvent interactions may not be strong enough to break the polymer-polymer bond. The second stage of solution will only take place when the polymer-polymer bond is broken to give true solution.

The structure of the polymer has an impact on its solubility in the solvent. Generally, a polymer with higher molecular weight is less soluble and takes a much longer time to dissolve than one with a lower molecular weight using the same solvent. The intermolecular forces between longer chain molecules are stronger and the solvent molecules take a longer time to diffuse into the polymer bulk. Crosslinked polymers do not dissolve, as covalent bonding between the molecules is much stronger than the secondary forces exerted from polymer-solvent interactions. Polymers of higher crystallinity have lower solubility as the solvent molecules have difficulty in penetrating the interior of the polymer bulk.

2.3.5.2 Processing parameters

Other important parameters that affect the electrospinning process are the various external factors exerting on the electrospinning jet such as the voltage applied, the feed rate, type of collector, diameter of needle and distance between the needle tip and collector. These parameters have a certain influence in the fiber morphology although they are less significant than the solution parameters [7].

Applied voltage

In the electrospinning process a crucial element is the applied voltage to the solution [8].

The applied voltage will induce the necessary charges on the solution and together with the external electric field, will initiate the electrospinning process when the electrostatic force in the solution overcomes the surface tension of the solution. Generally, both high negative or positive voltage of more than 6 kV is able to cause the solution drop at the tip of the needle to distort into the shape of a Taylor Cone during jet initiation. Depending on the flow rate of the solution, a higher voltage may be required so that the Taylor Cone is stable. The columbic repulsive force in the jet will then stretch the viscoelastic solution. If the applied voltage is higher, the greater amount of charges will cause the jet to accelerate faster and more volume of solution will be drawn from the tip of the needle. This may result in a smaller and less stable Taylor Cone. When the drawing of the solution to the collection plate is faster than the supply from the source, the Taylor Cone may recede into the needle [7].

It has been experimentally shown that an increase in applied voltage causes a change in the shape of the jet initiating point, and hence the structure and morphology of

fibers. It was observed that for the PEO/water system, the fiber morphology changed from a defect free fiber at an initiating voltage of 5.5 kV to a highly beaded structure at a voltage of 9.0 kV. The occurrence of beaded morphology has been correlated to a steep increase in the spinning current, which controls the bead formation in the electrospinning process [35].

Regarding the effect of the applied voltage on the fiber diameter there is no consensus.

Reneker and Chun have showed that there is not much effect of electric field on the fiber diameter with electrospinning of PEO. Researchers have suggested that when higher voltages are applied, there is more polymer ejection and this facilitates the formation of a larger diameter fiber. Other authors have reported that an increase in the applied voltage, increases the electrostatic repulsive force on the fluid jet which ultimately favours the narrowing of fiber diameter [8]. Megelski *et al*. investigated the voltage dependence on the fiber diameter using PS. The PS fiber size decreased from about 20 μm to 10 μm with an increase in voltage from 5 kV to 12 kV, while there was no significant change observed in the pore size distribution. These results concur with the interpretation of Buchko *et al*.,who observed a decrease in the fiber diameter with an increase in the applied field while spinning silk like polymer fiber with fibronectin functionality (SLPF) [35]. Larrondo and Manley have showed the decrease of fiber diameter by roughly half by doubling the applied electric field. Thus, voltage influences fiber diameter, but the level of significance varies with the polymer solution concentration and the distance between the tip and the collector. In most cases, a higher voltage causes greater stretching of the solution and this leads to the reduction in the fiber diameter and also rapid evaporation of solvent from the fibers [8].

The effect of high voltage is not only on the physical appearance of the fiber, it also affects the crystallinity of the polymer fiber. The electrostatic field may cause the polymer molecules to be more ordered during electrospinning thus induces a greater crystallinity in the fiber. However, above a certain voltage, the crystallinity of the fiber is reduced. With increased voltage, the acceleration of the fibers also increases. This reduces the flight time of the electrospinning jet. Since the orientation of the polymer molecules will take some time, the reduced flight time means that the fibers will be deposited before the polymer molecules have sufficient time to align

themselves. Thus, given sufficient flight time, the crystallinity of the fiber will improve with higher voltage [7].

Feed rate / Flow rate

This is the rate at which the polymer solution is pumped into the tip to replenish the Taylor's cone [38]. The flow rate of the polymer from the syringe is an important process parameter as it influences the jet velocity and the material transfer rate [35].

As a result of his work, Taylor realized that the cone shape at the tip of the capillary cannot be maintained if the flow of solution through the capillary is insufficient to replace the solution ejected as the fiber jet [42]. For a given voltage, there is a corresponding flow rate if a stable Taylor cone is to be maintained [7]. In other words the flow rate must match the rate of removal of solution from the tip which is determined by the applied voltage [38].

A lower feed rate is more desirable as the solvent will get enough time for evaporation [8]. When the feed rate is increased, there is a corresponding increase in the fiber diameter which is the result of the greater volume of solution that is drawn away from the needle tip [7] and high feed rates usually result in beaded fibers due to unavailability of proper drying time prior to reaching the collector [8,42].

Megelski *et al*., observed that the fiber diameter and the pore diameter increased with an increase in the polymer flow rate in the case of PS fibers. As the flow rate increased, fibers had pronounced beaded morphologies and the mean pore size increased from 90 to 150 nm [35,42].

Types of collector

One important aspect of the electrospinning process is the type of collector used. In electrospinning process, the collector serves as a conductive substrate where the nanofibers are collected [8]. There must be an electric field between the source and the collector for electrospinning to initiate. Thus in most electrospinning setup, the collector plate is made out of conductive material such as aluminum foil which is electrically grounded so that there is a stable potential difference between the source and the collector. In the case when a nonconducting material is used as a collector, charges on the electrospinning jet will quickly accumulate on the collector which will result in fewer fibers deposited. For a conducting collector, charges on the fibers

are dissipated thus allowing more fibers to be attracted to the collector. The fibers are able to pack closely together as a result [7].

Generally, aluminium foil is used as a collector but due to difficulty in transferring of collected fibers and with the need for aligned fibers for various applications, other collectors such as, conductive paper, conductive cloth, wire mesh, pin, parallel or grided bar, rotating rod, rotating wheel, liquid nonsolvent such as methanol coagulation bath and others are also common types of collectors nowadays. Wang *et al.*, compared wire screen with aluminium foil and wire screen without aluminium foil in the same conductive area and found that pure wire screen is a better collector for fiber collection because with the use of wire screen the transfer of fibers to other substrates became easy. The fiber alignment is determined by the type of the target/collector and its rotation speed. Several research groups have demonstrated the use of a rotating drum or a rotating wheel-like bobbin or metal frame as the collector, for getting aligned electrospun fibers more or less parallel to each other [8].

While rotating collector has been used to collect aligned fibers, it was found to assist in yielding fibers that are dry. This is useful because certain solvents such as DMF which is good for electrospinning but have a high boiling point that may result in the fibers being wet when they are collected. A rotating collector will give the solvent more time to evaporate and also increase the rate of evaporation of the solvents on the fibers. This will improve the morphology of the fiber where distinct fibers are required [7].

Several types of split electrodes have been used for getting aligned nanofibers and typically such collectors consist of two conductive substrates separated by a void gap where aligned nanofibers are deposited [8].

Diameter of pipette orifice / needle

The internal diameter of the needle or the pipette orifice has a certain effect on the electrospinning process. A smaller internal diameter was found to reduce the clogging as well as the amount of beads on the electrospun fibers. The reduction in the clogging could be due to less exposure of the solution to the atmosphere during electrospinning. Decrease in the internal diameter of the orifice was also found to cause a reduction in the diameter of the electrospun fibers. When the size of the droplet at the tip of the orifice is decreased, such as in the case of a smaller internal

diameter of the orifice, the surface tension of the droplet increases. For the same voltage supplied, a greater columbic force is required to cause jet initiation. As a result, the acceleration of the jet decreases and this allows more time for the solution to be stretched and elongated before it is collected. However, if the diameter of the orifice is too small, it may not be possible to extrude a droplet of solution at the tip of the orifice [7].

Tip-to-collector distance

One important physical aspect of the electrospinning nanofibers is their dryness from the solvent used to dissolve the polymer. Thus, there should be optimum distance between the tip and collector which favours the evaporation of solvent from the nanofibers [8].

The structure and morphology of electrospun fibers is easily affected by the tip-to-collector distance because of their dependence on the deposition time, evaporation rate, and whipping or instability interval. Buchko *et al*. examined the morphological changes in SLPF and polyamide electrospun fibers with variations in the distance between the tip and the collector screen. They showed that regardless of the concentration of the solution, lesser tip to collector distance produces wet fibers and beaded structures. SLPF fiber morphology changed from round to flat shape with a decrease in the tip-to-collector distance from 2 cm to 0.5 cm. This result shows the effect of the tip-to-collector distance on fiber morphology. The work also showed that aqueous polymer solutions require more distance for dry fiber formation than systems that use highly volatile organic solvents.

2.3.5.3 Ambient parameters

Environmental conditions around the spinneret, like the surrounding air, its relative humidity (RH), temperature, vacuum conditions, surrounding gas, etc., influence the fiber structure and morphology of electrospun fibers [35].

Mit-Uppatham *et al*. have investigated the effect of temperature ranging from 25º to 60 °C on the electrospinning of polyamide 6 fibers and found that with increase in temperature, there is a yield of fibers with decreased fiber diameter, and they attributed this decline in diameter to the decrease in the viscosity of the polymer solutions at increased temperatures as there is an inverse relationship between viscosity and temperature [8].

Baumgarten observed that when acrylic fibers are spun in an atmosphere of relative humidity more than 60%, they do not dry properly and get entangled on the surface of the collector [35]. The variation in humidity while spinning polystyrene solutions has been studied. The results show that by increasing humidity there is an appearance of small circular pores on the surface of the fibers and further increasing the humidity leads to the pores coalescing. It has also been suggested that the high humidity can help the discharge of the electrospun fibers. At very low humidity, a volatile solvent may dry rapidly. As a result, the electrospinning process may only be carried out for a few minutes before the needle tip is clogged [8].

The breakdown voltage of the atmospheric gases is said to influence the charge retaining capacity of the fibers. Srinivasarao *et al*. proposed a new mechanism for pore formation by evaporative cooling called 'breathe figures'. Breathe figures occur on the fiber surfaces due to the imprints of condensed moisture droplets caused by the evaporative cooling of moisture in the air surrounding the spinneret. Megelski *et al*. investigated the pore characteristics of PS fibers at varied RH and emphasized the importance of phase separation mechanisms in explaining the pore formation of electrospun fibers [35].

Hence, apart from solution and processing parameters, ambient parameters also affect the electrospinning process [8].

2.3.6 Applications of nanowebs

Recently, researchers have begun to look into various applications of electrospun fibers and mats as these provide several advantages such as high surface to volume ratio, very high porosity and enhanced physico-mechanical properties, as in the electrospinning process, manipulation of the solution and process parameters can be easily done to get the desired fiber morphology and mechanical strength. In addition to these, the electrospun fibers are required in a small amount and the electrospinning process itself is a versatile process as fibers can be spun into any shape using a wide range of polymers.

Electrospun nanofibers are mainly applied in biomedical applications, as tissue engineering scaffolds, medical prostheses, wound dressings, drug delivery carriers and in filtration and also suggested for use in biosensors, protective clothing, affinity membranes, enzyme immobilization, energy storage and generation, etc. [8,37]. It

should be realized that most of these applications have not reached their industry level, but just at a laboratory research and development stage. However, their promising potential is believed to be attracting attentions and investments from academia, governments, and industry all over the world [37]

2.3.6.1 Biomedical applications

As is clear from the majority of the patents devoted to the topic, biomedical applications remain the most intensely researched application area for electrospun nanofibers [38]. Particularly promising biomedical research areas are focused on nano-fiber based three-dimensional cell or tissue scaffolds, medical prostheses, wound dressings and drug delivery devices [37]. All of these application areas find the very high specific surface area of nanofibers to be an advantage in designing the next generation of devices. The finding that biodegradable polymers can be electrospun into nanofibers and that different cell types have been shown to adhere and proliferate on the fibrous scaffolding encourages applications research in this area [38].

For engineering living tissues, biodegradable scaffold is generally considered as an indispensable element as these are used as temporary templates for cell seeding, invasion, proliferation, and differentiation prior to the regeneration of biologically functional tissue or natural extracellular matrix (ECM), which is a complex structure made of proteins and glycosaminoglycans, giving strength and providing templates for cellular cultures in the body [8,46]. There has been an increased surge in the use of electrospinning techniques to create nanofibrous scaffolds for tissue engineering as there are reports that these scaffolds positively promote cell-matrix and cell-cell interactions [8]. The high surface to volume ratio of the nanofiber provides more room for the cell attachment than the regular fibers. The high porosity of the electrospun nanofiber scaffolds provides enough space for the cell accommodation and an easy passage for the nutrient intake and metabolic waste exchange [35]. The diameter of electrospun fibers is of similar magnitude as that of fibrils in ECM that mimics the natural tissue environment and has demonstrated effectiveness as a substrate for cell growth [8]. Choices in materials include both natural and synthetic (biodegradable and nondegradable) materials, as well as hybrid blends of the two, which can provide an optimal combination of mechanical and biomimetic properties [42]. Natural polymers such as collagen, alginate, silk protein, hyaluronic acid,

fibrinogen, chitosan, starch are often used for preparing nanofibrous scaffolds because of their enhanced biocompatibility and biofunctional motifs [8]. Using synthetic polymers for tissue engineering applications is advantageous because of the uniform chemical composition and consistency in the quality materials obtained from commercial sources. Also, a polymer with mechanical properties that best matches a particular scaffolding application can be readily selected or even designed. However, as most synthetic polymers are virtually nonbiodegradable, the available choices of synthetic polymers for scaffolding are somewhat limited. Electrospun biodegradable scaffolds reported in the literature are for the most part based on ε-poly(caprolactone) (PCL), poly(lactide) (PLA), poly(glycolide) (PGA), or copolymers composed of the repeat units of these [38]. A variety of polymeric nanofibers have been considered for use as scaffolds for engineering tissues such as cartilages, dermal tissue, bones, arterial blood vessels, heart, nerves, etc. [8]. Particularly exciting is the finding that mammalian stem cells survive and proliferate on the nanofiber surfaces [38]. In addition, electrospun biocompatible polymer nanofibers can also be deposited as a thin porous film onto a hard tissue prosthetic device designed to be implanted into the human body. This coating film with gradient fibrous structure works as an interphase between the prosthetic device and the host tissues, and is expected to efficiently reduce the stiffness mismatch at the tissue/device interphase and hence prevent the device failure after the implantation [37].

Nanowebs have also been applied as drug carriers in the drug delivery system because of their high functional characteristics and because the drug delivery system relies on the principle that dissolution rate of a particulate drug increases with increasing surface area of both the drug and the corresponding carrier [8]. Conventional delivery of a drug in successive doses results in a blood (or other tissue phase) concentration profile of the drug that fluctuates over the duration of the therapy. Therefore over significant durations, the concentrations may exceed the recommended maximum value with the risk of biotoxicity, or fall below the minimum effective concentration, limiting the therapeutic effect. To derive the highest therapeutic value an optimum concentration should be maintained in the body tissue over the full duration of treatment [38]. Controlled delivery of drugs at a defined rate over a definite period of treatment is possible with nanowebs [8]. Electrospinning affords great flexibility in selecting materials for drug delivery

applications. Either biodegradable or nondegradable materials can be used to control whether drug release occurs via diffusion alone or diffusion and scaffold degradation. Additionally, due to the flexibility in material selection a number of drugs can be delivered including antibiotics, anticancer drugs, proteins, and deoxyribonucleic acid (DNA). Using the various electrospinning techniques a number of different drug loading methods can also be utilized: coatings, embedded drug, and encapsulated drug (coaxial and emulsion electrospinning). These techniques can be used to give finer control over drug release kinetics [42]. A number of researchers have successfully encapsulated drugs within electrospun fibers by mixing the drugs in the polymer solution to be electrospun. A variety of solutions containing low molecular weight drugs have been electrospun, including lipophilic drugs such as ibuprofen, cefazolin, rifampin, paclitaxel and hydrophilic drugs such as mefoxin and tetracycline hydrochloride. Few, however, have encapsulated proteins in electrospun polymer fibers. Zong *et al.* have studied the effectiveness of electrospun non-woven bioabsorbable poly(lactide-co-glycolide) (PLGA) impregnated with antibiotics (mefoxin) in reducing post-surgery adhesion on an *in vivo* rat model. Zhang *et al.* have demonstrated encapsulation of a model protein, fluorescein isothiocyanate conjugated bovine serum albumin, along with poly(ethylene glycol) (PEG) in poly(e-caprolactone) (PCL) fibers by using a coaxial configuration and found a relatively smooth release of the drug over a period of five days from the electrospun nanofibrous mats [8].

Polymer nanofibers can also be used for the treatment of wounds or burns of a human skin, as well as designed for haemostatic devices with some unique characteristics [37]. For wound healing, an ideal dressing should have certain characterisctics such as haemostatic ability, efficiency as bacterial barrier, absorption ability of excess exudates (wound fluid/pus), appropriate water vapor transmission rate, adequate gaseous exchange ability, ability to conform to the contour of the wound area, functional adhesion, i.e., adherent to healthy tissue but non-adherent to wound tissue, painless to patient and ease of removal, and finally low cost. Current efforts using polymer nanofibrous membranes as medical dressing are still in its infancy but electrospun materials meet most of the requirements outlined for woundhealing polymer devices because their microfibrous and nanofibrous structures provide the nanoweb with desirable properties and there are also reports of

cytocompatibility and cell behaviour of normal human keratinocytes and fibroblasts onto electrospun silk fibroin nanowebs [8]. The same polymers, both biodegradable and nonbiodegradable used in scaffolds have also been suggested for woundhealing applications [38]. Rho *et al*. have investigated the wound-healing properties of mats of electrospun type I collagen fibers on wounds in mice and they found that healing of the wounds was better with the nanofiber mats than with conventional wound care, especially in the early stages of the healing process. Spasova *et al*., have prepared fibrous poly(L-lactide) (PLLA) and biocomponent PLLA/PEG mats by electrospinning which were coated with chitosan and found that with the increase of chitosan content, the haemostatic activity of the mats increased [8].

2.3.6.2 Filtration

Filtration is the leading nonbiomedical application of electrospun nanofibers, with products containing layers of nanofibers already in the marketplace [8]. It is also one of the areas where nanofibers are likely to make a significant and lasting impact [38]. Since the channels and structural elements of a filter must be matched to the scale of the particles or droplets that are to be captured in the filter, one direct way of developing high efficient and effective filter media is by using nanometer sized fibers in the filter structure. In general, due to the very high surface area to volume ratio and resulting high surface cohesion, tiny particles of the order of <0.5 mm can be easily trapped in the electrospun nanofibrous structured filters and hence the filtration efficiency can be improved [37].

Polymeric nanofibers have been used in air filtration applications for more than a decade [8]. The hazard to human health from exposure to air-borne dust is primarily due to the smaller particles with aerodynamic diameters of less than a few micrometers. Inhaled small particles including nanoparticles are well known to lodge deeper in the lungs causing asthma-like symptoms and other complications. The simplest means of removing these aerosols from air is by filtration. Filters are used in diverse applications including personel masks for inhalation protection, air cleaning of industrial effluents, in electronic equipment and in maintaining clean room manufacturing environments [38]. The nanofiber membrane shows an extremely effective removal (~100% rejection) of airborne particles with diameters between 1μm and 5μm not only by the physical entrapment mechanism but also by the electrokinetic capture in the air filter. Polymer nanofibers can also be

electrostatically charged to modify the ability of electrostatic attraction of particles without increase in pressure drop to further improve filtration efficiency [8]. In this regard, the electrospinning process has been shown to integrate the spinning and charging of polymer into nanofibers in one step. In addition to fulfilling the more traditional purpose in filtration, the nanofiber membranes fabricated from some specific polymers or coated with some selective agents can also be used as, for example, molecular filters. For instance, such filters can be applied to the detection and filtration of chemical and biological weapon agents [37].

2.3.6.3 Other applications

In addition to their use in biomedical area and filtration, nanowebs are also suggested for use in biosensors, protective clothing, energy generation applications, enzyme immobilization, cosmetics, etc.

Biosensors, which typically consist of bio-functional membrane and transducer, have been widely used for environmental, food, and clinical purposes. There are lots of parameters that affect the performance of a sensor which includes sensitivity, selectivity, response time, reproducibility, and aging, all of which are dependent directly on the property of the sensing membrane used. Because there is a strong need for detection of gases and biological substances at low concentration, sensitivity particularly, plays a very critical role [8]. It is reasonable to expect the sensitivity of a sensor that involves surface interaction with analyte molecules to increase with increasing surface area per unit mass of sensing material. The high specific surface area of nanofibers therefore suggests the possibility of more efficient and rapid sensor performance, particularly when sensing mechanism is via a surface reaction [38]. Modern biomedical sensors with advanced micro fabrication and signal-processing techniques are becoming more and more accurate and inexpensive nowadays. The main focus is now on miniaturization of bulky instrumentation and development of portable sensors in order to avoid the burden of accuracy and reliability and also in the development of various specific target molecules for different analytes that have exhausted all possibilities. Electrospun nanofibrous membranes have received great attention for their sensor applications because of their unique large surface area which is the most desirable property for improving the sensitivity of conductometric sensors, as larger surface area will absorb more of a gas analyte and change the sensor's conductivity more significantly. Silk fibroin

membranes-based biosensors have been extensively used for analysing various substances such as glucose, hydrogen peroxide and uric acid. Apart from this, the literature shows the involvement of other electrospun polymers such as polyaniline, polypyrrole, polyamic acid, polyamide-6, poly(vinyl alcohol)(PVA) and poly (acrylic acid)-poly (pyrene methanol), also as sensing interfaces. Recently, efforts have been made to produce nanofibers for electrochemical sensors as well. Optical sensors are relatively new and not much work has been carried out in this field.

Electrospun nanofiber membranes have been recognized as potential candidates for protective clothing applications, because of their light weight, large surface area, high porosity (breathable nature), great filtration efficiency, resistance to penetration of harmful chemical agents in aerosol form and ability to neutralize the chemical agents without impedance of the air and water vapour permeability to the clothing. A variety of methods for modification of nanofiber surfaces have been tried in order to get improved protection against toxins. One protection method that has been used includes chemical surface modification and attachment of reactive groups such as oximes, cyclodextrins, and chloramines that bind and detoxify warfare agents [8].

Conductive nanofibers are expected to be used in the fabrication of tiny electronic devices or machines such as Schottky junctions, sensors and actuators. Due to the well-known fact that the rate of electrochemical reactions is proportional to the surface area of the electrode, conductive nanofibrous membranes are also quite suitable for using as porous electrode in developing high performance battery [37]. Polymer batteries have been developed for cellular phones to replace conventional, bulky lithium batteries. The components of polymer batteries are a carbon anode, a lithium cobalt oxide cathode, and a polymer gel electrolyte. Conductive nanofibers offers noteworthy properties of polymer batteries, for example, less electrolyte leakage, high dimension flexibility, and high energy density per weight. However, there is still a need to improve energy density per weight of polymer batteries to increase their market share [8]. Conductive (in terms of electrical, ionic and photoelectric) membranes also have potential for applications including electrostatic dissipation, corrosion protection, electromagnetic interference shielding, photovoltaic device, etc. [37].

Immobilization of enzymes on inert, insoluble materials is an active area of research for improving the functionality and performance of enzymes for bioprocessing

applications as immobilized enzymes offer several advantages such as reusability, better control reaction and are more stable than soluble ones. The performance of immobilized enzymes depends greatly on the characters and structure of the carrier materials and on modification of the carriers, such as rendering biocompatibility, hydrophilicity, etc. Nevertheless, even for the modified supports, the enzyme loading is usually considerably low. Alternatively, porous material such as membranes, gel matrices, and porous particles have been used to achieve high enzyme loading. The fine porous structure of electrospun fibrous membranes can effectively relieve the diffusion resistance of the substrates/products and can greatly increase the catalyzing ability of the immobilized enzymes due to the large specific surface area. Nanofibrous membranes offer advantages such as; these can be processed into various structures such as non-woven mats, or well-aligned arrays and are more conveniently recovered and more durable than other nanoparticles or carbon nanotubes [8].

Affinity membranes are a broad class of membranes that selectively capture specific target molecules (or ligates) by immobilizing a specific or ligand onto the membrane surface and reflect technological advances in both fixed-bed liquid chromatography and membrane filtration, and combine both the outstanding selectivity of the chromatography resins and the reduced pressure drops associated with filtration membranes. Few works have been reported on the application of the electrospun nanofiber mesh as affinity membrane and for this the surface must be functionalized prior with ligands. In most cases, the ligand molecules should be covalently attached on the membrane to prevent leaching of the ligands. For protein purification, the affinity membrane should be made up of hydrophilic materials which usually have lower non-specific protein adsorption than hydrophobic synthetic polymers, for example, cellulose is a hydrophilic material widely used in membrane preparation. Affinity membranes also provide an alternative approach for removing organic molecules from waste water. For example, β-cyclodextrin, a cyclic oligosaccharide with a hydrophobic interior and hydrophilic exterior has been introduced into a poly (methyl methacrylate) nanofiber membrane using a physical mixing method for organic waste removal that can capture hydrophobic organic molecules from water by forming an inclusion complex is used for affinity membrane application.

Due to very small pore size and high surface area to volume ratio, electrospun nanofibers have the potential to be used as skin care masks [8], for the treatment of skin healing, skin cleansing, or other therapeutical or medical properties with or without various additives [37]. The electrospun nanofibrous skin mask has advantage of high surface area which facilitates better utilization and also speeds up the transfer rate of the additives to the skin. The electrospun nanofibrous cosmetic skin mask can be introduced gently and painlessly and also directly to the three-dimensional topography of the skin to provide healing or care treatment to the skin. For skin health and renewal, skin-revitalizing factors can be impregnated into nanofiber masks [8].

2.4 Electrospun Silk Fibroin Nanowebs

The availability of silk nanofibers introduces a new set of potential uses that previously were unattainable. Silk nanofibers are attractive candidates for biomedical, electrical and textile applications, including tissue-engineered scaffolds, wound dressings and drug delivery systems because of their high specific surface area, increased strength and surface energy and enhanced thermal and electrical conductivity [47].

Electrospun silk fibroin nanowebs are produced from aqueous or solvent formulations of silk fibroin.

Early attempts to electrospin *B. mori* fibroin from relatively dilute aqueous solutions were unsuccessful due to the surface tension and viscosity of the solution being too low to maintain a stable drop at the end of the needle tip. It was later found that using more concentrated solutions of *B. mori* fibroin (ca. 28 wt%) increased the surface tension and viscosity of the solution enough to enable the successful electrospinning of fibers. But the high concentration has been the disadvantage of this method.

Removal of water to get a dry silk fibroin material after dialysis and redissolution of the regenerated silk fibroin material in a solvent to obtain an electrospinnable solution is a more common method [21].

2.4.1 Processes in electrospinning of silk

2.4.1.1 Degumming

Degumming is the process which is used to eliminate the proteinaceous sericin coating that covers the fibers and maintains the integrity of the cocoon, so that the fibroin, the core of the fiber, can be recovered [4]. In degumming, sericin is removed using an alkali solution and/or an enzyme solution.

Traditionally, degumming of silk has been carried out by soap–soda ash method and it is considered as the best sericin removal method of silk. Recently, soap is replaced by synthetic detergents in continuous degumming systems, because it cannot compensate the acidity of sericin hydrolysis products accumulating in the bath, thus limiting the use of the degumming bath for weekly degumming cycles. In recent years, various studies have been dealt with the removal of sericin by using different types of enzymes as degumming agents. It has also been pointed out that the action of organic acids is generally milder and less aggressive than the action of alkali. Freddi *et al.* studied the degumming of silk with tartaric acid and showed the excellent performances of tartaric acid, both in terms of silk sericin removal efficiency and of intrinsic physico-mechanical characteristics of silk fibers. Recently citric acid is investigated as a degumming agent. It shows potential for possible industrial application [48].

2.4.1.2 Dissolving silk fibroin

Natural silk fibers dissolve only in a limited number of solvents, compared to globular proteins, because of the presence in fibroin of a large amount of intramolecular and intermolecular hydrogen bonds and its high crystallinity and specific physicochemical properties as wetting angle of 69±3 [26]**.** They are insoluble in common solvents including H_2O, dilute acids, and alkali [6] which make them hard to process.

The solvents that have up to this point been proposed to dissolve silk fibroin may be mainly classified into two classes as acidic solvents (e.g., formic acid) and high-ionic-strength aqueous salt solutions. A drawback of the former solvents, which tend to be harsh and may degrade the fibroin, is the poor stability of their silk fibroin solutions [49].

Fibroin is known to be soluble in certain high-ionic-strength aqueous salt solutions, for example, aqueous lithium thiocyanate (LiSCN), sodium thiocyanate (NaSCN), calcium thiocyanate ($Ca(SCN)_2$), magnesium thiocyanate ($Mg(SCN)_2$), calcium chloride ($CaCl_2$), lithium bromide (LiBr), zinc chloride ($ZnCl_2$), magnesium chloride ($MgCl_2$), and copper salts, such as copper nitrate ($Cu(NO_3)_2$), copper ethylene diamine ($Cu(NH_2CH_2CH_2NH_2)_2(OH)_2$). It has long been known that the salts can be dialyzed out of such aqueous salt/fibroin solutions to produce aqueous solutions of fibroin which are similar in some ways to the liquid contents of a silkworm's silk gland [50]. It should be noted that the concentrations of salts in such solutions reach the saturation limit [26].

It is preferable to dissolve the fibroin at room temperature, however elevated temperatures may be used, up to about 80°C., in order to increase the rate of dissolution. Heating should not be conducted at a temperature at which the fibroin may be degraded. Fibroin solutions in aqueous lithium thiocyanate are stable on standing several days. Preferably, the concentration of silk fibroin in the aqueous salt solution is in the range of about 5 to 40 wt%. If the concentration of fibroin is less than about 5 wt%, the solution is difficult to handle, since the salt must be dialyzed and high amounts of water removed. If the concentration of fibroin is greater than about 40 wt%, the solution is difficult to handle because of its high viscosity.

The main disadvantages of salt-containing aqueous, aqueous-organic, and organic solutions of fibroin are the long preparation time (aqueous solutions of fibroin should be dialyzed for several days) and large power consumption for the regeneration of the solvents for their reuse [26].

To overcome these drawbacks, hexafluoro-2-propanol (HFIP) was proposed as the solvent [49]. An attempt was made to dissolve purified silk fibroin fiber directly in HFIP 0.763 g of purified fiber was mixed with 4.35 g of HFIP in a heat-sealed polyethylene packet. The solvent had essentially no effect on the fiber beyond a slight swelling, even after 1 month. Gentle heating (to 40° C) also produced no apparent changes [50]. The solubility of *B. mori* silk fibroin is very low in HFIP which is attributed to the density of hydrogen bonding between highly oriented polymer molecules in β-sheet strcture of the fiber which cannot be overcome by HFIP. Due to the low solubility, the preparation time is very long and high cost is

another disadvantage [49]. HFA-hydrate was demonstrated to be a superior solvent to HFIP as it can dissolve naturally spun *B. mori* fibroin fibers [21].

The most common solvent used in dissolving of silk fibroin is aqueous 9.0-9.5 M LiBr, although mixtures of aqueous calcium chloride and ethanol ($CaCl_2/H_2O/EtOH$), calcium nitrate in methanol ($Ca(NO_3)_2$-MeOH), aqueous lithium bromide ($LiBr/H_2O/EtOH$) and ethanol are also used as well as aqueous lithium thiocyanate (LiSCN) and aqueous sodium thiocyanate (NaSCN) [51].

These solutions are subsequently dialysed to remove the salt and have a shelf life of about 1 week before the onset of gelation [52]. The concentrated dialysed aqueous solutions are directly used in some of the studies while preparation of stable fibroin solutions by lyophilizing the dialysed solutions and dissolving the resulting silk powder in another solvent suitable for electrospinning is a more common method.

2.4.1.3 Dialysis

Dialysis is carried out to remove the salt from the silk fibroin/salt solution and obtain an aquatic fibroin solution.

Dialysis is the most commonly used method for removing low molecular weight solutes from macromolecules in solution, buffer exchange, desalting or concentration of complex biomolecules [53]. Dialysis separates sample components based on selective diffusion across a semi-permeable membrane [54].

Sample is loaded into the dialysis cartridge by using a serological pipette (Figure 2.13a) or hypodermic needle attached to a syringe (Figure 2.13b)**.** The sample contained inside the dialysis membrane is put into a dialysate 200 to 300 times the volume of the sample (Figure 2.13c) which creates and maintains a concentration differential across the membrane [55].

Figure 2.13 : a.b. Loading samples into dialysis cartridges [54] c. Dialysis

Once the liquid-to-liquid interface (sample on one side of the membrane and dialysate on the other) is initiated, all molecules try to diffuse in either direction across the membrane to reach equilibrium [55]. Only those molecules that are small enough to fit through the membrane pores are able move through the membrane and reach equilibrium with the entire volume of solution in the system. Once equilibrium is reached, there is no further net movement of the substance because molecules will be moving through the pores into and out of the dialysis unit at the same rate. By contrast, large molecules that cannot pass through the membrane pores will remain on the same side of the membrane as they were when dialysis was initiated. To remove additional unwanted substance, it is necessary to replace the dialysis buffer so that a new concentration gradient can be established. Once the buffer is changed, movement of particles from high (inside the membrane) to low (outside the membrane) concentration will resume until equilibrium is once again reached. With each change of dialysis buffer, substances inside the membrane are further purified by a factor equal to the volume difference of the two compartments. For example, if one is dialysing 1 mL of sample against 200 mL of dialysis buffer, the concentration of the dialysable substance at equilibrium will be diluted 200 less than at the start. Each new exchange against 200 mL of new dialysis buffer will dilute the sample 200 times more. For example, for three exchanges of 200 mL, the sample will be diluted 200 x 200 x 200 or 8,000,000 times, assuming complete equilibrium was reached each time before the dialysis buffer was changed [56].

After the dialysis is complete, the purified solution is recovered from the cartridge by a serological pipette or a hypodermic needle attached to a syringe [53].

The membrane is the key to dialysis. The semipermeable membrane contains pores of a known size range that are large enough to let small molecular weight compounds pass through, but restrict large molecular weight compounds (e.g., proteins and nucleic acids). The ideal membrane is thin, has numerous pores of uniform diameter, and does not bind proteins and nucleic acids. Unfortunately, the ideal membrane does not exist. What scientists have been using for decades is an extruded regenerated cellulose membrane that is close to an ideal membrane [55].

Other important variables are sample and dialysate volume. The ideal scenario is to have a small sample volume and a large dialysate volume to maximize the concentration differential. The sample volume is important because subsequent

applications have certain minimum volume requirements. However, after the minimum volume requirements are met, it is not advantageous to dialyse more sample than is needed. Depending on the surface area of a given sample, a small volume sample will dialyse much faster than a large volume sample. Not only is expending additional time wasteful, it can result in sample loss because the longer a sample is in contact with solid-phase surfaces, the more likely proteins or nucleic acids will nonspecifically bind or denature [55].

Factors that affect the completeness of dialysis can be summarized as dialysis buffer volume, buffer composition, the number of buffer changes, time, temperature and particle size vs. pore size [56].

2.4.1.4 Removal of water

The fibroin is isolated from the desalted or dialysed solution by removal of the water. This may be done using a number of methods. A convenient means is by casting of films and removal of the water by evaporation. The solution may also be freeze-dried (lyophilized) or spray dried, or the solvent removed in a rotary evaporator [50].

Freeze drying is the most common method used to remove the water to obtain regenerated silk fibroin material in dry powder form. It is used to obtain dry fibroin powder that is readily soluble in the solvents which are convenient to be used in the electrospinning process.

Freeze drying (lyophilization) is a separation process based on the sublimation phenomenon. At its most basic, it is a drying process by which a solvent is removed from a frozen material or frozen solution by sublimation of the solvent and by desorption of the sorbed solvent, generally under reduced pressure [57], leaving the solutes or substrates in their anhydrous, or almost anhydrous states [58]. In other words, freeze-drying removes water from a frozen sample by sublimation and desorption [59].

It can be viewed as a three-step process consisting of freezing, primary drying and secondary drying [60].

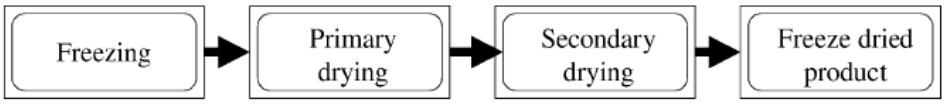

Figure 2.14 : Freeze-drying periods [60]

Freezing involves the formation of ice nuclei [60] and it reduces thermal denaturation of product, immobilizes solution components, and prevents foaming when the vacuum is applied [59]. The material to be processed is cooled down to a temperature below the solidification which may be well below 0ºC. The performance of the overall freeze drying process depends significantly on the freezing stage. The shape of the pores, the pore size distribution, and the pore connectivity of the porous network of the dried layer formed by the sublimation of the frozen water during the primary drying stage depend on the ice crystals formed during the freezing stage. Faster freezing rates give rise to small ice crystals. The result is faster sublimation at the primary drying phase, but slower secondary drying [57,60].

Primary drying is the stage at which ice is removed by sublimation under vacuum and heat addition. A significant amount of the sublimation latent heat is also consumed when the water molecules sublimate and enter to the vapor phase. Because of this, the temperature of the frozen product is reduced. It is then necessary to supply heat to the product, which could be provided by conduction, convection and/or radiation [57].

Secondary drying begins after all the frozen water has sublimed and is facilitated by increasing the product temperature. In the case of proteins, this temperature has to be chosen while keeping in view the thermal stability of proteins [60]. Resident moisture adsorbed to the apparently dry structure is removed by desorption at secondary drying stage [59]. The water is removed quickly up to the 2% level, and this process slows down thereafter. This is because, as the sample dries, diffusion of water molecules through the sample becomes more difficult. It is a function of the porosity of the sample and does not depend much upon the sample thickness [60].

This process has many advantages compared to the conventional drying process. The material structure is maintained, moisture is removed at low temperature, product stability during the storage is increased, the fast transition of the moisturized product to be dehydrated minimizes several degradation reactions [57].

2.4.1.5 Redissolution of regenerated silk

The fibroin, which is regenerated through dissolvation in concetrated salt solution, dialysis and freze drying, is readily soluble in HFIP, HFA, formic acid and some other solvents. It is believed that the fibroin molecules in the freeze-dried fibroin material are typically not in highly oriented β-sheet structure and are therefore not extensively involved in high-density hydrogen bonding. This reduced crystalline structure of the fibroin allows it to be redissolved easily in some solvents from which fibers may be spun.

Stable fibroin solutions are prepared by dissolving the lyophilized regenerated silk material in solvents such as formic acid, HFIP or HFA which are suitable to be used in the electrospinning process [50]. It has been demonstrated that electrospinning fibers from solutions of 0.2–1.5 wt% silk fibroin in HFIP and 10 wt% silk fibroin in formic acid is possible [21].

2.4.1.6 Electrospinning of silk

The general rules of electrospinning are applicable to the silk fibroin protein electrospinning.

Optimal combinations of the electrospinning parameters establish conditions to generate silk nano-scale fibers with narrow variations in diameter and absence of beads.

The effects of solution and process parameters such as concentration, pH, applied voltage, tip-to-collector distance on the fiber morphology and diameter have been discussed in many studies. However, no study involving the effect of the flow rate and the needle diameter on electrospun silk fiber characteristics has been conducted.

2.4.2 Previous studies about electrospinning of silk fibroin

Silk was first electrospun and patented by Zarkoob *et al*. in 2000.

Jin *et al*., added PEO to facilitate the electrospinning of silk in 2002. They studied electrospinning fibers from silk fibroin with a focus on blending with PEO and all aqueous processing. They dissolved the extracted silk fibroin in 9,3 M LiBr solution at 60 ºC yielding a 20% (w/v) solution, dialyzed in water using dialysis cassettes. To improve the processibility of silk solutions for electrospinning, while maintaining

biocompatibility, PEO with molecular weight of 900,000 g was successfully blended with the aqueous solution of fibroin by adding PEO directly into the silk aqueous solutions generating 4.8-8.8 wt% silk/PEO solutions. They demonstrated the possibility of using a lower concentration of aqueous silk fibroin solution for electrospinning by blending with as little as 12 wt% PEO. From this blend, nanofibers with comparable diameters to a pure aqueous silk system were generated (approximately 750 nm.), but more homogenous fiber diameters were observed with circular rather than ribbon-shaped cross-sections [6,61].

Ohgo *et al*. (2002) demonstrated the effect of the silk sources on the electrospinning processing parameters and fiber morphology. They successfully prepared nanofibers of *B. mori* and *Samia cynthia ricini* silk fibroins, and of the recombinant hybrid fiber involving the crystalline domain of *B. mori* silk and non-crystalline domain of *Samia cynthia ricini* silk from hexafluoroacetone (HFA) solution using electrospinning method. The concentration of silk in solution had a significant effect on nanofiber diameter. Continuous fibers were obtained only when a *B. mori* silk solution higher than 2% (w/v) concentration was used. Fibers with the smallest mean diameter and narrowest distribution were observed from silk solution of 3% (w/v), compared to those from 5 and 7% (w/v) solutions. When *Samia Cynthia ricini* silk and genetically engineered hybrid silk proteins were employed, the optimum conditions for fiber formation were found to be 10 and 12% solutions, respectively. This revealed the effect of silk sources on electrospinning processing parameters [6,62].

Kim *et al.* (2002) dissolved the degummed silk fibroin in a ternary solvent system of $CaCl_2/CH_3CH_2OH/H_2O$ (1/2/8 in mol ratio) at 70 ºC for 6 hours. After dialysis with cellulose tubular membrane in distilled water for 3 days, the SF solution was filtered and lyophilized to obtain the regenerated SF sponges. The SF solutions for electrospinning were prepared by dissolving the regenerated SF sponges in 98% formic acid for 3 hours. In the electrospinning process, a high electric potential of 15 kV was applied to a droplet of SF solution at the tip of a syringe needle with inner diameter of 0.495 mm. The electrospun nanofibers were collected on a target drum which was placed at a distance of 7 cm from the syringe tip. The flow rate of polymer solution was 1.5mL/h. They investigated the influence of the methanol treatment on the secondary structure of as-spun SF nanofibers [63]

Sukigara *et al.* (2003) studied the effect of electrospinning parameters on the morphology and fiber diameter of regenerated silk from *B. mori*. They dissolved the extracted fibers of 1.3 g in 50% aqueous $CaCl_2$ at 100 ºC to obtain silk concentration of 6% solution. The solution of 22 g was poured into regenerated cellulose dialysis to carry out dialysis against 1000 mL of deionized water for 48 h at 23 ºC. The regenerated silk fibroin sponge was obtained by lyophilization. Solutions of silk fibroin in formic acid with different concentrations were prepared for electrospinning. They used a needle of 18 Gauge and electrospun with a spinning angle of 45º. The tip-to-collector distance varied from 5 to 10 cm vertically under the needle tip. The electric field expressed in terms of voltage/distance between the collection plate and the needle tip ranged from 2 to 5 kV/cm. A factorial experiment was designed to investigate and identify the relative significance of the processing parameters on fiber diameter. The silk sponge solution (5–20%) was electrospun in formic acid (98–100%). Effects of electric field, tip-to-collector distance and solution concentration on fiber uniformity, morphology and diameter were measured. They showed that the silk concentration was the most important parameter in producing uniform cylindrical fibers less than 100 nm in diameter through statistical analysis [64].

Min *et al.* (2003) used the electrospinning method to fabricate SF nanowebs for cell culture of normal human keratinocytes and fibroblasts. To assay the cytocompatibility and cell behavior onto the electrospun SF nanofibers, cell attachment and spreading of normal human keratinocytes and fibroblasts seeded on the SF nanofibers and interaction between cells and SF nanofibers were studied. Cell morphology on SF nanofibers was examined by scanning electron microscopy. Their study indicated that the SF nanofibers may be a good candidate for the biomedical applications, such as wound dressing and scaffolds for tissue engineering.

Wang *et al*. (2005) prepared electrospun silk fibroin fibers with an average diameter of 700 nm from a concentrated aqueous solution with electrospinning technique. Their objectives were first to prepare a spinnable SF aqueous solution with a high SF content, second to produce ultrafine SF fibers from an aqueous solution by the environmentally friendly process of electrospinning, and third to investigate the fiber formation mechanism of the SF fibers spun from the aqueous solution. They dissolved the extracted silk fibroin in 9.3 M LiBr aqueous solution at room

temperature to obtain an SF aqueous solution with a concentration of 10 wt% which was diluted with four times the amount of water and then dialyzed against distilled water for 3 days. Then, the solution was filtered, and the final SF aqueous solutions with desired concentrations were prepared with a procedure developed in their laboratory. They used a needle with a diameter of 0.9 mm and a flat piece of aluminum foil placed 11 cm from the needle in the electrospinning process. A voltage of 10–40 kV was applied to the solutions with concentrations of 17%, 28% and 39%. The morphology, conformation, and crystalline structure of the SF fibers were characterized by scanning electron microscopy, Raman spectroscopy, and wide-angle X-ray diffraction, respectively. They concluded that the structure and morphology of the fibers were strongly influenced by the solution concentration and the processing voltage and they suggested concentration of 28 wt%, voltage of 20 kV, and working distance 11 cm as the optimum parameters for the preparation of beadless round electrospun silk fibroin fibers. In addition, they calculated the fiber formation parameters, including spinning velocity, elongation rate, and draw ratio and suggested that the high draw ratio was not the only factor in the transformation of SF from random-coil and α-helix conformations to a β-sheet conformation since even with the very high draw ratio random-coil conformation and α-helix structure could not fully transfer to β-sheet forms like those of silkworm silk [51].

Jeong *et al*. (2006) prepared nonwoven matrices of SF nanofibers by electrospinning a regenerated SF solution, followed by treatment with solvent vapor including water, methanol, ethanol, and propanol. They dissolved the extracted fibroin in a ternary solvent system composed of calcium chloride/ethanol/water (1:2:8 molar ratio) at 70ºC for 6 h and subsequently dialysed against distilled water for three days with cellulose tubular membrane. The resultant solution was filtered and lyophilized to obtain a white powder. The SF powder was then dissolved in HFIP to prepare a solution. SF nanofibers were prepared by electrospinning a 7% (w/v) fibroin solution and were collected on a target drum placed at a distance of 8 cm. A voltage of 16 kV was applied, and the flow rate of the solution was 2 mL/min. Electrospun SF nanofiber matrices were treated with solvent vapor, including water, methanol, ethanol, and propanol in order to achieve solvent-induced crystallization of fibroin. Structural changes of solvent vapor-treated SF nanofibers were investigated in a time-resolved manner using infra red spectroscopy. Conformational transitions of SF

nanofibers from random coil to β-sheet forms were dependent on the type of solvent vapor used, and their transition rates were strongly influenced by treatment temperatures. Methanol vapor treatment provided a fast and effective means to alter the secondary structure of SF nanofibers. However, treatment with water vapor, as compared to treatment with alcohol vapor, was also useful for inducing structural changes in SF nanofibers [65].

Chen *et al.* (2006) successfully prepared non-woven mats from stable regenerated silk fibroin aqueous solution at high concentration with the aim of improving the potential biocompatibility for use in biomedical applications. Scanning electronic microscope (SEM) was used to observe the morphology of the fibers. The structure of the fibers was characterized using Fourier transform infrared (FTIR), wide-angle X-ray diffraction (WAXD) and differential scanning calorimetry (DSC). The mechanical tests were also performed. In the as-spun fibers, silk fibroin was present in a random coil conformation, the stress and strain at break were 0.82 MPa and 0.76%, respectively, while after methanol treatment, the silk fibroin was transformed into a β-sheet-containing structure, the stress and strain at break increased to 1.49 MPa and 1.63%, respectively. Their study provided an option for the electrospinning of silk fibroin without using organic solvent or blending with any other polymers, which may be important in tissue engineering scaffold preparation [66].

Park *et al.* electrospun chitosan/silk fibroin before the solo electrospinning of chitosan was demonstrated. Chitosan/silk fibroin (30/70) fibers were created using formic acid as a solvent and the effect of methanol treatment on the secondary structure of silk fibroin versus chitosan/silk fibroin fibers was investigated [6].

Jeong *et al*. (2007) studied the effects of solvents as HFIP and formic acid on diameter and secondary structure of the *B. mori* silk nanofibers. They found the mean diameter of the electrospun nanofibers, composed of silk fibroin dissolved in formic acid, were smaller (80 nm) than those from HFIP (380 nm). This difference was due to the faster evaporation rate of HFIP than formic acid, which led to the formation of thicker fibers with less elongation. Higher solvent volatility increased fiber porosity in other polymer system, but this has not been observed in electrospun silk fibroin nanofibers [5].

Zhu *et al.* (2008) prepared regenerated silk fibroin aqueous solution to approach the environmental condition in the gland of silkworm, *B. mori* [67]. They employed the

electrospinning as a technique to help with understanding the spinning process of native silk fibers by silkworms and spiders. The effects of solution pH on electrospun fiber morphology and properties were investigated, since a decrease in pH of the silk dope from 6.9 to 4.8 was observed during the native flow from the posterior division to the anterior division of a silkworm gland [6]. The degummed fibers were dissolved in a 9.0 M LiBr aqueous solution at 40 ºC for 2 h yielding a 10% (w/v) solution. This solution was dialysed in deionized water for 3 days with a cellulose semipermeable membrane. To prepare condensed RSF aqueous solution, the water in the solution was slowly removed by forced airflow at 10ºC, the concentration of the solution was controlled by the velocity of the airflow and monitored by weighing the remaining solid after drying. After a certain time, a 20 wt% RSF aqueous solution was prepared. In order to approach the environmental condition in the gland of silkworm, RSF aqueous solutions at pH 6.9, 6.0, 5.6, 5.2 and 4.8, which are similar to the pH in the different divisions of the gland of *B. Mori*, were firstly prepared by adding 0.1 M citric acid, sodium hydroxide (NaOH), hydrochloric acid (HCl) buffer reagent into 20 wt% concentrated RSF aqueous solution in the volume ratio of 1:2. Then the solutions were condensed by forced airflow at an airflow rate of 5 ±1 m/s to different concentrations at 10 ºC and 50±5% relative humidity. Then electrospinning technique was used to prepare the silk fibers. In the electrospinning process, a high potential was applied to a wire connected with a syringe filled with 5 mL of RSF solution. The internal diameter of the syringe tip was 0.6 mm and the flow rate of the solution was 2.0 mL/h. The electric field was 4 kV/cm and the electrospinning process was carried out at ambient temperature [67]. The results indicated that reduction of solution pH caused a decrease in the concentration of aqueous silk fibroin solutions that could be electrospun. Moreover, the average diameter and diameter distributions of the electrospun silk fibers became smaller and narrower due to the decrease in spinnable solution concentration. With the combined reduction in pH and concentration, the morphology of the electrospun silk fibers changed from ribbon-like to a uniform cylinder. An average diameter of 265 nm was obtained from 25% (w/v) silk fibroin solution at pH of 4.8. However, when electrospinning was performed using silk fibroin solution at pH 6.9, mimicking the posterior division of silkworm gland, only a solution greater than 33% (w/v) was capable of forming fibers. An average diameter of 850 nm was obtained under these conditions, which is smaller than native silk fibers (~15μm) [6]. The conformation of the electrospun silk

fibers was characterized by RS, WAXD and DSC. It was found that electrospun fibers were predominantly random coil/silk I conformation [67].

Zhang *et al*. (2009) studied the structure of the electrospun SF nanowebs produced from HFIP and formic acid solutions and whether cell behaviour is affected by the solvent used in electrospinning. Their study proved that the SF nanowebs electrospun from HFIP and formic acid showed a difference in fiber diameter. Their results indicated that the electrospinning solvent of formic acid and HFIP would not affect the cytocompatibility of SF fiber mats, and the two kinds of electrospun SF fiber mats showed generally similar adhesion activity [68].

Zhou *et al*. (2009) investigated the producibility of seamless and porous tubular scaffold from silk fibroin without any additives and organic solvents and effects of electrospinning parameters including voltage, collection distance, solution concentration on the morphology and diameter distribution of regenerated silk fibroin fibers. Afterwards, SF tubular scaffold composed of homogenous fibers was fabricated at voltage of 18 kV, collection distance of 18 cm, concentration of 37%, and flow rate of 0.15 mL/min and the structure and properties of tubular scaffold before and after methanol treatment were further studied to evaluate its potential application [69].

3. EXPERIMENTAL

3.1 Materials and Equipment

3.1.1 Cocoons

'A' quality dried *B. mori* silkworm cocoons were kindly supplied from Kozabirlik. They were cut open and the pupas were removed before the process and cleared from the vegetative remnants. Then the cocoons were cut into small pieces.

3.1.2 Chemicals

Na_2CO_3, $CaCl_2.2H_2O$, CH_3CH_2OH, HFIP, 85% formic acid, 98% formic acid were used in the study and they were supplied from domestic suppliers.

3.1.3 Dialysis cassettes

Slide-A-Lyzer G2 Dialysis Cassettes with MWCO of 3.5K, sample volume capacity of 30mL were used for the fibroin purification. They were supplied from Thermo Fisher Scientific Inc.

The Slide-A-Lyzer Dialysis Cassettes are constructed of dialysis membranes separated by an inert gasket and sandwiched between two halves of a translucent plastic case that is sonically welded together.

The dialysis membrane is composed of low-binding regenerated cellulose for maximum sample recovery while maintaining maximum sample purity. The membranes have a symmetrical pore structure that allows small molecules to migrate across them in either direction.

For practical use, a membrane with a MWCO of 1/3 the molecular weight of the molecule of interest is chosen to ensure good sample recovery. However, the membrane MWCO should also be large enough to facilitate efficient separation of the small molecules that need to be removed. It is also important to consider the buffer system, as pH and other factors can alter the size, three-dimensional shape and

charge of proteins and thus affect their ability to pass through the pores of the membrane [54].

3.1.4 Freeze-dryer

Freeze dryer of Christ ALPHA 1-4 LD Plus type was used for the removal of water from the dialysed aqeous fibroin solution.

3.1.5 Electrospinning setup

The electrospinning setup used in this study was parallel positioned and consisted of a high voltage power supply which can supply positive voltage from 0 to 30 kV, a syringe pump and a rectangular (10×10cm) aluminum foil collecting plate.

3.2 Method

3.2.1 Preparation of regenerated silk fibroin

B. mori silk fibroin was prepared by boiling 25 g of cocoons in 500 mL aqueous solution of Na_2CO_3 (2 g/l) for 40 min, and then rinsing thoroughly with distilled water to extract the glue-like sericin proteins. The rinsed silk was air-dried and the degumming ratio was calculated as 27.8%. Then 5 grams of silk fibroin was dissolved in 50mL of $CaCl_2/H_2O/CH_3CH_2OH$ (mole ratio 1:8:2) solution at 80ºC in 40 minutes. The fibroin solution was filtered and dialysed against distilled water for 3 days, using Slide-A-Lyzer dialysis cassettes to remove $CaCl_2$ and CH_3CH_2OH. After filtrating, the clear fibroin aqueous solution was obtained and it was lyophilized to obtain regenerated SF sponges. The lyophilization was carried out at three stages as freezing at -25 ºC for 24 h, primary drying at -40 ºC for 24 h and secondary drying at -60 ºC for 24 h.

3.2.2 Preparation of the electrospinning solutions

SF solutions were prepared by dissolving the regenerated SF sponges in 85% formic acid and 98% formic acid for 3 hours. Concentrations of the SF solutions for electrospinning was in the range from 6% to 18% by weight.

3.2.3 Electrospinning

The first set of parameters was determined according to the literature. Due to the fact that SEM imaging of all the samples was not possible, the improvement was realized by visual evaluation of both the electrospinning process and the corresponding electrospun nanowebs.

The syringe was filled with 5 mL of fibroin solution and high voltage was applied to the needle. Constant volume flow rate was maintained using a syringe pump. The fibers were collected on the aluminum foil.

The purpose of the study which is to produce nanoscale uniform fibers from silk fibroin with electrospinning was achieved through electrospinning of 112 samples with different parameters as seen in Table 3.1.

Table 3.1: Parameters used in the electrospinning of silk fibroin

SAMPLE	concentration %	needle mm	voltage kV	flow rate mL/h	distance cm
es1	15%	0.8*	20	1.000	12
es2	15%	0.8*	20	1.000	10
es3	15%	0.8*	20	0.800	10
es4	15%	0.8*	20	0.600	10
es5	15%	0.8*	20	0.400	10
es6	15%	0.8*	20	0.200	10
es7	15%	0.8*	15	0.200	10
es8	15%	0.8*	17.5	0.200	10
es9	15%	0.8*	15	0.200	12
es10	15%	0.8*	15	0.200	7
es11	15%	0.8*	15	0.400	10
es12	15%	0.8*	15	0.400	12
es13	15%	0.8*	15	0.400	8
es14	15%	0.7*	15	0.200	10
es15	15%	0.7*	15	0.400	10
es16	15%	0.7*	15	0.600	10
es17	15%	0.7*	20	0.600	10
es18	15%	0.7*	20	0.400	10
es19	15%	0.7*	20	0.200	10
es20	15%	0.7*	20	0.100	10
es21	15%	0.7*	17	0.200	10
es22	15%	0.7*	22	0.200	10
es23	15%	0.8*	15	0.200	15
es24	15%	0.8*	20	0.400	12

Table 3.1 (continued): Parameters used in the electrospinning of silk fibroin

SAMPLE	concentration %	needle mm	voltage kV	flow rate mL/h	distance cm
es25	15%	0.9*	20	0.400	12
es26	15%	0.7*	20	0.200	10
es27	15%	0.7*	20	0.100	10
es28	15%	0.9*	15	0.200	10
es29	15%	0.9*	15	0.100	10
es30	15%	0.9*	17,5	0.100	10
es31	15%	0.9*	20	0.100	10
es32	15%	0.9*	22	0.100	10
es33	15%	0.9*	17,5	0.200	10
es34	15%	0.9*	20	0.200	10
es35	15%	0.9*	20	0.200	7
es36	15%	0.9*	20	0.100	7
es37	15%	0.9*	20	0.100	5
es38	15%	0.9*	17	0.100	5
es39	15%	0.9*	15	0.100	5
es40	15%	0.9*	15	0.200	5
es41	15%	0.9*	15	0.400	5
es42	15%	0.8*	15	0.200	5
es43	15%	0.8*	15	0.100	10
es44	15%	0.8*	15	0.100	7
es45	15%	0.8*	15	0.100	12
es46	15%	0.7*	15	0.400	10
es47	15%	0.7*	17	0.400	10
es48	15%	0.7*	22	0.400	10
es49	15%	0.7*	20	0.200	7
es50	15%	0.7*	20	0.200	12
es51	15%	1.2	15	0.100	10
es52	12%	0.8*	15	0.100	10
es53	12%	0.8*	15	0.100	7
es54	12%	0.8*	15	0.200	7
es55	12%	0.8*	15	0.200	5
es56	12%	0.8*	15	0.200	12
es57	12%	0.8*	15	0.200	10
es58	12%	0.8*	15	0.300	10
es59	12%	0.8*	17,5	0.300	10
es60	12%	0.8*	18	0.200	10
es61	12%	0.8*	15	0.250	10
es62	12%	0.8*	20	0.300	10
es63	12%	0.8*	20	0.400	10
es64	12%	0.8*	15	0.400	10
es65	10%	0.8*	15	0.200	7

Table 3.1 (continued): Parameters used in the electrospinning of silk fibroin

SAMPLE	Concentration %	needle mm	voltage kV	flow rate mL/h	distance cm
es66	10%	0.8*	15	0.200	10
es67	15%	0.8*	15	0.100	10
es68	15%	0.8*	15	0.100	7
es69	10%	0.8*	15	0.130	10
es70	10%	0.8*	15	0.130	7
es71	12%	18g	15	0.030	10
es72	12%	18g	15	0.048	10
es73	12%	18g	15	0.100	10
es74	12%	18g	15	0.066	10
es75	15%	18g	15	0.066	10
es76	10%	18g	15	0.030	10
es77	15%	18g	15	0.030	10
es78	15%	18g	15	0.018	10
es79	12%	1.2	15	0.050	10
es80	12%	1.2	15	0.050	7
es81	12%	1.2	15	0.050	13
es82	12%	1.2	15	0.080	10
es83	12%	1.2	15	0.110	10
es84	12%	1.2	18	0.080	10
es85	12%	1.2	21	0.080	10
es86	12%	0.9*	15	0.080	10
es87	12%	0.8*	15	0.080	10
es88	12%	0.7*	15	0.080	10
es89	18%	18g	15	0.030	10
es90	18%	18g	15	0.018	10
es91	18%	18g	20	0.030	10
es92	18%	18g	10	0.030	10
es93	18%	1.25	15	0.018	10
es94	18%	0.70	15	0.018	10
es95	18%	0.90	15	0.018	10
es96	18%	1.06	15	0.018	10
es97	18%	0.8*	15	0.018	10
es98	12%	1.25	15	0.018	10
es99	12%	0.70	15	0.018	10
es100	12%	0.90	15	0.018	10
es101	12%	1.06	15	0.018	10
es102	12%	0.8*	15	0.018	10
es103	12%	18g	15	0.018	10
es104	18%	0.7	15	0.006	10
es105	18%	0.8*	15	0.006	10
es106	18%	0.7	15	0.003	10

Table 3.1 (continued): Parameters used in the electrospinning of silk fibroin

SAMPLE	concentration %	needle mm	voltage kV	flow rate mL/h	distance cm
es107	12%	1.25	15	0.030	10
es108	12%	0.7	20	0.018	10
es109	12%	0.7	10	0.018	10
es110	12%	0.7	15	0.018	5
es111	12%	0.7	15	0.018	13
es112	12%	0.7	25	0.018	10

After determining the parameters which were best for the production of uniform silk fibroin fibers, silk fibroin nanowebs were electrospun from solutions with concentrations of 6, 8, 10, 12, 15 and 18 wt%, by changing the high voltage from 10 kV to 25 kV, distance from 5 cm to 15 cm, flow rate from 0.003mL/h to 2.0 mL/h. Needles with diameters of 1.25 mm, 1.06 mm, 0.90 mm and 0.70 mm were used to determine the effect of needle diameter on the bead formation and fiber diameter.

3.2.4 Characterization

Fourier transform infrared (FTIR) spectrum was obtained in the spectral region of 400–4,000 cm^{-1} to observe the structural and conformational changes in silk fibroin.

Fourier transform infrared spectroscopy (FTIR) is an analytical technique for material analysis. An infrared spectrum represents a fingerprint of a sample with absorption peaks which correspond to the frequencies of vibrations between the bonds of atoms making up the material. Because each different material is unique in combination of atoms, no two compounds produce the exact same infrared spectrum. Therefore infrared spectroscopy can result in qualitative analysis of every different kind of material [70].

In protein analysis, the FTIR provides information about the secondary structure of proteins. Characteristic bands found in the infrared spectra of proteins include the amide I and amide II which arise from the amide bonds that link the aminoacids. The absorption associated with the Amide I band leads to stretching vibrations of C=O bond of the amide, the absorption associated with the amide II band leads to bending vibrations of the N-H bond.

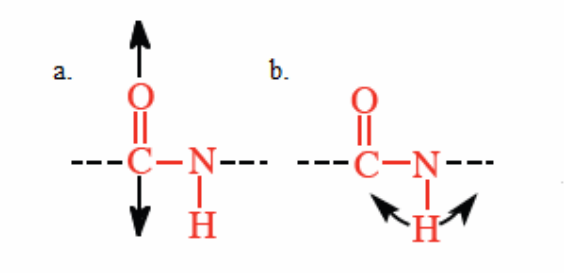

Figure 3.1 : Vibrations of a. Amide I; b.Amide II

Because both the C=O and the N-H bonds are involved in the hydrogen bonding that takes place between the different elements of secondary structure, the locations of both the amide I and amide II bands are sensitive to the secondary structure content of a protein. (Figure 3.2) [71].

Since silk fibroin is also a protein, the structural and conformational changes can be examined from the characteristic bands of silk fibroin which are located in the range of 1,600 – 1,690 cm^{-1} for amide I and 1,480 – 1,575 cm^{-1} for amide II.

The bead formation and fiber diameters were examined by field emission scanning electron microscope (Supra 50 VP FESEM) after the nanowebs had been coated with gold.

The average fiber diameter and its distribution were determined from 100 random fibers obtained from each spinning conditions. The diameters were measured using Analyzing Digital Images Software.

3.2.5 Statistical analysis

The fiber diameter distributions were assumed as normal to carry out statistical analysis on data. SPSS (**S**tatistical **P**ackage for the **S**ocial **S**ciences) program was used for statistical analysis and Oneway Anova was applied in order to approve whether the differences between mean diameters were of real importance.

3.3 Results and Discussion

3.3.1 FTIR spectroscopy

The FTIR spectrum of degummed silk fibroin and electrospun SF nanoweb is represented in Figures 3.2 and 3.3 respectively.

Fibroin protein in the electrospun nanowebs was confirmed by absorption bands at amide I, amide II and amide III regions on the FTIR spectrum.The degummed silk fibroin was characterized by absorption bands at 1,621 cm^{-1} (amide I) and 1,514cm^{-1} (amide II) which is attributed to the β-sheet conformation and the structure of the electrospun nanowebs was characterized by absorption bands at 1648 cm^{-1} (amide I) and 1535 cm^{-1} (amide II) which is attributed to the random coil or α-helix (random coil form and silk I were not differentiated because of the similarity between their infrared spectra).

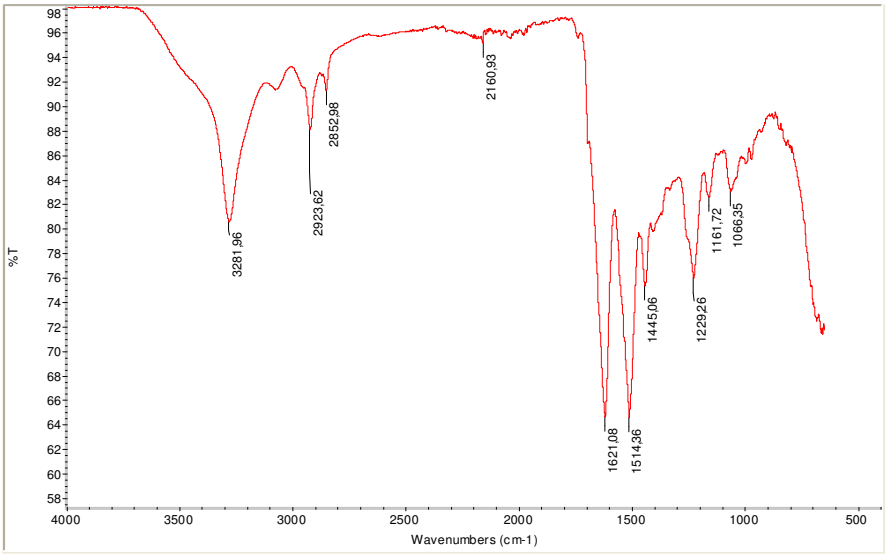

Figure 3.2 : FTIR spectra of degummed silk fibroin

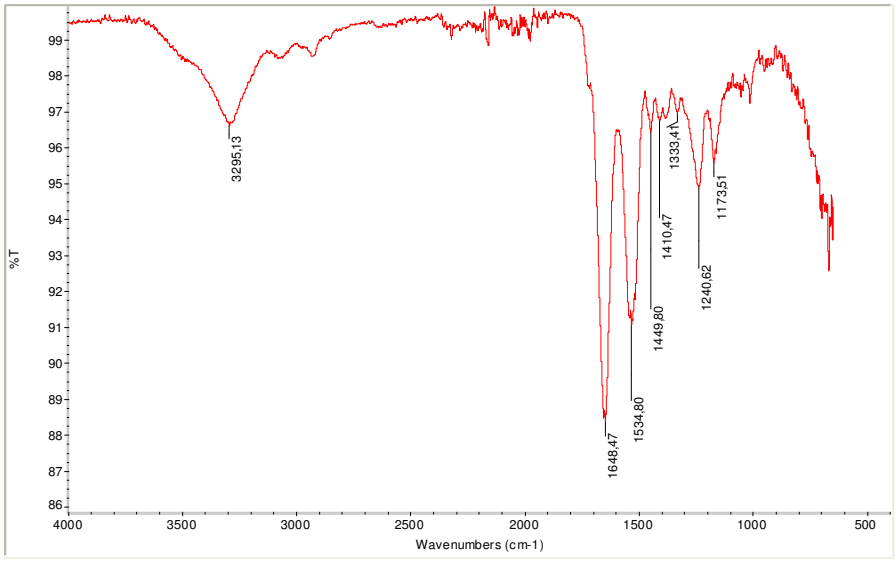

Figure 3.3 : FTIR spectra of electrospun SF nanoweb

These band shifts occurred because of the distinct hydrogen bonding states produced by the different conformations adopted by the protein chains [72].

3.3.2 Effect of concentration on bead formation and fiber diameter

SF solutions with concentrations of 6, 8, 10, 12, 15, and 18 wt% were prepared. During the electrospinning process, it was observed that silk fibroin concentration played a major role in fiber spinnability. No fibers were formed at concentrations below 10% for any electric field and spinning distances and only drops of solution were seen on the collector. For fiber formation to occur, a minimum solution concentration of 10% was required.

Samples were prepared from the solutions with concentrations of 10, 12, 15 and 18% in order to study the effect of concentration on bead formation and fiber diameter. The samples and the parameters used in the electospinning process are listed in Table 3.2.

Table 3.2: Samples prepared from solutions with different concentrations

Sample Nr.	concentration %	needle mm	voltage kV	flow rate mL/h	distance cm
es76	10%	18G	15	0.03	10
es71	12%	18G	15	0.03	10
es77	15%	18G	15	0.03	10
es89	18%	18G	15	0.03	10

SEM images of the samples are shown in Figure 3.4.

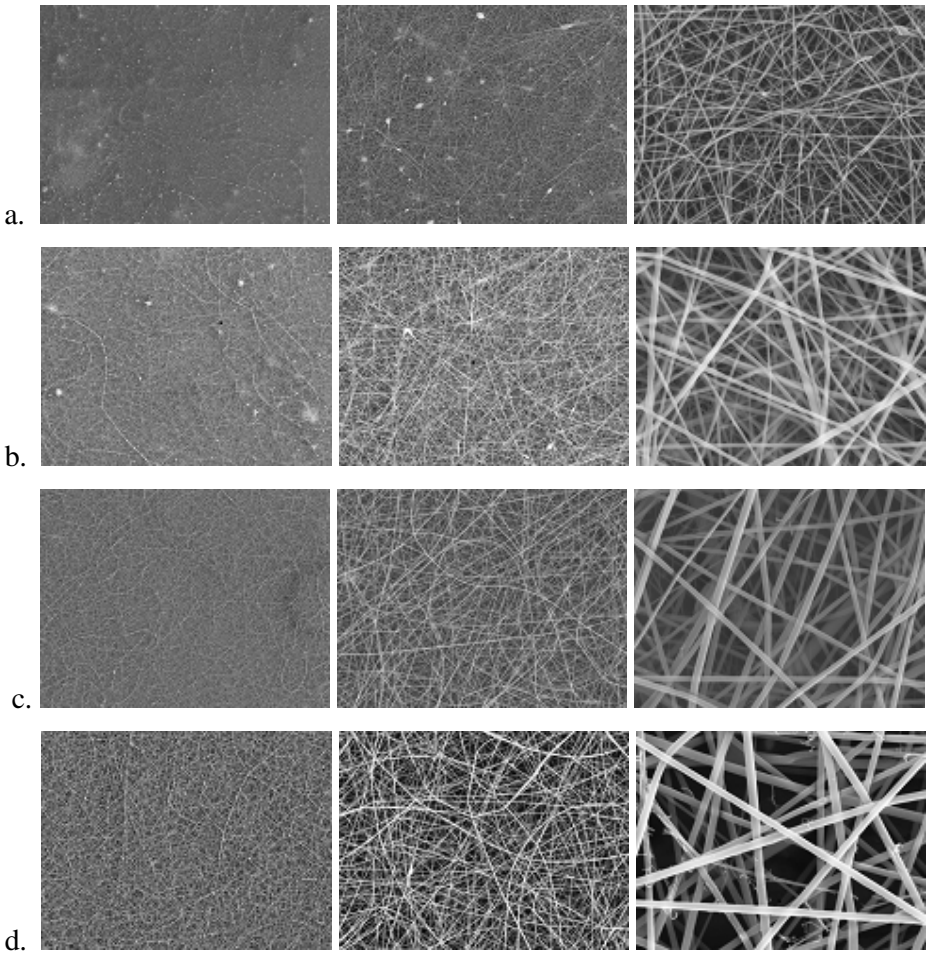

Figure 3.4 : SEM images of nanowebs which were electrospun from solutions with different concentrations a. es76, b. es71, c. es77 d. es89

The increase in concentration affected the formation of beads. At the concentration of 10%, fibers together with droplets and beads were observed. Also there were some broken ends. This showed that the fiber formation was intermittent which can be attributed to the inadequate entanglement of the macromolecules in the fibroin solution. At a higher concentration of 12%, the fibers were continuous and beaded fibers became fewer. Continuous and more uniform fibers were obtained at the concentrations above 12%. The concentration of 12% appears to correspond to the onset of the viscosity as represented in Figure 3.5. At concentrations above 12%, the viscosity increases dramatically, which indicates that there are extensive chain entanglements at this concentration. At the concentrations of 15% and 18%, beads disappeared and uniform fibers were obtained regardless of electric field and distance [73].

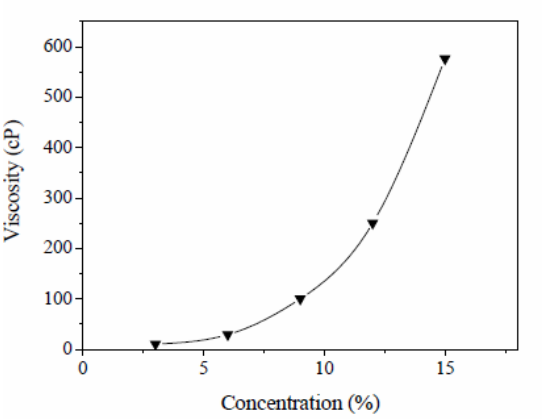

Figure 3.5 : Variation in viscosity with the concentration of SF in formic acid.

Therefore, it can be concluded that extensive chain entanglements are necessary to produce continuous fibers by electrospinning.

It is also reported in the literature that the beads and droplets form if the solution reaches the collection plate before the solvent fully evaporates [64]. This explains the formation of droplets and beads at the concentrations below 12%.

Diameters of randomly selected 100 fibers were measured and fiber diameter distributions of each sample can be seen in Figure 3.6

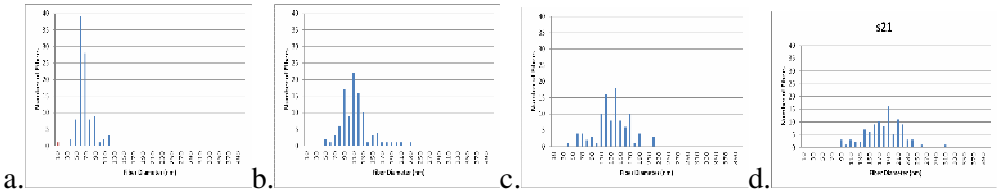

Figure 3.6 : Fiber diameter distributions of nanowebs which were electrospun from solutions with different concentrations a.es76; b.es71; c.es77; d.es89

The sample es76 which was electrospun from the solution with a concentration of 10% had the smallest mean diameter and narrowest fiber diameter distribution. Fiber diameter distributions became broader with the increasing concentration.

The mean fiber diameters of each sample together with the minimum and maximum values, standard deviation, and lower and upper bounds of 95% confidence interval can be seen in Table 3.3.

Table 3.3: Descriptives for the samples es76, es71, es77, es89

Sample Nr (concentration%)	N	Mean	Std. Deviation	Std. Error	95% Confidence Interval for Mean Lower Bound	95% Confidence Interval for Mean Upper Bound	Min.	Max.
es76 (10%)	100	**63.46**	15.89707	1.58971	60.3087	66.6173	37.50	112.50
es71 (12%)	100	**107.53**	31.15303	3.11530	101.3506	113.7134	41.20	223.50
es77 (15%)	100	**130.83**	45.34823	4.53482	121.8399	139.8361	37.50	418.80
es89 (18%)	100	**173.83**	38.58498	3.85850	166.1829	181.4951	81.30	306.30
Total	400	**118.91**	52.70647	2.63532	113.7371	124.0989	37.50	418.80

The mean diameters calculated from the measurements of 100 random fibers were 63.46 nm, 107.53 nm, 30.84 nm, and 173.84 nm for the concentrations of 10, 12, 15, and 18%, respectively. The change of mean fiber diameter versus concentration is illustrated in Figure 3.7.

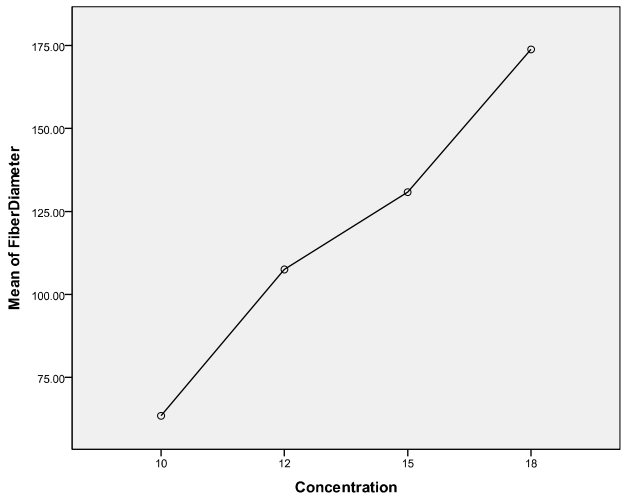

Figure 3.7 : Mean plots for nanowebs which were electrospun from solutions with different concentrations

The diameters of fibers increased with the increase in concentration. At 18%, the mean fiber diameter was much larger than that of fibers spun at lower concentrations.

The increase in fiber diameter with increase in concentration is thought to be the reason of increased SF macromolecule entanglements in the solution [69]**.**

The variance analysis was carried out by applying Oneway Anova Method to decide whether the diferences were of real importance. The Oneway Anova statistical evaluation can be seen in Table 3.4.

Table 3.4: Oneway Anova table for the samples es76, es71, es77, es89

Fiber Diameter

	Sum of Squares	df	Mean Square	F	**Sig.**
Between Groups	636330.066	3	212110.022	177.926	**0.000**
Within Groups	472080.564	396	1192.123		
Total	1108410.630	399			

It is approved that the difference between the mean diameters of the samples electrospun with different concentrations are significant at 95% confidence interval since the significance is 0.0 which is less than 0.05.

Multiple comparisons showed that the differences within groups were of real significance. The multiple comparisons can be seen in Table 3.5.

Table 3.5: Multiple comparisons for the samples es76, es71, es77, es89

Fiber Diameter

		Mean			95% Confidence Interval	
(I) % Concentration	**(J) % Concentration**	Difference (I-J)	Std. Error	**Sig.**	Lower Bound	Upper Bound
10	**12**	-44.06900*	4.88287	**0.00**	-53.6686	-34.4694
	15	-67.37500*	4.88287	**0.00**	-76.9746	-57.7754
	18	-110.37600*	4.88287	**0.00**	-119.9756	-100.7764
12	**10**	44.06900*	4.88287	**0.00**	34.4694	53.6686
	15	-23.30600*	4.88287	**0.00**	-32.9056	-13.7064
	18	-66.30700*	4.88287	**0.00**	-75.9066	-56.7074
15	**10**	67.37500*	4.88287	**0.00**	57.7754	76.9746
	12	23.30600*	4.88287	**0.00**	13.7064	32.9056
	18	-43.00100*	4.88287	**0.00**	-52.6006	-33.4014
18	**10**	110.37600*	4.88287	**0.00**	100.7764	119.9756
	12	66.30700*	4.88287	**0.00**	56.7074	75.9066
	15	43.00100*	4.88287	**0.00**	33.4014	52.6006

*. The mean difference is significant at the 0.05 level.

These results proved that the concentration was of great importance in affecting the bead formation and fiber diameter. The results were consistent with the studies in the literature.

3.3.3 Effect of applied voltage on bead formation and fiber diameter

The effect of the applied voltage was studied on two sets of samples prepared by changing only the applied voltage (and keeping all the other parameters constant).

Itis observed that the applied voltage had an effect on electrospinning in terms of fiber jet formation. Fiber jets were induced when a voltage of 8 kV was applied to the 12% SF solution. It was also observed that higher voltages were needed to initiate the fiber formation when working with higher concentrations. This suggested that the increased macromolecular entanglements could be overcome by the increased electrostatic forces.

The samples prepared are listed in Table 3.6 together with the parameters used in the electrospinning process. The samples were prepared from a solution with a concentration of 12% in order to see the effect of voltage on both bead formation and fiber diameter. Then a solution with a concentration of 18% was electrospun to see the effect of applied voltage on beadless fibers.

Table 3.6: Samples prepared at different voltages

Sample Nr.	concentration %	needle mm	voltage kV	flow rate mL/h	distance cm
Sample Set 1					
es82	12%	1.2	15	0.080	10
es84	12%	1.2	18	0.080	10
es85	12%	1.2	21	0.080	10
Sample Set 2					
es109	12%	0.7	10	0.018	10
es99	12%	0.7	15	0.018	10
es108	12%	0.7	20	0.018	10
es112	12%	0.7	25	0.018	10

SEM images of the samples are shown in Figure 3.8 and 3.9 for the sample set 1 and sample set 2, respectively.

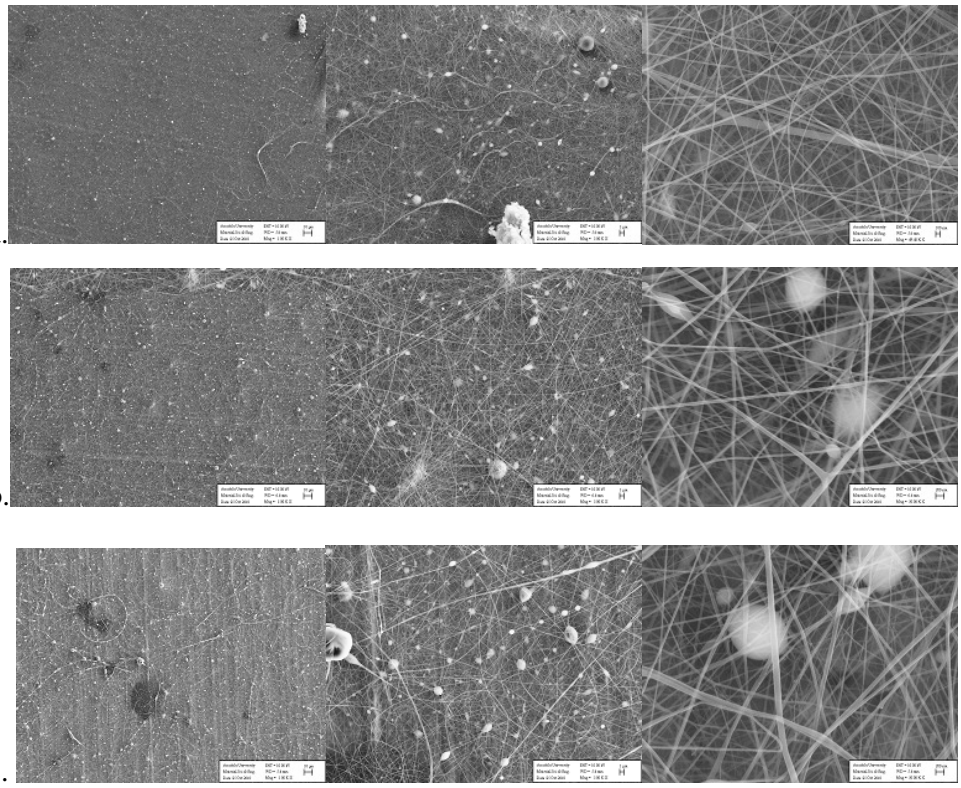

Figure 3.8 : SEM images of nanowebs which were electrospun at different voltages a. es82; b. es84; c. es85 (sample set 1)

a.

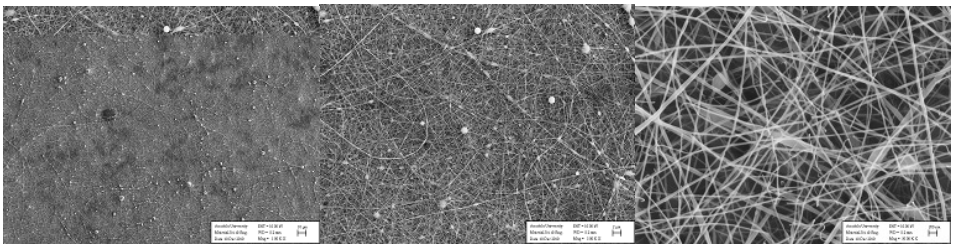

b.

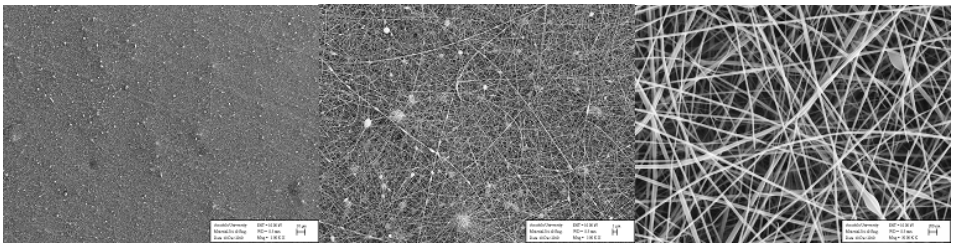

c.

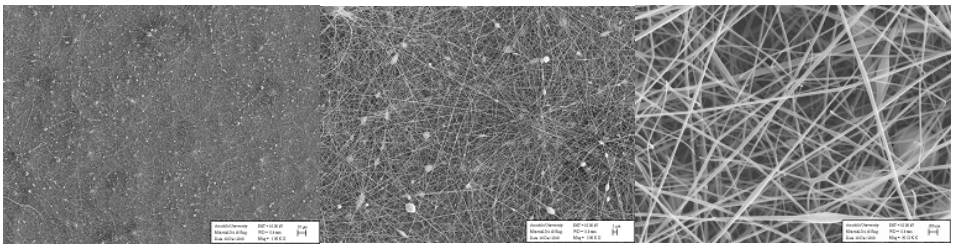

d.

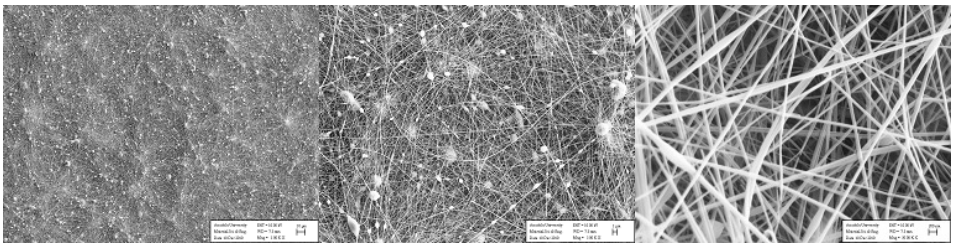

Figure 3.9 : SEM images of nanowebs which were electrospun at different voltages a. es109; b. es99; c. es108; d. es112 (sample set 2)

The number and size of the beads increased in response to the increase in applied voltage in both of the sample sets. With the increase in applied voltage, the acceleration of the jet increases and this allows less time for the solvent to evaporate and polymer to be elongated [7] which results in increased bead formation. This result is consistent with the studies in the literature. It was observed that for the PEO/water system, the fiber morphology changed from a defect free fiber at an initiating voltage of 5.5 kV to a highly beaded structure at a voltage of 9.0 kV. The occurrence of beaded morphology has been correlated to a steep increase in the spinning current, which controls the bead formation in the electrospinning process [35].

Diameters of randomly selected 100 fibers were measured and fiber diameter distributions of each sample can be seen in Figure 3.6

a. 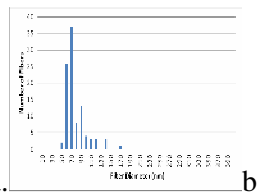 b. 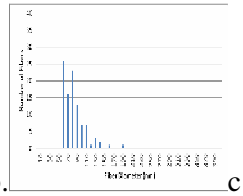 c. 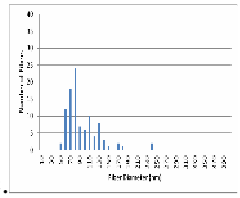

Figure 3.10 : Fiber diameter distributions of nanowebs which were electrospun at different voltages a. es82, b. es84, c. es85 (sample set 1)

a. 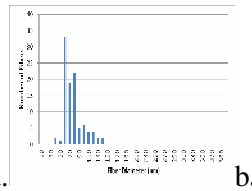 b. 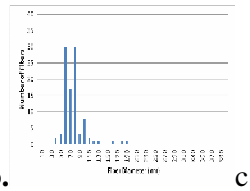 c. 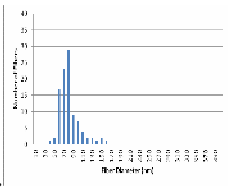 d. 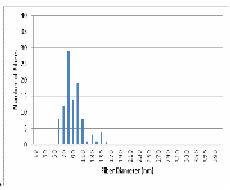

Figure 3.11 : Fiber diameter distributions of nanowebs which were electrospun at different voltages a.es109; b.es99; c.es108; d.es112 (sample set 2)

In Sample Set 1, broader fiber diameter distributions were observed in response to increase in applied voltage. Fiber diameters were distributed in 43.80–168.80 nm range at the voltage of 15 kV, compared with the fiber diameters electrospun at 18kV which were distributed in 51.61–187.10 nm and at 21kV which were mainly distributed in 45.16–238.71 nm. In Sample Set 2, there wasn't any important difference observed between the distributions.

The mean fiber diameters of each sample together with the minimum and maximum values, standard deviations, and lower and upper bounds of 95% confidence interval can be seen in Table 3.7 and 3.8 for sample set 1 and sample set 2 respectively.

Table 3.7: Descriptives for sample set 1

Fiber Diameter

Sample Nr (Voltage)	N	Mean	Std. Deviation	Std. Error	95% Confidence Interval Lower Bound	95% Confidence Interval Upper Bound	Min.	Max.
es82 (15kV)	100	**71.9000**	21.55355	2.15536	67.6233	76.1767	43.80	168.80
es84 (18kV)	100	**77.9997**	23.96714	2.39671	73.2441	82.7553	51.61	187.10
es85 (21kV)	100	**88.8392**	35.44181	3.54418	81.8068	95.8716	45.16	238.71
Total	300	**79.5796**	28.44559	1.64231	76.3477	82.8116	43.80	238.71

Table 3.8: Descriptives for sample set 2

Fiber Diameter

Sample Nr. (Voltage)	N	Mean	Std. Deviation	Std. Error	95% Confidence Interval Lower Bound	95% Confidence Interval Upper Bound	Min.	Max.
es109 (10kV)	100	**71.2270**	21.67824	2.16782	66.9256	75.5284	38.70	135.50
es99 (15kV)	100	**71.6190**	23.39954	2.33995	66.9760	76.2620	38.70	180.60
es108 (20kV)	100	**76.3890**	21.29672	2.12967	72.1633	80.6147	38.70	154.80
es112 (25kV)	100	**85.5510**	21.78472	2.17847	81.2284	89.8736	51.60	154.80
Total	400	**76.1965**	22.71842	1.13592	73.9634	78.4296	38.70	180.60

For both set of samples, an increasing trend is observed in the mean fiber diameters in response to the increase in applied voltage. The change of mean fiber diameter versus applied voltage is illustrated in Figure 3.13 for Sample Set 1 and Sample 2.

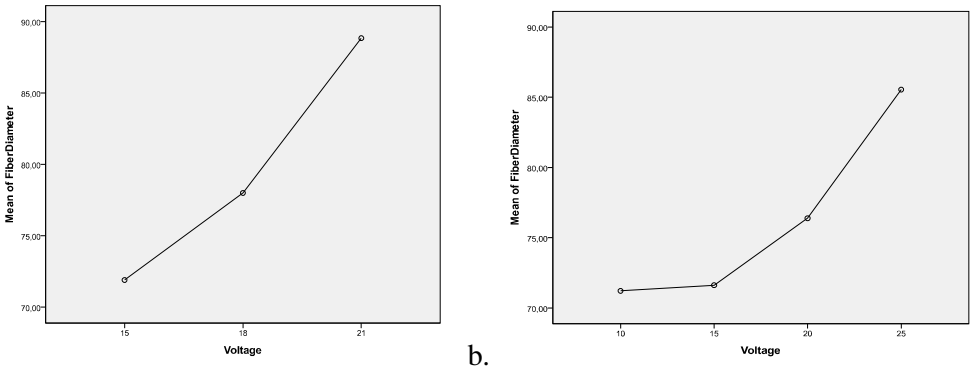

a. b.

Figure 3.12 : Mean plots for nanowebs which were electrospun at different voltages a. sample set 1, b. sample set 2

When the applied voltage was increased from 10 to 21 kV, the mean fiber diameter increased from 71.9 to 88.8 nm in Sample Set 1 and when the applied voltage was increased from 10 to 25 kV, the mean fiber diameter increased from 71.2 to 85.5 nm in Sample Set 2.

The increase in fiber diameter with increase in concentration is thought to be the reason of more solution ejection which facilitates the formation of larger diameter fibers [69**].**

The variance analysis was carried out by applying Oneway Anova Method to decide whether the diferences were of real importance. The Oneway Anova statistical evaluation can be seen in Table 3.9 and 3.10 for sample set 1 and 2, respectively.

Table 3.9: Oneway Anova table for sample set 1

Fiber Diameter

	Sum of Squares	df	Mean Square	F	**Sig.**
Between Groups	14721.253	2	7360.627	9.621	**0.000**
Within Groups	227215.074	297	765.034		
Total	241936.327	299			

Table 3.10: Oneway Anova table for sample set 2

Fiber Diameter

	Sum of Squares	df	Mean Square	F	**Sig.**
Between Groups	13319.316	3	4439.772	9.128	**0.000**
Within Groups	192615.279	396	486.402		
Total	205934.595	399			

It is approved that the difference between the mean diameters of the samples electrospun at different voltages are significant at 95% confidence interval since the significance is 0.0 which is less than 0.05.

There is no consensus in the literature regarding the effect of the applied voltage on the fiber diameter. Some of the researchers have suggested that when higher voltages are applied, there is more polymer ejection and this facilitates the formation of a larger diameter fiber. Other authors have reported that an increase in the applied voltage, increases the electrostatic repulsive force on the fluid jet which ultimately favours the narrowing of fiber diameter [8]. The results found in this study, are not consistent with Reneker and Chun who showed that there is not much effect of electric field on the fiber diameter with electrospinning of PEO, Megelski *et al.* who observed a decrease from 20 μm to 10 μm with an increase in voltage from 5 kV to 12 kV while electrospinning PS, Buchko *et al.*,who observed a decrease in the fiber diameter with an increase in the applied voltage while spinning silk like polymer fiber with fibronectin functionality (SLPF) [35], and Larrondo and Manley who showed the decrease of fiber diameter by roughly half by doubling the applied electric field [8].

Multiple comparisons were carried out to evaluate the significance of differences between the two means, results of which are represented in Table 3.11 and Table 3.12 for the Sample Set 1 and Sample Set 2, respectively.

Table 3.11: Multiple comparisons for sample set 1

(I) Voltage	(J) Voltage	Mean Difference (I-J)	Std. Error	Sig.	95% Confidence Interval Lower Bound	95% Confidence Interval Upper Bound
15	**18**	-609970	3.91161	**0.120**	-13.7977	1.5983
	21	-16.93920*	3.91161	**0.000**	-24.6372	-9.2412
18	**15**	6.09970	3.91161	**0.120**	-1.5983	13.7977
	21	-10.83950*	3.91161	**0.006**	-18.5375	-3.1415
21	**15**	16.93920*	3.91161	**0.000**	9.2412	24.6372
	18	10.83950*	3.91161	**0.006**	3.1415	18.5375

*. The mean difference is significant at the 0.05 level.

Table 3.12: Multiple comparisons for sample set 2

(I) Voltage	(J) Voltage	Mean Difference (I-J)	Std. Error	Sig.	95% Confidence Interval Lower Bound	95% Confidence Interval Upper Bound
10	**15**	-0.39200	3.11898	**0.900**	-6.5238	5.7398
	20	-5.16200	3.11898	**0.099**	-11.2938	0.9698
	25	-14.32400*	3.11898	**0.000**	-20.4558	-8.1922
15	**10**	0.39200	3.11898	**0.900**	-5.7398	6.5238
	20	-4.77000	3.11898	**0.127**	-10.9018	1.3618
	25	-13.93200*	3.11898	**0.000**	-20.0638	-7.8002
20	**10**	5.16200	3.11898	**0.099**	-0.9698	11.2938
	15	4.77000	3.11898	**0.127**	-1.3618	10.9018
	25	-9.16200*	3.11898	**0.004**	-15.2938	-3.0302
25	**10**	14.32400*	3.11898	**0.000**	8.1922	20.4558
	15	13.93200*	3.11898	**0.000**	7.8002	20.0638
	20	9.16200*	3.11898	**0.004**	3.0302	15.2938

*. The mean difference is significant at the 0.05 level.

Multiple comparisons show that the difference between the mean diameters of fibers which were electrospun at voltages of 10 and 15 kV was not of real importance (Sig.= 0.9>0.05), whereas the difference between the mean diameters of fibers which were electrospun at voltages of 10 and 25 kV was of real importance (Sig.= 0.0<0.05). Increase in voltage from 10 to 25 kV, 15 to 25 kV and 20 to 25 kV resulted in significant differences in mean fiber diameters (at 95% confidence interval). It can be concluded that, at higher voltages, important differences are obtained in response to minor changes in the applied voltage whereas at lower voltages, important differences are only obtained in response to major changes in the applied voltage.

Thus, voltage influences the bead formation and fiber diameter, but the level of significance varies with the range of the applied voltage.

3.3.4 Effect of flow rate on bead formation and fiber diameter

The flow rate is to be set to a value which keeps the solution at the tip of the needle without dripping and maintains a stable Taylor cone. It is observed that the cone shape at the tip of the needle cannot be maintained if the flow of the solution through the needle is insufficient. However, if the flow rate is higher, the stability of the cone shape cannot be maintained at the constant voltage.

In the literature, generally flow rates in the range of 1-4 mL/h have been used in electrospinning of silk fibroin. In this study, the optimal conditions were achieved by controlling the shape of the Taylor cone and it was not possible to maintain a stable cone shape when the flow rate exceeded the value of 0.03 mL/h at the applied voltage of 15 kV. A lot of solution waste occured without adequately differentiating into fibers with higher flow rates.

The effect of the flow rate was studied on two sets of samples prepared by changing only the flow rate (keeping all the other parameters constant). The samples prepared are listed in Table 3.13 together with the parameters used in the electrospinning process.

Table 3.13: Samples electrospun with different flow rates

Sample Nr.	concentration %	needle mm	voltage kV	flow rate mL/h	distance cm
Sample Set 1					
es71	12%	18g	15	0.030	10
es72	12%	18g	15	0.048	10
es74	12%	18g	15	0.066	10
Sample Set 2					
es106	18%	0.7	15	0.003	10
es104	18%	0.7	15	0.006	10
es94	18%	0.7	15	0.018	10

SEM images and fiber diameter distributions of sample set 1 are shown in Figure 3.14.

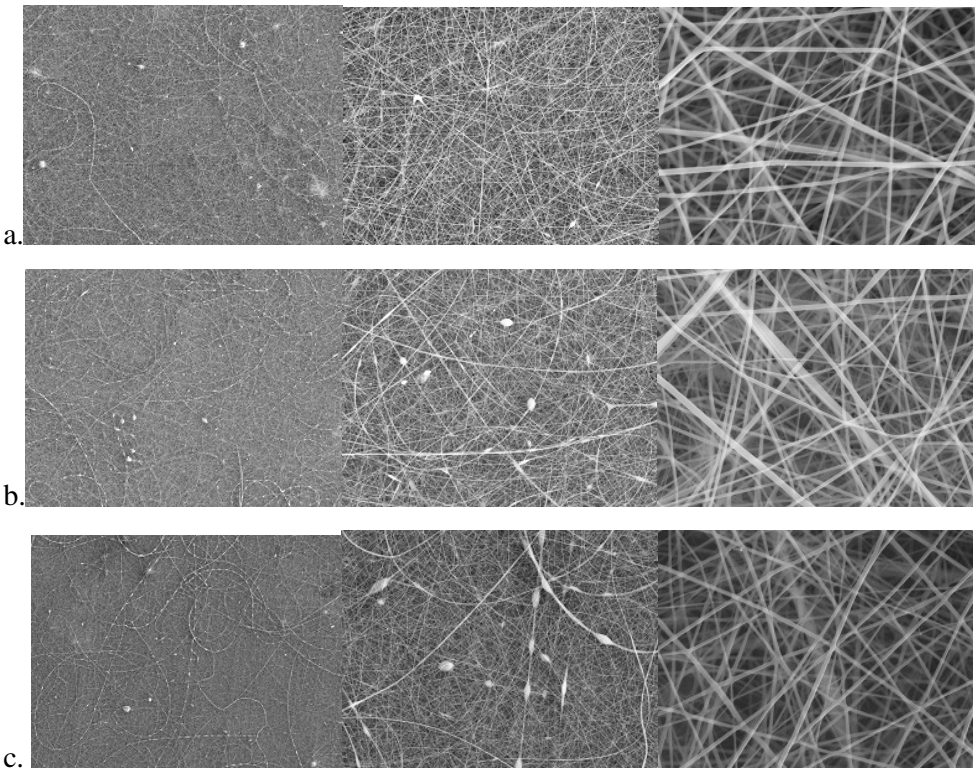

Figure 3.13 : SEM images of nanowebs which were electrospun with different flow rates a.es71; b.es72; c.es74 (sample set 1)

SEM images of set 1 depict the affect of flow rate on bead formation very clearly. During electrospinning, the voltage was kept at a constant value of 15kV and the flow rate was increased from 0.03mL/h to 0.066mL/h. With the flow rate of 0.03 mL/h, more uniform fibers were obtained (Figure 3.14a). Increasing the flow rate while keeping the voltage constant resulted in the accumulation of the solution at the tip of the needle and a sudden jet occured with higher volume of polymer solution which was believed to be the reason of the beaded coarser fibers seen in the SEM images (Figure 3.14b and 3.14c). After this sudden ejection, the electrospinning continued with smaller volume of polymer solution which resulted in finer fibers.

Increase in flow rate resulted in bead formation and decrease in uniformity. The SF fibers appeared inhomogeneous under higher flow rates. There were beaded fibers, coarser fibers and solution droplets pronounced with the increase in the flow rate. This can be explained by the inharmony between the fiber formation speed and flow rate. It indicated that flow rate was a dominant factor on uniformity of fibers.

Diameters of randomly selected 100 fibers were measured and fiber diameter distributions of each sample can be seen in Figure 3.15.

a. 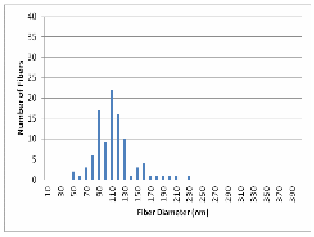 b. 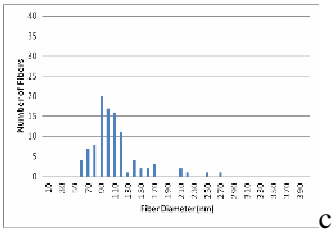 c. 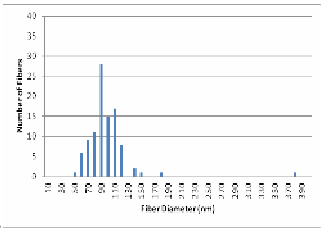

Figure 3.14 : Fiber diameter distributions of nanowebs which were electrospun with different flow rates a. es71, b. es72, c. es74

Fiber diameters were distributed in 41.2–223.5 nm range at 0.03 mL/h, compared with 0.048 mL/h which were distributed in 50–268.8 nm and 0.066 mL/h which were mainly distributed in 43.8–375 nm. The distributions are not very dispersed distributions. 87% of the fibers had diameters below 180 nm at flow rate of 0.03 mL/h and the percentages were 91% and 97% at the flow rates of 0.048 mL/h and 0.066 mL/h, respectively. The peak values increased in response to the increase in flow rates. The peak values were 223 nm for the flow rate of 0.03 mL/h ; 268 nm for the flow rate of 0.048 mL/h and 375 nm for the flow rate of 0.066 mL/h. The reason for the increase in the peak values was the solution accumulation caused by the inadequateness of fiber formation speed against the increase in flow rates.

The mean fiber diameters of each sample together with the minimum and maximum values, standard deviations, and lower and upper bounds of 95% confidence interval can be seen in Table 3.14 for sample set 1.

Table 3.14: Descriptives for sample set 1

Fiber Diameter

Sample Nr. (Flow Rate)	N	Mean	Std. Deviation	Std. Error	95% Confidence Interval		Min.	Max.
					Lower Bound	Upper Bound		
es71 (0.030mL/h)	100	**107.5320**	31.15303	3.11530	101.3506	113.7134	41.20	223.50
es72 (0.048mL/h)	100	**103.8420**	37.91130	3.79113	96.3196	111.3644	50.00	268.80
es74 (0.066mL/h)	100	**91.8410**	35.00222	3.50022	84.8958	98.7862	43.80	375.00
Total	300	**101.0717**	35.32562	2.03953	97.0580	105.0853	41.20	375.00

The mean fiber diameters were calculated as 108 nm, 104 nm, 92 nm for the flow rates of 0.03 mL/h, 0.048 mL/h and 0.066mL/h., respectively. Despite the increase in

the peak values, decrease was observed in the mean fiber diameters. The mean fiber diameters versus flow rate can be seen in Figure 3.16.

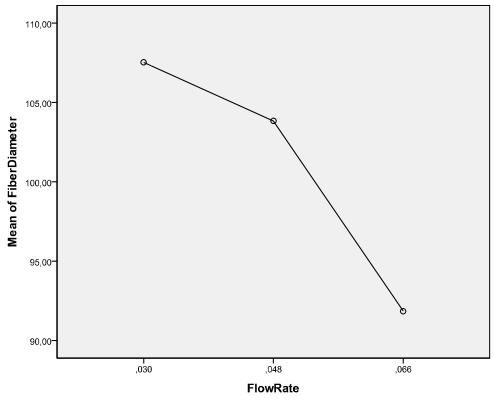

Figure 3.15 : Mean plots for nanowebs which were electrospun with different flow rates sample set 1

The variance analysis was carried out by applying Oneway Anova Method to decide whether the diferences were of real importance. The Oneway Anova statistical evaluation can be seen in Table 3.15.

Table 3.15: Oneway Anova table for sample set 1

Fiber Diameter

	Sum of Squares	df	Mean Square	F	**Sig.**
Between Groups	13461.586	2	6730.793	5.558	**0.004**
Within Groups	359660.383	297	1210.978		
Total	373121.969	299			

It is approved that the difference between the mean fiber diameters of the samples electrospun at different voltages are significant at 95% confidence interval since the significance is 0.004 which is less than 0.05.

Multiple comparisons, as represented in Table 3.16 showed that the increase in flow rate from 0.030 mL/h to 0.048 mL/h did not result in significant changes in diameter (Sig.=0.454 >0.05) whereas increase in the flow rate from 0.048mL/h to 0.066mL/h and from 0.030mL/h to 0.066mL/h caused significant changes in fiber diameters (Sig.=0.015<0.05 and Sig.=0.002<0.05, respectively).

Table 3.16: Multiple comparisons for sample set 1

Fiber Diameter

(I) Flow Rate (mL/h)	(J) Flow Rate (mL/h)	Mean Difference (I-J)	Std. Error	Sig.	95% Confidence Interval	
					Lower Bound	Upper Bound
0.030	**0.048**	3.69000	4.92134	**0.454**	-5.9951	13.3751
	0.066	15.69100*	4.92134	**0.002**	6.0059	25.3761
0.048	**0.030**	-3.69000	4.92134	**0.454**	-13.3751	5.9951
	0.066	12.00100*	4.92134	**0.015**	2.3159	21.6861
0.066	**0.030**	-15.69100*	4.92134	**0.002**	-25.3761	-6.0059
	0.048	-12.00100*	4.92134	**0.015**	-21.6861	-2.3159

*. The mean difference is significant at the 0.05 level.

The results were inconsistent with the studies in the literature. It is thought that the results were affected by the presence of beads and droplets in the structure. Due to the formation of beads, less solution differentiated into fibers which led to finer fibers. Thus it can be concluded that the uniformity decreased in response to the flow rate increase and as a result of this more finer and more coarser fibers formed.

The flow rate was set to keep the solution at the tip of the needle without dripping at the voltage of 15 kV and sample set 2 was prepared to see the effect of flow rate on fiber diameter. Solution with concentration of 18% was especially chosen in order to electrospin beadless fibers and to see the effect of flow rate on fiber diameter. SEM images of Set 2 can be seen in Figure 3.17.

a.

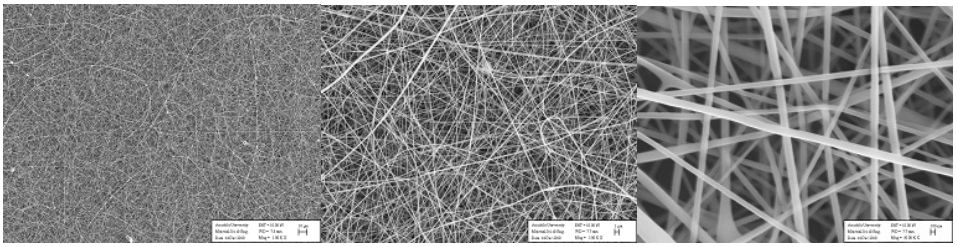

b.

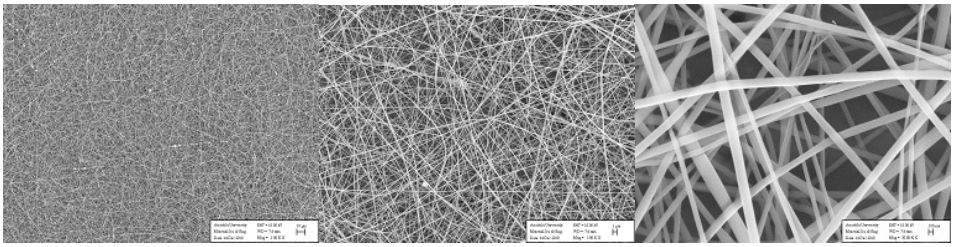

c.

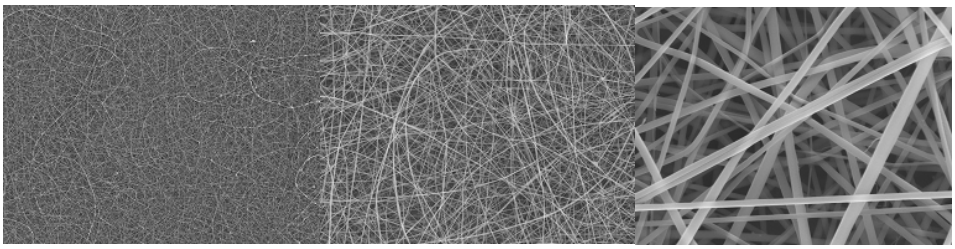

Figure 3.16 : SEM images of nanowebs which were electrospun with different flow rates a.es106, b. es104, c.es94 (sample set 2)

The diameter distributions are represented in Figure 3.18

a.

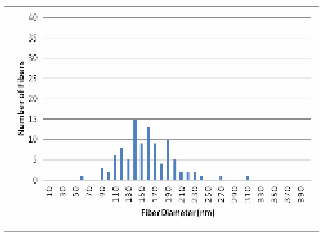

b.

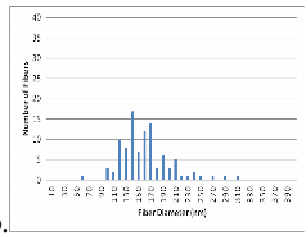

c.

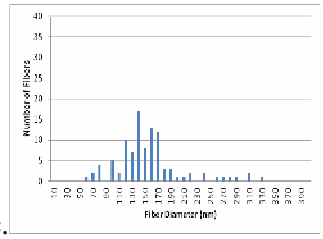

Figure 3.17 : Fiber diameter distributions of nanowebs which were electrospun with different flow rates a. es106, b. es104, c. es94 (sample set 2)

The distributions became broader with increase in flow rate.

The mean fiber diameters of each sample together with the minimum and maximum values, standard deviation, and lower and upper bounds of 95% confidence interval can be seen in Table 3.17.

Table 3.17: Descriptives for sample set 2

Fiber Diameter

Sample Nr. (Flow Rate)	N	Mean	Std. Deviation	Std. Error	95% Confidence Interval Lower Bound	95% Confidence Interval Upper Bound	Min.	Max.
es106 (0.003mL/h)	100	**154.7760**	48.56583	4.85658	145.1395	164.4125	50.00	437.50
es104 (0.006mL/h)	100	**157.9000**	47.60141	4.76014	148.4548	167.3452	56.30	412.50
es94 (0.018mL/h)	100	**149.7780**	50.78154	5.07815	139.7018	159.8542	50.00	325.00
Total	300	**154.1513**	48.95167	2.82623	148.5895	159.7131	50.00	437.50

The mean diameters calculated from the measurements of 100 random fibers were 155 nm, 158 nm, and 149 nm for the flow rates of 0.003, 0.006 and 0.018 mL/h, respectively. The small differences in the mean diameters are statistically evaluated by Oneway Anova method, results of which is represented in Table 3.18.

Table 3.18: Oneway Anova table for sample set 2

Fiber Diameter

	Sum of Squares	df	Mean Square	F	**Sig.**
Between Groups	3356.875	2	1678.438	0.699	**0.498**
Within Groups	713126.574	297	2401.100		
Total	716483.449	299			

It is approved that the differences in the mean fiber diameters were not of real significance at 95% confidence interval. (Sig.=0.498>0.05).

Multiple comparisons can be seen in Table 3.19. It can be concluded from the multiple comparisons that the flow rate increase from 0.003 mL/h to 0.018 mL/h was not sufficient to cause any significant change (Sig.= 0.47 >0.05)

Table 3.19: Multiple comparisons for sample set 2

Fiber Diameter

(I) Flow Rate (mL/h)	(J) Flow Rate (mL/h)	Mean Difference (I-J)	Std. Error	Sig.	95% Confidence Interval Lower Bound	95% Confidence Interval Upper Bound
0.003	**0.006**	-3.12400	6.92979	**0.65**	-16.7617	10.5137
	0.018	4.99800	6.92979	**0.47**	-8.6397	18.6357
0.006	**0.003**	3.12400	6.92979	**0.65**	-10.5137	16.7617
	0.018	8.12200	6.92979	**0.24**	-5.5157	21.7597
0.018	**0.003**	-4.99800	6.92979	**0.47**	-18.6357	8.6397
	0.006	-8.12200	6.92979	**0.24**	-21.7597	5.5157

These results proved that the flow rate is of great importance in affecting mainly the fiber uniformity in the electrospinning process.

For a given voltage, there is a corresponding flow rate if a stable Taylor cone is to be maintained. Increasing the flow rate only results in bead formation which leads to low quality nanowebs.

3.3.5 Effect of tip-to-collector distance on bead formation and fiber diameter

The effect of the tip-to-collector distance was studied on two sets of samples prepared by changing only the tip-to-collector distance (keeping all the parameters constant). The samples prepared are listed in Table 3.20 together with the parameters used in the electrospinning process.

Table 3.20: Samples electrospun at different tip-to-collector distances

Sample Nr.	concentration %	needle mm	voltage kV	flow rate mL/h	distance cm
Sample Set 1					
es80	12%	1.2	15	0.050	5
es79	12%	1.2	15	0.050	10
es81	12%	1.2	15	0.050	13
Sample Set 2					
es110	12%	0.7	15	0.018	5
es99	12%	0.7	15	0.018	10
es111	12%	0.7	15	0.018	13

SEM images of the samples are shown in Figure 3.18 and 3.19 for sample set 1 and sample set 2, respectively.

a.

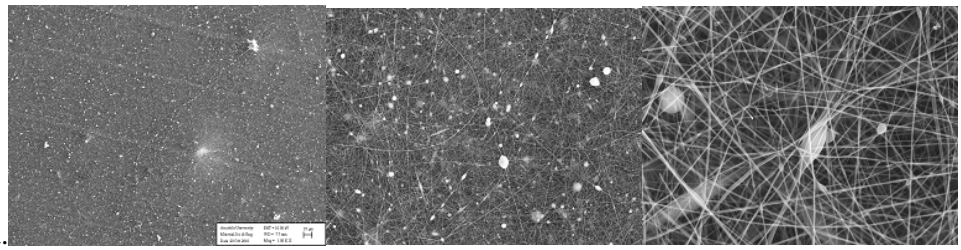

b.

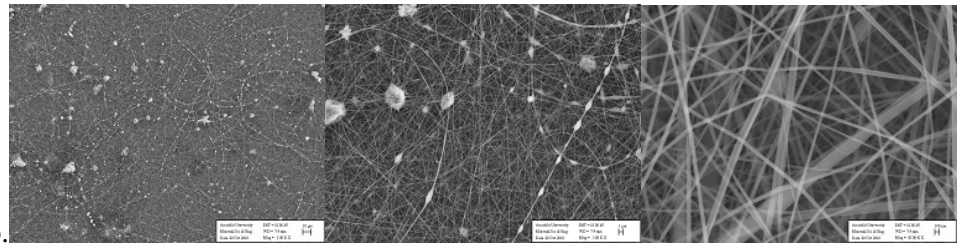

c.

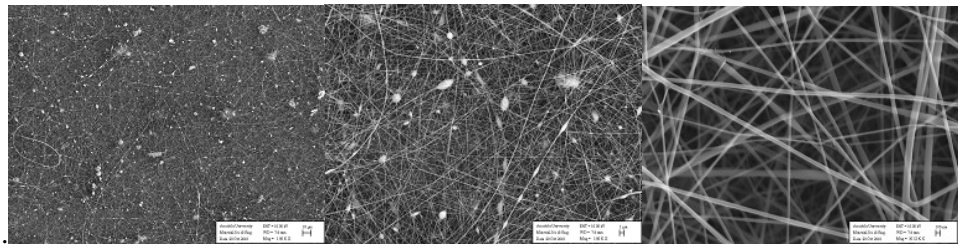

Figure 3.18 : SEM images of nanowebs which were electrospun at different tip-to-collector distances a. es80; b. es79; c. es81 (sample set 1)

a.

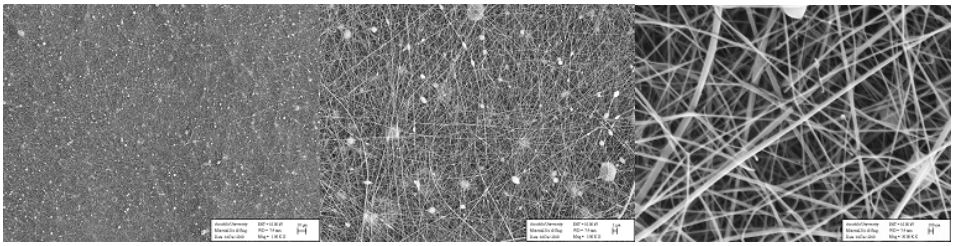

b.

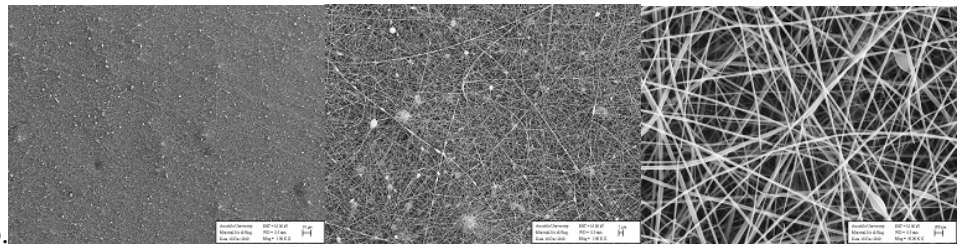

c.

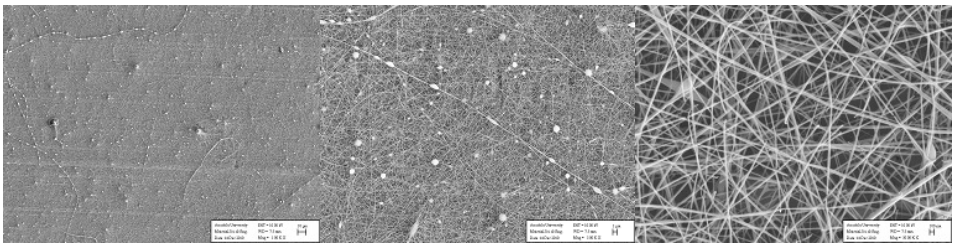

Figure 3.19 : SEM images of which were electrospun at different tip-to-collector distances a.es110; b. es99; c. es111 (sample set 2)

The effect of tip-to-collector distance on bead formation is clear from the SEM images of sample set 2. The number of beads decreased with the increase in distance from 5 cm to 13 cm.

The diameter distributions are represented in Figure 3.20 and 3.21 for Sample Set 1 and Sample Set 2, respectively.

a.

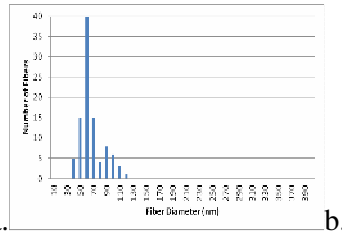

b.

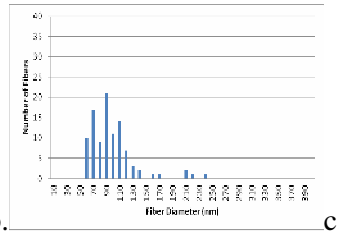

c.

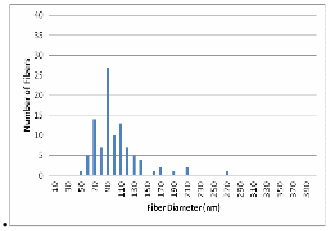

Figure 3.20 : Fiber diameter distributions of nanowebs which were electrospun at different tip-to-collector distances a.es80, b.es79, c.es81 (sample set 1)

a. 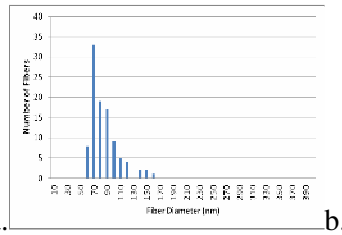 b. 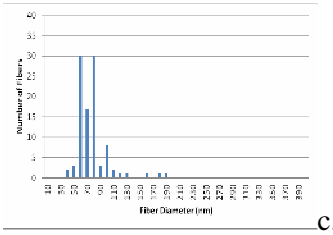 c. 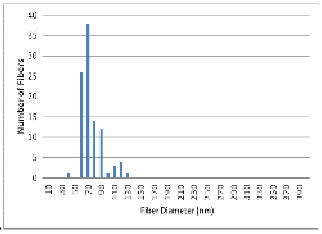

Figure 3.21 : Fiber diameter distributions of nanowebs which were electrospun at different tip-to-collector distances a. es110, b. es99, c. es111 (sample set 2)

The mean fiber diameters of each sample together with the minimum and maximum values, standard deviation, and lower and upper bounds of 95% confidence interval can be seen in Table 3.21.

Table 3.21: Descriptives for sample set 1

Fiber Diameter

Sample Nr. (Distance)	N	Mean	Std. Deviation	Std. Error	95% Confidence Interval		Min.	Max.
					Lower Bound	Upper Bound		
es80 (5 cm)	100	**60.3380**	17.44125	1.74412	56.8773	63.7987	37.50	112.50
es79 (10 cm)	100	**92.0260**	33.76021	3.37602	85.3272	98.7248	50.00	231.30
es81 (13 cm)	100	**96.2770**	34.59885	3.45988	89.4118	103.1422	43.80	262.50
Total	300	**82.8803**	33.65122	1.94285	79.0569	86.7037	37.50	262.50

Table 3.22: Descriptives for sample set 2

Fiber Diameter

Sample Nr. (Distance)	N	Mean	Std. Deviation	Std. Error	95% Confidence Interval		Min.	Max.
					Lower Bound	Upper Bound		
es110 (5 cm)	100	**79.6460**	20.44355	2.04436	75.5896	83.7024	50.00	150.00
es99 (10 cm)	100	**71.6190**	23.39954	2.33995	66.9760	76.2620	38.70	180.60
es111 (13 cm)	100	**69.4590**	16.23110	1.62311	66.2384	72.6796	37.50	125.00
Total	300	**73.5747**	20.64399	1.19188	71.2291	75.9202	37.50	180.60

For sample set 1, the mean diameters calculated from the measurements of 100 random fibers were 60 nm, 92 nm, and 96 nm at the distances of 5, 10, and 13 cm, respectively. For Sample Set 2, the mean diameters were calculated as 79 nm, 71 nm and 69 nm at the distances of 5, 10 and 13 cm, respectively. The mean fiber diameter change versus tip-to-collector distance can be seen in Figure 3.22.

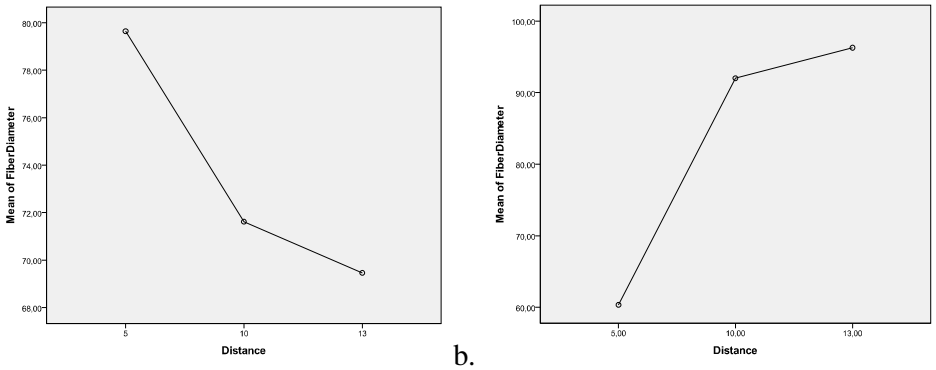

a. b.

Figure 3.22 : Mean plots for nanowebs which were electrospun at different tip-to-collector distances a.Sample set 1, b.Sample set 2

In sample set 1, there is a decrease in fiber diameters in response to the increase in distance whereas there is an increase in fiber diameter with increase in distance in sample set 2.

The variance analysis was carried out by applying Oneway Anova Method to decide whether the diferences were of real importance. The Oneway Anova statistical evaluation can be seen in Table 3.23 and 3.24 for sample set 1 and sample set 2, respectively.

Table 3.23: Oneway Anova table for sample set 1

Fiber Diameter

	Sum of Squares	df	Mean Square	F	**Sig.**
Between Groups	77127.069	2	38563.534	43.805	**0.000**
Within Groups	261461.865	297	880.343		
Total	338588.934	299			

Table 3.24: Oneway Anova table for sample set 2

Fiber Diameter

	Sum of Squares	df	Mean Square	F	**Sig.**
Between Groups	5762.443	2	2881.222	7.034	**0.001**
Within Groups	121663.664	297	409.642		
Total	127426.107	299			

It is approved that the differences in the mean diameter was of real significance at 95% confidence interval for both of the sets. (Sig.=0.0<0.05 for Sample Set 1 and Sig.=0.001<0.05 for Sample Set 2).

Multiple comparisons, as represented in Table 3.25 (Sample Set 1) and 3.26 (Sample Set 2) showed that the increase in distance from 5 cm to 10 cm and 5 to 13 cm had a

significant effect on fiber diameter with the significance value of 0. The effect of the increase in distance from 10 cm to 13 cm was not of real importance. (Sig.=0.312>0.05)

Table 3.25: Multiple comparisons for sample set 1

Fiber Diameter

(I) Distance (cm)	(J) Distance (cm)	Mean Difference (I-J)	Std. Error	Sig.	95% Confidence Interval	
					Lower Bound	Upper Bound
5.00	**10.00**	-31.68800*	4.19605	**0.000**	-39.9458	-23.4302
	13.00	-35.93900*	4.19605	**0.000**	-44.1968	-27.6812
10.00	**5.00**	31.68800*	4.19605	**0.000**	23.4302	39.9458
	13.00	-4.25100	4.19605	**0.312**	-12.5088	4.0068
13.00	**5.00**	35.93900*	4.19605	**0.000**	27.6812	44.1968
	10.00	4.25100	4.19605	**0.312**	-4.0068	12.5088

*. The mean difference is significant at the 0.05 level.

Table 3.26: Multiple comparisons for sample set 2

Fiber Diameter

(I) Distance (cm)	(J) Distance (cm)	Mean Difference (I-J)	Std. Error	Sig.	95% Confidence Interval	
					Lower Bound	Upper Bound
5	**10**	8.02700*	2.86231	**0.005**	2.3940	13.6600
	13	10.18700*	2.86231	**0.000**	4.5540	15.8200
10	**5**	-8.02700*	2.86231	**0.005**	-13.6600	-2.3940
	13	2.16000	2.86231	**0.451**	-3.4730	7.7930
13	**5**	-10.18700*	2.86231	**0.000**	-15.8200	-4.5540
	10	-2.16000	2.86231	**0.451**	-7.7930	3.4730

*. The mean difference is significant at the 0.05 level.

It is thought that the fiber diameter measurements were affected by the presence of beads in the structure. Some more evidence is needeed before reaching a definite conclusion.

3.3.6 Effect of needle diameter on bead formation and fiber diameter

The effect of the needle diameter on bead formation and fiber diameter was studied on two sets of samples for four different needle gauges. The samples prepared are listed in Table 3.27 together with the parameters used in the electrospinning process.

Table 3.27: Samples which were electrospun with different needles

Sample Nr.	concentration %	needle mm	voltage kV	flow rate mL/h	distance cm
Sample Set 1					
es99	12%	0.70 (22G)	15	0.018	10
es100	12%	0.90 (20G)	15	0.018	10
es101	12%	1.06 (19G)	15	0.018	10
es98	12%	1.25 (18G)	15	0.018	10
Sample Set 2					
es94	18%	0.70 (22G)	15	0.018	10
es95	18%	0.90 (20G)	15	0.018	10
es96	18%	1.06 (19G)	15	0.018	10
es93	18%	1.25 (18G)	15	0.018	10

There were no problems as clogging of the needle or dripping of the solution observed during the electrospinning process with any of the needles.

SEM images of electrospun fibers fabricated with needles of different diameters are shown in Figures 3.23 and 3.24 for sample set 1 and 2, respectively.

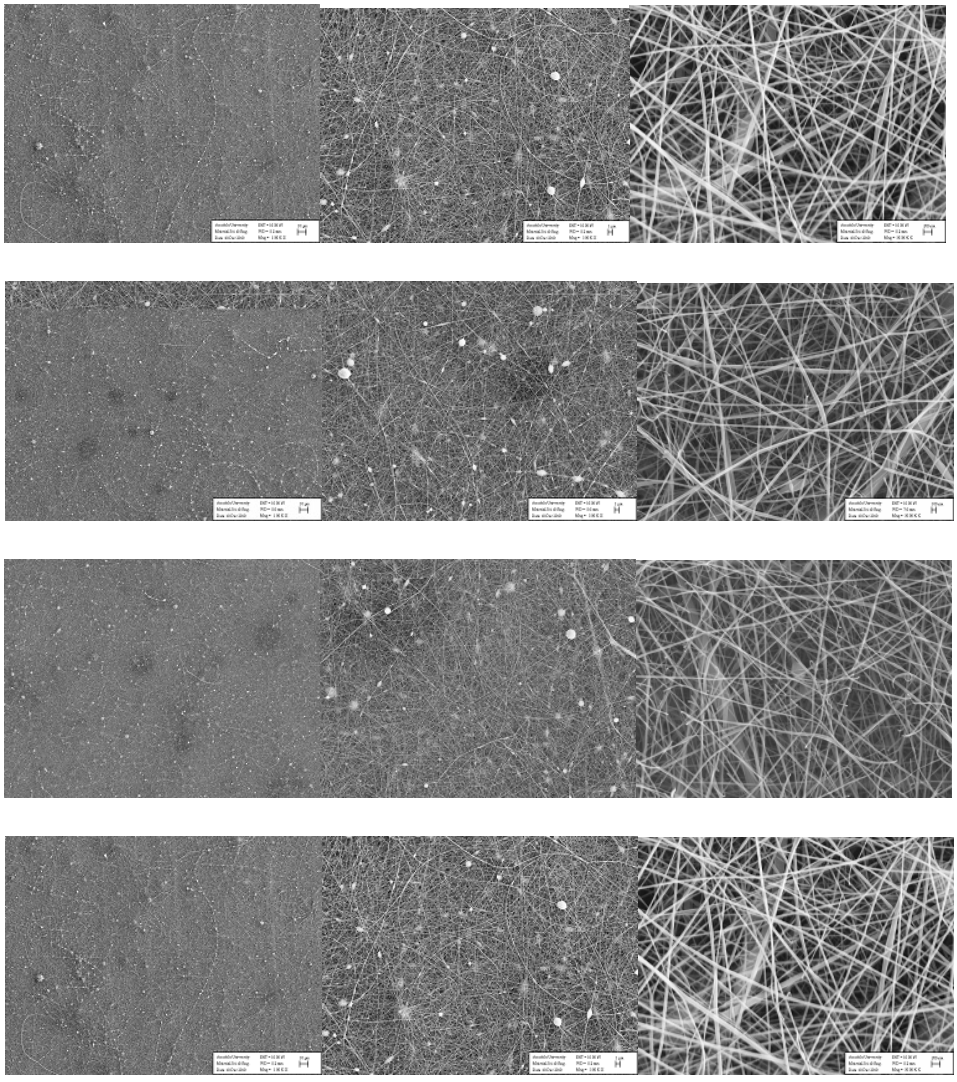

Figure 3.23 : SEM images of nanowebs which were electrospun with different needles a.es99;b. es100; c. es101; and d. es98 (sample set 1)

a.

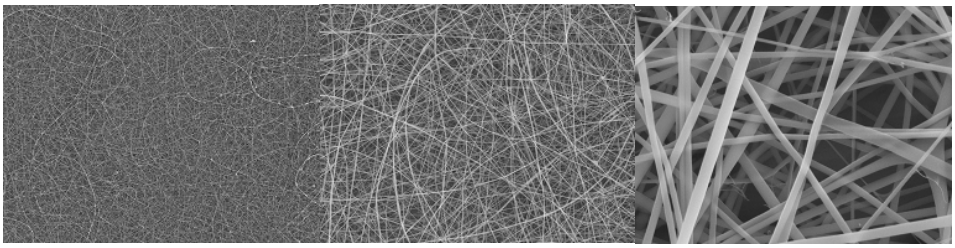

b.

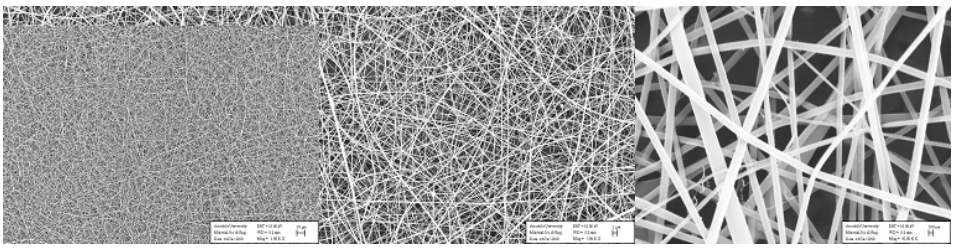

c.

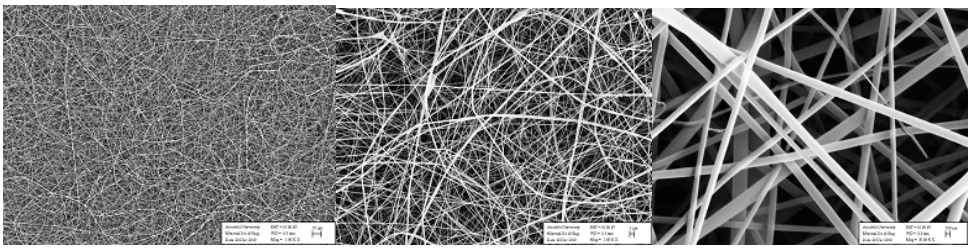

d.

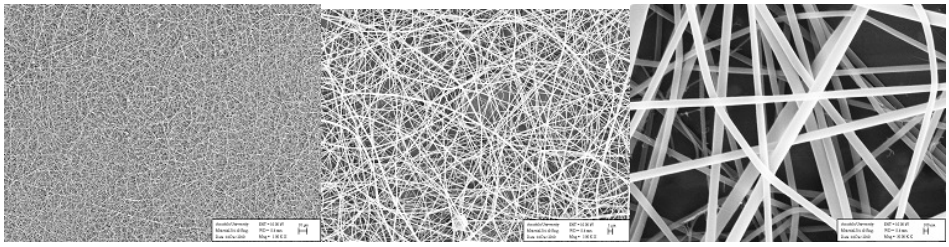

Figure 3.24 : SEM images of nanowebs which were electrospun with different needles a. es94; b. es95; c. es96; d. es93 (sample set 2)

From the SEM images of sample set 1, it is clear that increase in needle diameter did not have any improving effects on bead formation. In other words, the beaded fiber structure could not be improved by using a needle of differet gauge. Also using needles of different gauges did not lead to bead formation on fibers as can be seen from the SEM images of sample set 2.

The diameter distributions are represented in Figures 3.25 and 3.26 for sample set 1 and sample set 2, respectively.

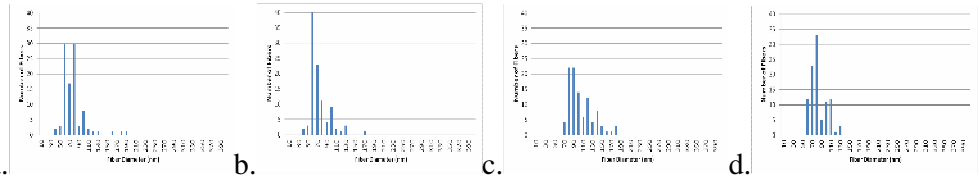

Figure 3.25 : Fiber diameter distributions of nanowebs which were electrospun with different needles a. es99, b. es100, c. es101, d. es98 (sample set 1)

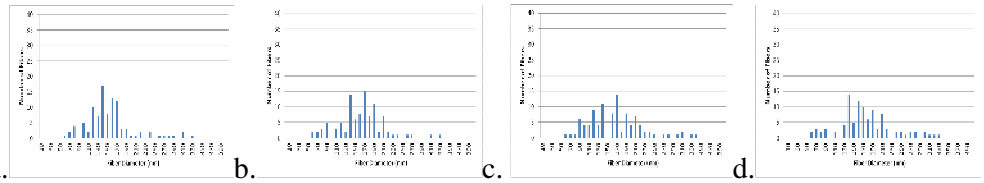

Figure 3.26 : Fiber diameter distributions of of nanowebs which were electrospun with different needles a. es94, b. es95, c. es96; d.es93 (sample set 2)

In Figure 3.25, it is observed that the fiber diameter distributions become more concentrated with the increase in needle diameter. Fiber diameters were distributed in 51.60–129 nm range for needle diameter of 1.25 mm. compared with the fiber diameters which were distributed in the ranges of 66.70-171.40 nm, 38.70-161.30 nm, 38.70-180.60 nm for the needle diameters of 1.06 mm, 0.90 mm and 0.70 mm, respectively. In Figure 3.26 which represents the fiber diameter distributuions of sample set 2, no important differences were observed between the fibr diameter distributions.

The mean fiber diameters of each sample together with the minimum and maximum values, standard deviation, standard error, and lower and upper bounds of 95% confidence interval can be seen in Tables 3.28 and 3.29 for sample set 1 and sample set 2, respectively.

Table 3.28: Descriptives for sample set 1

Fiber Diameter

Sample Nr. (Needle Dia.)	N	Mean	Std. Deviation	Std. Error	95% Confidence Interval		Min.	Max.
					Lower Bound	Upper Bound		
es99 (0.70mm)	100	**71.6190**	23.39954	2.33995	66.9760	76.2620	38.70	180.60
es100 (0.90mm)	100	**68.2620**	20.33750	2.03375	64.2266	72.2974	38.70	161.30
es101(1.06mm)	100	**67.6160**	17.06210	1.70621	64.2305	71.0015	45.20	116.10
es98 (1.25mm)	100	**77.9350**	17.84013	1.78401	74.3951	81.4749	51.60	129.00
Total	400	**71.3580**	20.16067	1.00803	69.3763	73.3397	38.70	180.60

Table 3.29: Descriptives for sample set 2

Fiber Diameter

Sample Nr. (Needle Dia.)	N	Mean	Std. Deviation	Std. Error	95% Confidence Interval Lower Bound	95% Confidence Interval Upper Bound	Min.	Max.
es94 (0.70mm)	100	**149.7780**	50.78154	5.07815	139.7018	159.8542	50.00	325.00
es95 (0.90mm)	100	**155.3360**	48.09470	4.80947	145.7930	164.8790	56.30	325.00
es96 (1.06mm)	100	**162.4375**	57.29938	5.72994	151.0681	173.8069	56.25	331.25
es93 (1.25mm)	100	**171.4640**	58.26897	5.82690	159.9022	183.0258	56.30	325.00
Total	400	**159.7539**	54.19268	2.70963	154.4269	165.0808	50.00	331,25

The mean plots versus needle diameter can be seen in Figure 3.27 for sample set 1 and sample set 2, respectively.

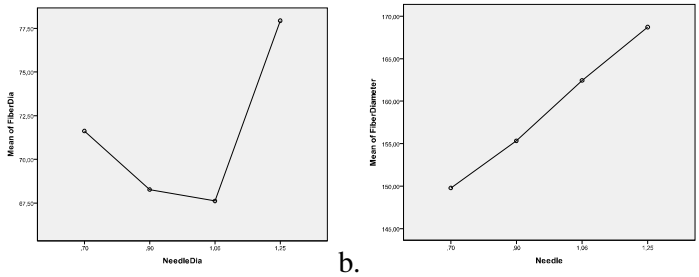

a. b.

Figure 3.27 : Mean plots for of nanowebs which were electrospun with different needles a. sample set 1, b. sample set 2

For sample set 1, mean fiber diameters were calculated as 71.6, 68.2, 67.6 and 77.9 nm for the needle diameters of 0.70, 0.90, 1.06 and 1.25 mm respectively (Table 3.28, Figure 3.27) and for sample set 2, mean values were calculated as 149.8, 155.3, 162.4 and 171.5 nm for the needle diameters of 0.70, 0.90, 1.06 and 1.25 mm, respectively (Table 3.29, Figure 3.27) which suggested a correlation between needle diameter and fiber diameter.

The variance analysis was carried out by applying Oneway Anova Method to decide whether the diferences were of real importance. The Oneway Anova statistical evaluation can be seen in Table 3.30 and 3.31 for sample set 1 and 2, respectively.

Table 3.30: Oneway Anova table for sample set 1

Fiber Diameter

	Sum of Squares	df	Mean Square	F	**Sig.**
Between Groups	6691.283	3	2230.428	5.681	**0.001**
Within Groups	155483.271	396	392.635		
Total	162174.554	399			

Table 3.31: Oneway Anova table for sample set 2

Fiber Diameter

	Sum of Squares	df	Mean Square	F	**Sig.**
Between Groups	26336.457	3	8778.819	3.035	**0.029**
Within Groups	1145465.264	396	2892.589		
Total	1171801.721	399			

From the variance analysis, it is concluded that the differences between the mean diameters were of real significance, since Sig.=0.0 < 0.05 and Sig.=0.029<0.05 for sample set 1 and 2, respectively.

Multiple comparisons for sample set 1 (Table 3.32) showed that the needle diameter change from 0.70 to 1.25 mm, 0.90 to 1.25mm and 1.06 to 1.25mm, resulted in significant changes in fiber diameter.

Table 3.32: Multiple comparisons for sample set 1

(I) Needle Dia. (mm)	**(J) Needle Dia. (mm)**	Mean Difference (I-J)	Std. Error	**Sig.**	95% Confidence Interval	
					Lower Bound	Upper Bound
0.70	**0.90**	3.35700	2.80227	**0.232**	-2.1522	8.8662
	1.06	4.00300	2.80227	**0.154**	-1.5062	9.5122
	1.25	-6.31600*	2.80227	**0.025**	-11.8252	-0.8068
0.90	**0.70**	-3.35700	2.80227	**0.232**	-8.8662	2.1522
	1.06	0.64600	2.80227	**0.818**	-4.8632	6.1552
	1.25	-9.67300*	2.80227	**0.001**	-15.1822	-4.1638
1.06	**0.70**	-4.00300	2.80227	**0.154**	-9.5122	1.5062
	0.90	-.64600	2.80227	**0.818**	-6.1552	4.8632
	1.25	-10.31900*	2.80227	**0.000**	-15.8282	-4.8098
1.25	**0.70**	6.31600*	2.80227	**0.025**	.8068	11.8252
	0.90	9.67300*	2.80227	**0.001**	4.1638	15.1822
	1.06	10.31900*	2.80227	**0.000**	4.8098	15.8282

*. The mean difference is significant at the 0.05 level.

Multiple comparisons for sample set 2 (Table 3.33) showed that the needle diameter change from 0.70 to 0.90 mm, 0.70 to 1.06mm, 0.90 to 1.06 mm and 1.06 to 1.25mm resulted in increases which were not of real importance ($Sig._{0.70\text{-}0.90}$= 0.465 >0.05, $Sig._{0.70\text{-}1.06}$= 0.097 >0.05, $Sig._{0.90\text{-}1.06}$= 0.351 >0.05, $Sig._{1.06\text{-}1.25}$=0.236 >0.05) whereas the needle diameter change from 0.70 to 1.25 mm and 0.90 to 1.25 mm resulted in significant increases in fiber diameter ($Sig._{0.70\text{-}1.25}$= 0.005<0.05, $Sig._{0.90\text{-}1.25}$= 0.035<0.05).

Table 3.33: Multiple comparisons for sample set 2

(I) Needle Dia. (mm)	(J) Needle Dia. (mm)	Mean Difference (I-J)	Std. Error	Sig.	95% Confidence Interval	
					Lower Bound	Upper Bound
0.70	**0.90**	-5.55800	7.60604	**0.465**	-20.5113	9.3953
	1.06	-12.65950	7.60604	**0.097**	-27.6128	2.2938
	1.25	-21.68600*	7.60604	**0.005**	-36.6393	-6.7327
0.90	**0.70**	5.55800	7.60604	**0.465**	-9.3953	20.5113
	1.06	-7.10150	7.60604	**0.351**	-22.0548	7.8518
	1.25	-16.12800*	7.60604	**0.035**	-31.0813	-1.1747
1.06	**0.70**	12.65950	7.60604	**0.097**	-2.2938	27.6128
	0.90	7.10150	7.60604	**0.351**	-7.8518	22.0548
	1.25	-9.02650	7.60604	**0.236**	-23.9798	5.9268
1.25	**0.70**	21.68600*	7.60604	**0.005**	6.7327	36.6393
	0.90	16.12800*	7.60604	**0.035**	1.1747	31.0813
	1.06	9.02650	7.60604	**0.236**	-5.9268	23.9798

*. The mean difference is significant at the 0.05 level.

The results obtained from the sample set 2 are thought to be more important in reflecting the effect of needle diameter on fiber diameter because of the uniform fiber structure obtained in this set of samples. As a result of their uniform structure the measurements were not affected from the exclusion of the droplets.

The increase in fiber diameter as a result of increase in needle diameter is attributed to the increased size of the droplet at the tip of needle. When the size of the droplet at the tip of the needle increases, the surface tension of the droplet decreases. For the same voltage supplied, a smaller columbic force is required to cause jet initiation. As a result, the acceleration of the jet increases and this allows less time for the solution to be stretched and elongated before it is collected which results in increased fiber diameters [7].

4. CONCLUSIONS

Electrospinning process of regenerated silk fibroin in formic acid was conducted successfully and fibers with diameters in the range of 37 to 437 nm which were much thinner than natural silk fiber were fabricated.

The effect of electrospinning process on the structure of silk fibroin was investigated by FTIR spectroscopy. The structure of as-spun fibers was predominantly α-helical because there was not enough time for molecular arrangement and crystallization.

Bead formation on fibers and distribution of fiber diameter were investigated by varying concentration of the regenerated silk solution, and processing parameters such as flow rate, applied voltage, tip-to-collector distance, and needle diameter in order to find an optimum set of settings for the fabrication of nanoscale, uniform, and continuous silk fibroin fibers.

The concentration of regenerated silk solution played a major role in fiber spinnability, bead formation and fiber diameter. For fiber formation to occur, a minimum solution concentration of 10% was required. At the concentration of 10%, fibers together with droplets and beads were observed. Also there were some broken ends which showed that the fiber formation was intermittent. At a higher concentration of 12%, droplets disappeared and the beaded fibers became fewer; no droplets or beaded fibers were observed at the concentration of 15% or 18%. At 18%, the average fiber diameter was much larger than that of fibers spun at lower concentrations. The diameters of the fibers increased with the increase in concentration.

Flow rate was found to affect the fiber uniformity significantly. It was necessary to keep the flow rate at 0.03mL/h or below to obtain defect-free nanowebs at the voltage of 15kV. Higher flow rates only provided more polymer solution than needed. The excess polymer solution accumulated at the tip of the needle and resulted in instability of the Taylor cone. The resultant nanoscale SF fibers appeared inhomogeneous. There were beaded fibers, coarser fibers and solution droplets

pronounced with the increase in the flow rate. It is concluded that the flow rate should be in harmony with the applied voltage in order to obtain uniform fibers. For a given voltage, there is a corresponding flow rate if a stable Taylor cone is to be maintained. Increasing the flow rate only results in bead formation which leads to low quality nanowebs.

Increase in applied voltage resulted in increase in bead formation. For beaded fibers, fiber diameter increased as a result of an increase in applied voltage. The fiber diameter became more sensitive to changes when working at higher voltages. An increase in the voltage from 20 to 25 kV resulted in significant changes in mean diameters whereas an increase from 10 to 15 kV and even from 10 to 20 kV resulted in changes that were statistically not of real importance. An increase from 10 kV to 25kV was required to obtain significant change in the mean fiber diameters.

Increase in fiber diameter was observed as a result of increase in needle diameter from 0.70 to 0.90 mm, from 0.90 to 1.06mm and from 1.06 to 1.25mm but not at the required level of significance. Important variation was identified between the mean diameters of fibers produced with the needles of 0.70mm and 1.25mm. Fiber diameter increased in response to the increase in needle diameter.

As a result of observation and SEM image analysing, nanowebs with uniform nanoscale fibers were obtained by using a polymer concentration of 15%, a voltage of 15kV, a flow rate of 0.03 mL/h, tip-to-collector distance of 10cm and a needle with an outer diameter of 0.70mm. Lower polymer concentration, shorter spinneret-collector distance, and higher flow rate led to various kinds of defects, such as noncontinuous fibers, beads, solution droplets, fusing of wet fibers, etc., thus leading to poor quality nanowebs.

REFERENCES

[1] Vepari, C., Kaplan, D. L., (2007), Silk as a biomaterial, *Prog. Polym. Sci*., **32**, 991–1007

[2] Kweon H., Yeo J. H., Lee K. G., Lee H.C., Na H.S., Won Y.H., Cho C.S., (2008), Semi-interpenetrating polymer Networks composed of silk fibroin and poly(ethylene glycol) for wound dressing, *Biomedical materials,* **3**, 34115,

[3] WILEY VCH., (2008), *Ullmann's fibers 1 Fiber Classes, Production and Characterization,* WILEY-VCH Verlag GmbH & Co KgaA, Weinheim

[4] Plaza, G. R., Corsini, P., Pe´rez-Rigueiro, J., Marsano, E., Guinea, G. V., Elices, M., (2008), Effect of Water on Bombyx mori Regenerated Silk Fibers and Its Application in Modifying Their Mechanical Properties*, Journal of Applied Polymer Science*, **109**, 1793–1801.

[5] Zhang X., Reagan, M. M., Kaplan, D. L., (2009), Electrospun silk biomaterial scaffolds for regenerative medicine, *Advanced Drug Delivery Reviews*, **61**, 988–1006.

[6] Schiffman, J. D., Schauer, C. L., (2008), A Review: Electrospinning of Biopolymer Nanofibers and their Applications, *Polymer Reviews*, **48**, 317–352.

[7] Ramakrishna, S., Fujihara, K., Teo, W. E., Lim, L. C., MA, Z., (2005), *An Introduction to Electrospinning and Nanofibers*, World Scientific Publishing Company, Incorporated, River Edge, NJ, USA.

Retrieved from http://0-site.ebrary.com.divit.library.itu.edu.tr/

[8] Bhardwaj, N., Kundu, S. C., (2010), Electrospinning: A fascinating fiber fabrication technique, *Biotechnology Advance,* **28**, 3, 325-347.

[9] Saville, B. P., Greaves, P. H., (1995), *Microscopy of textile fibres,* BIOS Scientific Publishers, Oxford.

[10] Url-1 < *http://www.tex.in/education/nextiles/fib/reg/reg.html*>, accessed at 13.11.2010.

[11] Hearle J. W. S., (2007), Protein fibers: structural mechanics and future opportunities**,** J Mater Sci., **42**, 8010–8019

[12] Tatsuya, H., Glyn, O. P., Machiko T., (2005), *new millennium fibers*, Woodhead, Cambridge

[13] Url-2 < *http://www.organicexchange.org/Documents/eco-fibre.pdf* >, accessed at 13.11.2010

[14] Poole, A. J., Church, J. S., Huson, M. G., (2009), Environmentally Sustainable Fibers from Regenerated Protein, *Biomacromolecules,* **10**, No. 1.

[15] Zhang, Y., Ghasemzadeh, S., Kotliar, A. M., Kumar, S., Presnell, S., Williams, L. D., (1999), Fibers from Soybean Protein and Poly(vinyl alcohol) *Journal of Applied Polymer Science*, **71**, 11–19.

[16] Aluigi, A., Zoccola, M., Vineis, C., Tonin, C., Ferrero, F., Canetti, M., (2007), Study on the structure and properties of wool keratin regenerated from formic acid, *International Journal of Biological Macromolecule,* **41**, 266–273.

[17] Kaplan, D., Adams, W. W., Farmer, B., Viney, C., (1993), *Silk Polymers Materials Science and Biotechnolog,* American Chemical Society, Washington

[18] Url-3 < *http://corbis.co.in/* > accessed at 13.11.2010.

[19] Url-4 <*http://www.fibrecrafts.com/resource/fact_file/fibres/silk.asp*> accessed at 13.11.2010.

[20] Nazarov, R., Jin, H.J., Kaplan, D. L., (2004), Porous 3-D Scaffolds from Regenerated Silk Fibroin, *Biomacromolecules*, **5**, 718-726

[21] Hardy, J. G., Roemer, L. M., Scheibel T. R., (2008), Polymeric materials based on silk proteins, *Polymer,* **49**, 4309–4327

[22] Houck, M. M., (2009), *Identification of textile fibers,* Woodhead Pub., Cambridge.

[23] Franck, Robert R., (2001), *silk, mohair, cashmere, and other luxury fibres,* Woodhead Pub., Cambridge

[24] Url-5 < *http://en.wikipedia.org/wiki/History_of_silk* > accessed at 13.11.2010.

[25] Warner, S. B., (1995), *Fiber Science,* Prentice Hall, Inc, New Jersey

[26] E. S. Sashina, A. M. Bochek, N. P. Novoselov, and D. A. Kirichenko, (2006), Structure and Solubility of Natural Silk Fibroin, *Russian Journal of Applied Chemistry,* 2006, **79**, 6, 869-876.

[27] M. S. Alger, *Polymer Science Dictionary*, Elsevier, New York, 1989.

[28] Url-6 < *http://chemed.chem.wisc.edu* > accessed at 13.11.2010.

[29] Url-7 < *http://en.wikipedia.org/wiki/File: Silk_fibroin_primary_structure.svg* **>** accessed at 13.10.2010

[30] Gregory H. Altman, Frank Diaz, Caroline Jakuba, Tara Calabro, Rebecca L. Horan, Jingsong Chen, Helen Lu, John Richmond, David L. Kaplan, (2003), Silk-based biomaterials, *Biomaterials*, **24**, 401–416

[31] Url-8 <*http://cosmos.ucdavis.edu/archives/2008/cluster8/ghezelayagh_ava.pdf***>** accessed at 13.11.2010

[32] Url-9 < *http://en.wikipedia.org/wiki/Silk* **>** accessed at 13.10.2010

[33] Url-10 <*http://ezinearticles.com/Properties-and-Characteristics-of-Silk&id=488797***>** accessed at 13.11.2010

[34] A. Schneider, X.Y. Wang, D.L. Kaplan, J.A. Garlick, C. Egles, (2009), Biofunctionalized electrospun silk mats as a topical bioactive dressing for accelerated wound healing, *Acta Biomaterialia,* **5**, 2570–2578

[35] Thandavamoorthy Subbiah, G. S. Bhat, R. W. Tock, S. Parameswaran, S. S. Ramkumar, (2005, Electrospinning of Nanofibers, *Journal of Applied Polymer Science*, **96**, 557–569.

[36] Kristin J. Pawlowski, Catherine P. Barnes, Eugene D. Boland, Gary E. Wnek, Gary L. Bowlin, Biomedical Nanoscience: Electrospinning Basic Concepts, Applications, and Classroom Demonstration, Mat. Res. Soc. Symp. Proc., **827E**, Retrieved from < http://www.mrs.org >

[37] Zheng-Ming Huanga, Y.-Z. Zhang, M. Kotakic, S. Ramakrishna, (2003), A review on polymer nanofibers by electrospinning and their applications in nanocomposites*, Composites Science and Technology,* **63**, 2223–2253.

[38] Andrady, A. L., (2008), *Science and Technology of polymer nanofibers,* John Wiley & Sons, Inc., Hoboken, New Jersey

[39] Stranger, J., Tucker, N., Staiger, M., (2005), Electrospinning, *Rapra Review Reports*, **16**, 10. Retrieved from http://site.ebrary.com.

[40] Url-11 < *http://en.wikipedia.org/wiki/Electrospinning* **>** accessed at 13.11.2010

[41] Vrieze, S., Clerck, K., (2009), 80 Years of Electrospinning

Retrieved from < *http://biblio.ugent.be/record/767594* >

[42] Sill T., Recum, H. A., (2008), Electrospinning: Applications in drug delivery and tissue engineering Biomaterials, **29**, 1989-2006.

[43] Url-12 < *http://prc.ac.nctu.edu.tw/www* **>** accessed at 13.11.2010

[44] A. K. Moghe, B. S. Gupta, (2008), Co-axial Electrospinning for Nanofiber Structures: Preparation and Applications, *Polymer Reviews*, **48**, 353–377.

[45] Chen Chen, Cao Chuanbao, Ma Xilan, Tang Yin, Zhu Hesun, (2006), Preparation of non-woven mats from all-aqueous silk fibroin solution with electrospinning method, *Polymer,* **47**, 6322-6327.

[46] Christina Kriegel, Alessandra Arrechi, Kevin Kit, D. J. Mc lements, Jochen Weiss, (2008), Fabrication, Functionalization, and Application of Electrospun Biopolymer Nanofibers, *Critical Reviews in Food Science and Nutrition*, **48**, 775–797

[47] Jonathan Ayutsede, Milind Gandhi, Sachiko Sukigara, Michael Micklus, Hung-En Chen, Frank Ko, (2005), Regeneration of Bombyx mori silk by electrospinning.Part 3: characterization of electrospun nonwoven mat, *Polymer*, **46**, 1625–1634.

[48] Md. Majibur Rahman Khan, Masuhiro Tsukada, Yasuo Gotoh, Hideaki Morikawa, Giuliano Freddi, Hideki Shiozaki, (2010), Physical properties and dyeability of silk fibers degummed with citric acid, *Bioresource Technology*, **101**, 8439–8445

[49] Hong Wang, Huili Shao, Xuechao Hu, (2005), Structure of Silk Fibroin Fibers Made by an Electrospinning Process from a Silk Fibroin Aqueous Solution, *Journal of Applied Polymer Science,* **101**, 961–968.

[50] Process for making silk fibroin fibers, United States Patent 5252285

[51] Chen, X., Knight, D. P., Shao Z., Vollrath, F., (2001), Regenerated Bombyx silk solutions studied with rheometry and FTIR, *Polymer*, **42**, 9969-9974

[52] David M. Phillips, Lawrence F. Drummy, Deborah G. Conrady, Douglas M. Fox, Rajesh R. Naik, Morley O. Stone, Paul C. Trulove, Hugh C. De Long, Robert A.Mantz, (2004), Dissolution and Regeneration of Bombyx mori Silk Fibroin Using Ionic Liquids, *J. AM. CHEM. SOC.,* **126**, 14350-14351

[53] Url-12 < *http://www.piercenet.com/files/2132as8.pdf* **>** accessed 13.11.2010

[54]Url-13 < *http://www.piercenet.com/previews/Vol13Iss3/1601847_Previews_13_3.pdf* **>** accessed at 13.11.2010

[55] Url-14 <*http://www.piercenet.com/dialysis handbook***>**accessed at 13.11.2010

[56] Url-15 < *http://www.piercenet.com/files/TR0020-Dialysis-overview.pdf* **>**

[57] Edinara Adelaide Boss, Rubens Maciel Filho, Eduardo Coselli Vasco de Toledo, (2004), Freeze drying process: real time model and optimization, *Chemical Engineering and Processing,* **43**, 1475–1485

[58] Felix Franks, (1998), Freeze-drying of bioproducts: putting principles into practice, *European Journal of Pharmaceutics and Biopharmaceutics,* **45**, 221–229.

[59] Gerald Adams, (2007), The Principles of Freeze-Drying, *Cryopreservation and Freeze Drying Protocols, Methods in Molecular Biology*, **368**, 15-38.

[60] Ipsita Roy, Munishwar Nath Gupta, (2004), Freeze-drying of proteins: some emerging concerns, *Biotechnol. Appl. Biochem*., **39**, 165–177.

[61] Hyoung-Joon Jin, Sergey V. Fridrikh, Gregory C. Rutledge, David L. Kaplan, (2002), Electrospinning Bombyx mori Silk with Poly(ethylene oxide), *Biomacromolecules,* **3**, *1233-1239.*

[62] Ohgo, K., Zhao, C., Kobayashi, M., Asakura, T., (2003), Preparation of non-woven nanofibers of Bombyx mori silk, Samia cynthia ricini silk and recombinant hybrid silk with electrospinning method, *Polymer*, **44**, 841–846.

[63] Kim, S. H., Nam, Y. S., Lee, T. S., Park, W. H., (2003), Silk Fibroin Nanofiber: Electrospinning, Properties, and Structure, *Polymer Journal*, **35**, 2, 185-190.

[64] Sachiko Sukigara, Milind Gandhi, Jonathan Ayutsede, Michael Micklus, Frank Ko, (2003), Regeneration of Bombyx mori silk by electrospinning-part 1: processing parameters and geometric properties, *Polymer,* **44**, 5721–5727

[65] Lim Jeong, Kuen Yong Lee, Ju Whan Liu, Won Ho Park, (2006), Time-resolved structural investigation of regenerated silk fibroin nanofibers treated with solvent vapor, *International Journal of Biological Macromolecules*, **38**, 140–144

[66] Chen Chen, Cao Chuanbao, Ma Xilan, Tang Yin, Zhu Hesun, (2006), Preparation of non-woven mats from all-aqueous silk fibroin solution with electrospinning method, *Polymer,* **47**, 6322-6327

[67] Jingxin Zhu, Yaopeng Zhang, Huili Shao, Xuechao Hu, (2008), Electrospinning and rheology of regenerated Bombyx mori silk fibroin aqueous solutions: The effects of pH and concentration, *Polymer*, **49**, 2880–2885

[68] Feng Zhang, Bao Q. Zuo, Lun Bai, (2009), Study on the structure of SF fiber mats electrospun with HFIP and FA and cells behavior, *J Mater Sci*, **44**, 5682–5687

[69] Juan Zhou, Chuanbao Cao, Xilan Ma, (2009), A novel three-dimensional tubular scaffold prepared from silk fibroin by electrospinning, *International Journal of Biological Macromolecules,* 45, 504–510

[70] Url-16 < http://mmrc.caltech.edu/FTIR/FTIRintro.pdf **>** accessed at 13.10.2010

[71]Url-17 <http://www.chem.uwec.edu/Chem455_S05/Pages/Manuals/FTIRofproteins.pdf > accessed at 13.10.2010

[72] Yesim Iridag, Murat Kazanci, (2006), Preparation and Characterization of *Bombyx mori* Silk Fibroin and Wool Keratin, *Journal of Applied Polymer Science*, **100**, 4260–4264

[73] Byung-Moo Min, Gene Lee, So Hyun Kim, Young Sik Nam, Taek Seung Lee, Won Ho Park, (2004), Electrospinning of silk fibroin nanofibers and its effect on the adhesion and spreading of normal human keratinocytes and fibroblasts in vitro, *Biomaterials*, **25**, 1289–1297

CURRICULUM VITAE

Candidate's full name: Nuray KIZILDAG

Place and date of birth: Dortmund – 20.01.1978

Permanent Address: Istanbul - TURKEY

Universities and
Colleges attended: Ege University, 2000

Publications:

- **Kizildag, N.**, Iridag Y., *Tekstil Takviyeli Kompozit Malzemeler,* tekstil&teknik, *Ağustos 2010*, Issue 307, 72-86.